Arnold Schwarzenegger
Governor

TRACE METAL MOBILIZATION DURING COMBUSTION OF BIOMASS FUELS

PIER FINAL PROJECT REPORT

Prepared For:

California Energy Commission
Public Interest Energy Research Program

Prepared By:

University of California Davis
UCDAVIS

AUGUST 2007
CEC-500-2007-XXX

Prepared By:
Peter Thy, Charles E. Lesher, Bryan M. Jenkins, Michelle A. Gras, and Ryoji Shiraki
University of California Davis, Davis, CA 95616
Christian Tegner
University of Aarhus, 8000 Århus C, Denmark
Commission Contract No. 500-02-004
Commission Work Authorization No: MR 043-05

Prepared For:
Public Interest Energy Research (PIER) Program
California Energy Commission

Insert: Commission Manager Name
Contract Manager

Insert: Program Area Lead Name
Program Area Lead
Insert: Program Area Name

Insert: Office Manager Name
Office Manager
Insert: Office Name

Martha Krebs
Deputy Director
ENERGY RESEARCH & DEVELOPMENT DIVISION

B.B. Blevins
Executive Director

Jackalyne Pfannenstiel
Chair

Acknowledgements

Wheelabrator Shasta Energy Company, Anderson, California, kindly provided the raw wood fuel. We are grateful to Professor Sidsel Grundvig, University of Aarhus, for analyzing the major and minor element compositions of many of our ashes. We also acknowledge the help of John Neil and the access to the X-ray diffraction laboratory at the NEAT-ORU, Thermochemistry Facility, UC Davis.

Please cite this report as follows:

Thy, P., C.E. Lesher, B.M. Jenkins, M. A. Gras, and R. Shiraki, 2007. Trace Metal Mobilization During Combustion of Biomass Fuels. California Energy Commission, PIER Energy-Related Environmental Research Program. CEC-500-2007-XXX.

Preface

The Public Interest Energy Research (PIER) Program supports public interest energy research and development that will help improve the quality of life in California by bringing environmentally safe, affordable, and reliable energy services and products to the marketplace.

The PIER Program, managed by the California Energy Commission (Energy Commission), conducts public interest research, development, and demonstration (RD&D) projects to benefit California.

The PIER Program strives to conduct the most promising public interest energy research by partnering with RD&D entities, including individuals, businesses, utilities, and public or private research institutions.

PIER funding efforts are focused on the following RD&D program areas:

- Buildings End-Use Energy Efficiency
- Energy Innovations Small Grants
- Energy-Related Environmental Research
- Energy Systems Integration
- Environmentally Preferred Advanced Generation
- Industrial/Agricultural/Water End-Use Energy Efficiency
- Renewable Energy Technologies
- Transportation

Trace Metal Mobilization During Combustion of Biomass Fuels is the final report for 'A Pilot Study of Trace Metal Mobilization During Combustion of Biomass Fuels' project (contract number 500-02-004, grant number MEX-06-05, WA No. MR-043-05) conducted by University of California Davis. The information from this project contributes to PIER's Energy-Related Environmental Research Program.

For more information about the PIER Program, please visit the Energy Commission's website at www.energy.ca.gov/pier or contact the Energy Commission at 916-654-5164.

Table of Contents

List of Figures

List of Tables

Abstract[1]

Systematic mineralogical and chemical changes occur in the ash or slag of biomass during combustion. These changes are a function of fuel composition, firing temperature, and firing duration. Controlled temperature experiments were conducted using clean samples of wood, rice straw, and wheat straw to evaluate trace element mobility as a function of firing temperature. The concentrations of major and trace elements in ash and slag were analyzed using various multi-element instrumental techniques. The recommended analytical methods and element combinations consists of X-ray fluorescence (XRF) (or similar methods) for major and minor elements, the majority of trace elements using inductively coupled plasma mass spectroscopy (ICPMS), and short irradiation duration instrumental neutron activation analysis (INAA) for the alkali metals and chlorine.

There are distinct differences between the individual fuel ash types that easily allow fuel sources to be identified based on knowledge of ash compositions. A general increase occurs in residual concentrations of many elements with the removal of volatile constituents and increasing temperature. Depletion with increasing firing temperature was in this study particularly observed for the alkali metals (Na, K, Rb, Cs), but could also be seen for other elements (Cl, Ag, Cd, As, Se, and Pb).

Fly ash from fuel-intake controlled experiments was also analyzed. Observations include: 1) strong fractionation occurs during combustion; 2) trace element concentrations are often strongly affected by contamination from plant construction materials; and 3) incorporation of urban fuel types can strongly affect many heavy metal concentrations.

Among the fuel samples tested, enrichment of both barium and lead in wood ash resulted in concentrations slightly exceeding US Environmental Protection Agency's (EPA) total constituent analysis limits for heavy metals. In ashes and fly ashes for which a significant component of urban wood material is involved, As, Cr, and Pb may variably exceed EPA limits. Metals in all straw ashes tested were below the permitted limits. Leaching of straw ashes also depletes many alkali major and trace elements, although concerns may then arise as to concentrations in water or other solvent employed.

Key Words*: biomass fuel, biomass ash, biomass slag, major and minor elements, trace elements, fly ash, wood ash, straw ash, rice straw, wheat straw*

[1] See Appendix 1 for abbreviations of the atomic elements and Appendix 2 for non-technical dictionary and list of used acronyms.

Executive Summary[2]

Introduction

Use of wood and straw materials for power and fuel generation based on heat treatment procedures results in atmospheric emissions and a significant volume of solid residue, including fly ash. Utilizing of such byproducts as a partial substitute for soil fertilizers also has lead to concern, particularly as increase use is made of municipal and industrial solid wastes. Understanding of the partitioning of major and trace elements between solid and gas during thermal conversion is thus critical for environmental and regulatory purposes and for plant operation.

Objectives

This study examines major, minor, and trace element concentrations and their mobility during biomass combustion. Three series of temperature-controlled, experimental ashes of clean wood with low bark content, rice straw, and wheat straw were analyzed to assess trace element partitioning among combustion products. Also analyzed was a series of fly ash produced in either a fuel-intake controlled, laboratory-scale fluidized bed-combustor or a commercial biomass-fueled power plant. The results allow predictions of the concentrations of the trace elements in common biomass materials and provide a necessary foundation for monitoring heavy element emission and the utilization and disposal of waste from biomass fueled power plants.

Approaches

The concentrations of major and trace elements were analyzed using a selection of multielement instrumental techniques. The majority of major and minor elements were analyzed using X-ray fluorescence (XRF) spectroscopy (Si, Ti, Al, Fe, Mn, Mg, Ca, Na, K, P). Some major and minor elements (Fe, Mn, Na, K) were in addition analyzed by instrumental neutron activation analysis (INAA) techniques using both short and long irradiation exposures. The majority of the trace elements were analyzed by inductively coupled plasma mass spectroscopy (ICPMS) with about

[2] See Appendix 1 for abbreviations of the atomic elements and Appendix 2 for non-technical dictionary and list of used acronyms.

40 elements detected in most ashes. INAA using short irradiation duration techniques proved very successful in analyzing Na, Cl, K, Mn, and Sr. These results supplemented the XRF results and added chloride to the list of analyzed elements. The remaining trace elements were analyzed using long irradiation duration INAA with variable success because of very low concentrations encountered particularly in fuels containing straw materials. It was possible to detect many of the transition and alkali metals, however, most of the rare earth and heavier elements could not be detected using INAA.

Outcomes

Wood fuel thermally decomposes leaving significant carbonates in the solid fraction together with amorphous silicates, while straw fuels decompose leaving amorphous silicate and halite salts in the solid. Residual organic components and graphitic carbon are also often present in ashes in concentrations that depend on combustion conditions and efficiency. Combustion temperatures above 700 ^{o}C for wood ash drive off the remaining carbon bound in carbonate and give way to silicate and oxide minerals in the residuum prior to partial melting at very high temperatures beginning at about 1350 ^{o}C. The straw ashes become increasingly void of graphite with increasing crystallinity and the appearance of silica minerals (tridymite) together with the breakdown of halite salts from about 1000 ^{o}C. The straw ashes melt at relatively low temperatures from 800 ^{o}C, dependent on potassium content. Potassium and sodium are for all fuels lost as a function of firing temperature. The total weight loss above a temperature of 525 ^{o}C can amount to a maximum of 40 % for wood ash and 20 % for straw ashes. These fundamental processes are manifested in two competing factors when considering trace element abundances in the solid fraction: enrichments controlled by volatile releases of organic and inorganic components (amounting to a maximum of about 60 % increase in concentrations) and depletions resulting from removal with the volatile components. The latter depletion can be so severe that an element can be completely removed from the solid fraction (e.g., alkali metals).

There are clear differences among the individual fuel types (Table E1). Wood ash is dominantly composed of SiO_2 and CaO (~60 % of total). Trace elements in the highest concentrations in wood ash are strontium (2,200 ppm) and barium (2,200 ppm). Manganese occurs in major element concentrations of 20,000 ppm. Elements in intermediate concentrations (100-10 ppm range) are

many of the transition metals (V, Cr, Co, Ni, Cu, Zn), Zr, and Rb. Elements in the 10-1 ppm range include Be, As, Se, Cd, Sn, La, Ce, Nd, and Pb. The lead concentration average 7 ppm. Chlorine was not detected in the clean wood ash.

Table E1. Average Trace Element Concentrations

Element	Wood		Wheat Straw		Rice Straw		Detection Limit
	ppm	RSD%	ppm	RSD%	ppm	RSD%	ppb
Be	1.05	13.73%	0.92	16.65%	0.9	28.94%	0.034
V	33.0	3.33%	16.1	3.54%	3.4	2.35%	0.013
Cr	118	2.82%	36.2	2.97%	14.5	2.13%	0.150
Mn	20584	3.07%	829	3.35%	3923	2.56%	0.053
Co	10	3.71%	6	3.04%	4	2.86%	0.014
Ni	78	2.76%	20	3.44%	9.8	1.97%	0.013
Cu	177	2.78%	51	3.07%	35	2.17%	0.213
Zn	936	2.70%	80	3.47%	190	1.98%	0.064
As	16.1	4.17%	5.2	5.23%	5.6	2.07%	0.024
Se	1.0	10.67%	2.0	6.75%	0.1	7.38%	0.615
Rb	120	2.62%	49	3.39%	62	2.48%	0.026
Sr	2213	2.24%	262	3.11%	86	2.61%	0.021
Zr	15.6	2.99%	7.8	2.65%	1.5	10.69%	0.003
Ag	1.5	4.62%	0.1	6.13%	0.1	8.96%	0.023
Cd	6.7	2.38%	1.6	4.55%	0.3	7.63%	0.042
Sn	1.3	3.26%	0.9	4.45%	0.4	6.70%	0.071
Sb	0.73	3.84%	0.42	3.14%	0.22	4.52%	0.014
Cs	0.60	4.76%	0.35	2.62%	0.31	3.94%	0.029
Ba	2222	2.14%	743	2.64%	112	2.07%	0.056
La	1.84	3.27%	0.61	2.50%	0.30	2.79%	0.001
Ce	2.29	2.94%	1.63	2.78%	0.64	2.34%	0.002
Pr	0.14	4.19%		3.58%	0.09	4.24%	0.001
Nd	1.69	3.80%	1.12	2.80%	0.36	5.74%	0.006
Sm	0.38	7.28%	0.29	4.52%	0.15	10.02%	0.003
Gd	0.33	22.55%	0.21	5.18%	0.03	12.14%	0.006
Tb	0.04	9.41%	0.03	5.87%	0.01	12.67%	0.001
Dy	0.24	6.88%	0.18	4.37%	0.03	10.05%	0.007
Er	0.25	8.12%	0.24	4.55%	0.07	8.92%	0.002
Tm	0.03	12.80%	0.03	8.30%	0.02	12.93%	0.001
Yb	0.06	7.43%	0.03	4.74%		9.12%	0.004
Lu	0.02	15.00%	0.01	6.58%		14.12%	0.001
Hf	0.47	4.24%	0.28	5.00%	0.17	10.25%	0.005
Ta	0.28	4.10%	0.37	3.68%	0.53	4.38%	0.002
W	0.93	2.42%	0.35	4.22%	0.20	4.38%	0.002
Tl	0.25	10.08%		16.07%	0.01	17.99%	0.014
Pb	7.1	2.63%	5.7	3.04%	4.0	1.94%	0.042
Th	0.17	8.49%		3.73%		6.62%	0.002
U	0.30	9.45%	0.10	4.31%	0.02	3.67%	0.027

ppm, parts per million; ppb, parts per billion; RSD%, relative standard deviation in %.
See appendix 1 for abbreviations of the atomic elements.

Rice straw ash is composed principally of SiO_2 and K_2O (~90 % of total). The only trace element in high concentration in rice straw ash is manganese (4,000 ppm). Other elements in intermediate

concentrations (200-10 ppm range) include many transition and alkali metals (Cr, Cu, Zn, Rb, Sr, Ba). Elements in the range 1-10 ppm include V, Co, Ni, Zr, and Pb. The average lead concentration is 4 ppm. Chlorine occurs as a major element in concentrations to 3.5 wt. %.

Wheat straw ash shows many features in common with rice straw ash and is dominantly composed of the major oxides SiO_2 and K_2O (~80 % of total). The only trace elements in high concentrations in wheat straw ash are Mn (800 ppm), Ba (750 ppm), and Sr (250 ppm). Other elements in intermediate concentrations (100-10 ppm range) are many transition and alkali metals (V, Cr, Ni, Cu, Zn, Rb). Elements in the 1-10 ppm range include Co, As, Se, Zr, Cd, Ce, Nd, and Pb. The average lead concentration is 6 ppm. Chlorine also occurs as a major element in concentrations to 4.5 wt. %.

The concentrations of many major and trace elements depend on firing temperature. The alkali metals, Na, K, Rb, and Cs, show for wood ash strong depletion with increasing temperature above 800 ^{o}C, attributable to the removal of these elements as a result of the decomposition of carbonate minerals. Chlorine in addition shows depletion from the straw ashes. Depletion with increasing firing temperature was in this study variably observed for Cl, Na, K, Rb, Cs, Ag, Cd, As, Se, and Pb.

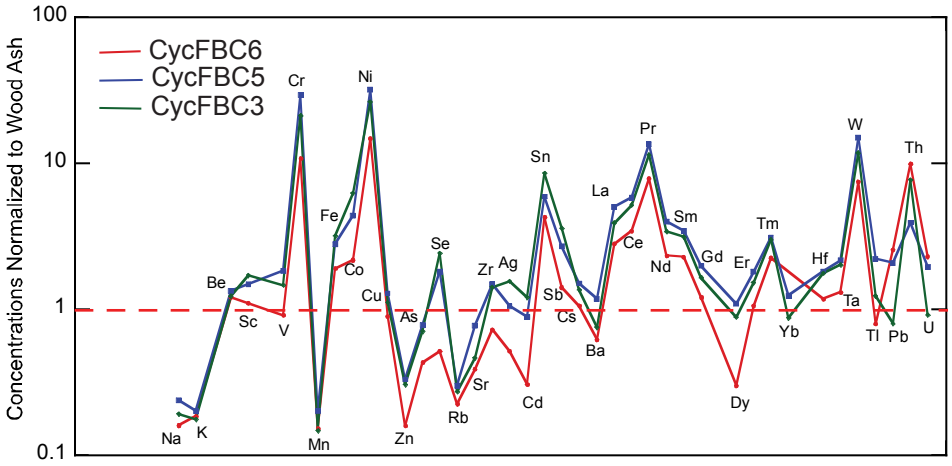

Figure E1. Fly ashes produced in laboratory scale fluidized bed combustor using blended wood and rice straw fuels. Arranged in order of increasing atomic number and normalized to wood ash of Table E1.

Two sets of fly ashes produced in controlled laboratory and full-scale experiments were also analyzed (Figure E1). Very strong fractionation occurs during combustion to the extent that trace element concentrations in fly ash show little similarities to those observed in the corresponding whole fuel ash prior to combustion. Fly ash collected over the duration of the experiments remained remarkably similar in composition. Blending of straw, either leached or unleached, at low concentrations in wood had little effect on trace element concentrations in fly ash. Trace element concentrations can be strongly affected by contamination, such as from steel and other materials making up the conversion facility. Incorporation of some urban fuel types may also strongly affect heavy metal trace element, including lead. It is for this reason that biomass power plants control the source of fuel in order to avoid heavy metal enrichment above federal and state limits. Our results show that this intake control can be very efficient and can produce remarkably near identical trace element characteristics over years of operation.

Enrichment of both barium and lead in the examined wood ash resulted in concentrations slightly exceeding US Environmental Protection Agency's (EPA) total constituent analysis limits for heavy metals (Table E2). Metals in all straw ashes tested were all below the permitted limits.

Table E2. Toxicity of Fuel Ashes

EPA Hazardous Waste Code	Element	EPA limits* (ppm)	Wood Ash (ppm)	C/20	Rice Straw Ash (ppm)	C/20	Wheat Straw Ash (ppm)	C/20
D004	Arsenic (As)	5	16.1	0.81	6	0.28	5.2	0.26
D005	Barium (Ba)	100	2222	**111**	112	5.6	743	37
D005	Cadmium (Cd)	1	6.7	0.34	0.3	0.02	1.6	0.08
D007	Chromium (Cr)	5	118	**6**	14.5	0.73	36	1.8
D008	Lead (Pb)	5	7.1	0.36	4	0.2	5.7	0.29
D009	Mercury (Hg)	0.2	(35 ppb)					
D010	Selenium (Se)	1	1	0.05	0.1	0.01	2	0.1
D011	Silver (Ag)	5	1.5	0.08	0.1	0.01	0.1	0.01

*Elemental limits following the EPA Toxic Characteristic Leaching Procedure.
C/20, concentration divided by 20. Bold indicate adjusted concentrations exceeding EPA limits.

Conclusions

Most major and trace elements are readily analyzed in ashes and slag using commonly available multielement instrumental techniques. The majority of major and minor elements can be

analyzed using X-ray fluorescence spectroscopy or similar techniques. Instrumental neutron activation using short irradiation duration techniques proved valuable for analyzing chlorine and some of the alkali metals. The majority of trace elements can be analyzed by inductively coupled plasma mass spectroscopy. The trace element concentrations are distinctly dependent on fuel type. The wood ash tested contains strontium and barium in high concentrations above 2,000 ppm in addition to many elements in concentrations above 1 ppm (V, Cr, Co, Ni, Cu, Zn, Zr, Rb, Be, As, Se, Cd, Sn, La, Ce, Nd, and Pb). Managanese was a major element in the wood ash with concentrations around 2 wt. % MnO. The straw ashes contain in general lower concentration of many of the same elements including Mn, Ba, and Sr above 200 ppm in addition to several elements variably in concentrations above 1 ppm (Cr, Ni, Cu, Zn, Rb, Cd, Nd, Sr, Ba, V, Co, As, Se, Zr, and Pb). Chlorine occurs as a major element in straw ashes. Many major and trace elements are depleted with increasing firing temperature (Cl, Na, K, Rb, Cs, Ag, Cd, As, Se, and Pb) due to release with volatile components. Fly ashes from controlled pilot and full-scale experiments show very strong fractionation to the extent that trace element concentrations may show little similarities to those observed in the original fuel ashes. Sources of contamination in fly ashes include plant construction material, such as steel, and blended urban wood fuels. Enrichment for some elements including Ba, As, Cr, and Pb caused concentrations in ash to approach or in some cases to exceed federal toxicity standards. Blending with straws poses few problems in terms of trace element abundances, due to their generally low concentrations in straw ash, although major element effects on slag forming and fouling remain of concern.

Recommendations

The present study was principally conducted using three fuels and cannot be generalized to represent the fuels options of California. It is recommended that a broad survey of trace element contents of potential biomass fuels are conducted in order to determine for example the dependencies of soil type, irrigation water quality, and atmospheric pollution. It is also recommended that a detailed study be initiated of the fractionation of trace elements during combustion in model boilers as well as full-scale power plants (and during other types of thermal processing). Such broad knowledge of the distribution of the trace elements in biomass products and their fractionation during thermal conversion are central for formulating environmental and analytical monitoring programs.

Accurate and precise analyses of trace element abundances are critical for future investigations. A major obstacle in defining environmental performance is currently the lack of well-characterized biomass standards applicable for multielement analytical quality control. It is thus recommended that a set of biofuel multielement analytical standards be developed; including common biomass ashes as well of fly ashes from biomass fueled power plants. The current situation is that the only relevant multielement standard available is a fly ash from a coal-fueled power plant (NIST 1633). The potential for high heavy element abundance in some fuel types warrant precise analyses of biomass and byproducts from thermal conversions. Such analyses would be greatly aided by high quality analytical standards resembling the fuel material in question.

Public Benefits to California

The present results allow predictions of the concentrations of the trace elements in common biomass materials and provide a necessary foundation for monitoring heavy element emission and the utilization and disposal of residues from biomass fueled power plants and other conversion facilities.

1. Introduction[3]

The possibility of utilizing ash products from biomass power plants as a partial substitute for soil fertilizers has led to a growing concern about the trace metal content of such ashes, particularly as increasing use is made of municipal and industrial solid wastes in conversion technologies. In part, these concerns relate to the fertilizer value of the biomass byproducts, but as well as to compliance with standards for atmospheric emissions and for the disposal and utilization of solid waste products (e.g., California Health and Safety Code Sections 25140-25145.4). Use of biomass fuels, such as wood and straw materials, for power generation results in atmospheric emissions and a significant volume of solid wastes (slag, bottom and fly ash) that may contain leachable toxic elements. There is, therefore, a need for knowing the trace element contents of biomass materials as well as for understanding the behavior of such elements during combustion (e.g., K, Cl, B, Be, Cd, Cr, Li, Pb, U, Hg, Se). Some information is available on the trace element content of pure biomass (e.g., PHYLLIS databases, http://www.phyllis.nl/) as well as products of fluidized bed and coal co-firing experiments (e.g., Kouvo and Backman, 2003; Richaud et al., 2004). However, little information is available on the fate of trace elements (toxic or beneficial) in biomass fuels commonly used for power generation in California. This is despite a large interest in the behavior of trace elements in coal-fired power plants (Roy et al., 1981; Raask, 1985; Querol et al., 1995; Llorens et al., 2001).

Following the incentives provided under the 1978 Public Utilities Regulatory Policy Act (PURPA), the existing US electricity generating capacity from biomass fuels stands currently at around 10 GW_e (www.eia.doe.gov, 2004), with California representing about one-tenth of this. Increasing mandates such as renewable portfolio standards and demand for renewable energy have created opportunities for increasing power generation from biomass. Mature wood fuels are proposed for much of this expansion. However, their availability is in some instances limited and herbaceous fuels and annual growth woods are expected to be used in increasing quantities. An annual consumption of between 60 million and 90 million metric tons of wood is currently required to fuel the existing biomass based power output. This could amount to a nationwide

[3] See Appendix 1 for abbreviations of the atomic elements and Appendix 2 for non-technical dictionary and list of used acronyms. Note that this note applies to all following report chapters.

annual production of 2.4 million to 3.6 million tons of waste ash, assuming a 4 % mean ash content. Biomass ash contains high amounts of plant nutrients such as Ca, K, and P that in part could substitute for traditional agricultural soil amendments. However, the ash also contains trace elements in concentrations sometime high enough to raise concern. As an example, wood fuel ash can contain 40 ppm of lead or higher (Tillmann, 1994). This will translate into more than 100 tons of lead in ash and slag annually. Similarly, mercury concentrations of 2 ppm in wood ash will translate into 5-7 tons of mercury that will either be released to the atmosphere or be retained in the ash waste. These values may be much higher depending on the actual source of the fuel. Toxic elements may locally reach such high concentrations that the waste products will require special handling and disposal considerations.

The volume of waste products will significantly increase as the forecasted expansion in biomass fuel consumption materializes, resulting in even stronger pressures on the power industry to find alternative uses for their waste products. The use of domestic and industrial waste products, such as urban demolition woods, may result in strongly increased concentrations of some toxic trace elements like lead. The concentrations of trace metals and their behavior during combustion are therefore of considerable practical and economic interest to the power industry.

Trace metals are mobilized and fractionated during combustion between bottom ash and slag, heat exchanger deposits, fly ash, and atmospheric emission. Additional fractionation involves fall-out and mobilization by leaching from solid waste deposits such as in landfills. In a typical coal fired U.S. power plant, Se, I, As, Sb, Br, Zn, Cd, and Pb are enriched in fly ash (Chadwick et al., 1987). The elements Br, Hg and I are strongly partitioned into the gas phase and released into the atmosphere. Studies of coal fueled operating power plants have mainly centered on understanding the fractionation of trace elements between size fractions of fly- and bottom-ashes (Roy et al., 1981; Tillmann, 1994; Querol et al., 1995; Llorens et al., 2001). Few studies have attempted to understand biomass-fueled systems (Tillmann, 1994; Obernberger and Biedermann, 1997; Kouvo and Backman, 2003; Richaud et al., 2004; Spears, 2004). The result is that little is known about the heavy metals and other environmentally critical pollutants associated with biomass combustion, although heavy metals, especially Pb and Zn, are known to influence the

char reactivity and gasification rate for wood and other biomass waste (Struis, et al., 2002; Hasler, et al., 1994).

The behavior of the major and trace elements in biomass systems are controlled by the nature and composition of the solid components and combustion temperature (among other possible factors). It is not possible to predict the trace element behavior across the large temperature range encountered in biomass boilers from ignition of fuel to partial or complete melting of ash and slag without direct experimental observations. It is plausible that elements in trace amounts, such as the halogens (F, I, Br) and alkalis (Be, Rb, Cs, Sr, Ba) behave in a similar fashion as observed for their major element counter parts (K, Cl) (Thy et al., 1999, 2000). Of particular interest is the group of heavy metals (Cr, Co, Ni, Cu, Zn, Pb, Hg, As, Se, Sb, and Cd) that is toxic to many organisms. Many of these trace metals are according to Environmental Protection Agency (EPA) and state regulations used to define a particular waste product as hazardous or non-hazardous. Therefore, it is important that we understand their behavior during combustion and know their concentrations in ash waste products.

In this report, the trace element concentrations and their mobility in three series of temperature-controlled, experimental ashes produced from wood, rice straw, and wheat straw fuels were discussed. The fuels utilized were void of domestic and industrial components and provide the base for evaluating trace elements and their behavior in potential biomass fuels. The experimental results were tested using a series of fly ashes produced by a fuel-intake controlled laboratory bed-combustor and an operating biomass-fueled power plant. The results are also compared to fuel types that are either leached or are strongly contaminated by urban wood waste. The results allow predictions of the concentrations of the trace elements in common biomass materials and provide a necessary foundation for monitoring heavy element emission and for the utilization and disposal of waste from biomass fueled power plants.

2. Experimental Ash and Slag Procedures

This study principally determines trace element concentrations and mobility during combustion for three representative and common California biomass fuels (wood, rice straw, and wheat straw). This is done by direct analyses of the inorganic ash and slag residues experimentally produced under controlled temperatures between 525 and 1500 ^{o}C. The selected biomass materials for the study are compositionally well characterized and serve as a basis for understanding the behavior of trace metals during biomass combustion. The study involves ashing at controlled temperatures and the analyses of these ashes using a selection of analytical techniques best suited to the range of trace constituents present in the ashes of the biomass materials.

The principal goal of the analytical program is to analyze all trace elements detectable in common biomass fuel ashes with a precision below 3 %, a lower limit of detection of at least 1-2 ppm, and a reasonable and demonstrable accuracy. The selected analytical techniques (instrumental neutron activation, inductively coupled plasma-mass spectrometry, and X-ray fluorescence spectrometry) use different sample preparation methods in order to monitor possible elemental losses during sample preparation. A further consideration is that the various analytical techniques have their strength for particular elements or group of elements. It is thus necessary to employ several techniques to assemble a list of elements of interest to biomass fuels.

The analytical results are used to quantify the depletion factors in trace element concentrations caused by volatilization as well as the enrichment factors caused by breakdown of inorganic and organic matter during combustion. The partitioning of trace elements between the inorganic residue and the combustion gas depends on fuel type as well as combustion temperature and the mineralogical composition of the inorganic residue. The results are used to evaluate the severity of trace element release to the atmosphere and the concentrations in solid waste from combustion of common fuel types and their blends. The results form the practical and regulatory basis from which more complex domestic and industrial fuel types can be evaluated.

2.1. Fuel Selection and Preparation

The samples selected for the ashing experiments are three commonly available biomass materials in California. The first is a mixed-conifer, whole-tree chips obtained from Wheelabrator-Shasta Energy Company, Inc., Anderson, California. The trees, white fir and ponderosa pine, were harvested from the northeastern slopes of Mt. Shasta. The content of bark in the wood fuel is less that 5 % by volume. This relatively clean and high quality fuel is one of many types received at the plant. The second sample is a medium grain Japonica (variety M202) rice straw from Colusa County, California. The third sample is a wheat straw from Yolo County, California. Neither of the straw fuels is currently used as boiler fuel in California, although several facilities are permitted to use straw.

The fuels were dried in ambient air for a week and then milled to a maximum 1/8" particle size. The final moisture content for the samples determined after oven-drying at 105 ^{o}C were 10.4 % for wood, 7.5 % for rice straw, and 7.7 % for wheat straw. The fuels were ashed in air in a large-volume, electric muffle furnace. Temperature was ramped at 20 ^{o}/min to 100 ^{o}C and then at 2 ^{o}/min to a maximum of 525 ^{o}C. Temperature was dwelled at 400 ^{o}C for 3 hours and again at 525 ^{o}C for 4 hours. The furnace temperature was then dropped from the maximum 525 ^{o}C at 8 ^{o}/min until 30 ^{o}C. The furnace and sample temperatures were monitored during ashing by thermocouples inserted through the roof of the furnace. The rice and wheat straw samples were ashed in open ceramic containers. The wood sample was ashed in a semi-closed, steel container with an airflow of 4.5 l/min admitted to the container when the temperature reached its maximum value. These ashing procedures allowed relatively large ash volumes to be produced under controlled temperatures without ignition. Such ignition could have resulted in uncontrolled high temperature and possible elemental losses. The ash samples were stored in airtight containers before and between uses.

The total amounts of dried fuel ashed were 22.2 kg wood giving an ash content on a dry basis of 1.2 %, 2.3 kg rice straw giving an ash content 22.1 % (20.38 ± 0.29 %, N=66), and 4.5 kg wheat straw giving an ash content of 9.8 % (8.95 ± 0.57 %, N=244). The ultimate elemental

compositions for the fuels were determined following the analytical recommendations of Miles et al. (1995) and Baxter et al. (1998) and are summarized in Table 1.

Table 1. Compositions of Fuels Used as Starting Materials

	Wood		Rice Straw		Wheat Straw	
Ultimate Analysis (%, wet basis)						
Carbon	48.54		38.50		43.81	
Hydrogen	5.22		3.56		5.1	
Nitrogen	0.07		0.55		0.58	
Sulfur	0.02		0.06		0.12	
Oxygen	36.55		36.30		35.27	
Chlorine	<0.012		0.648		0.402	
Potassium	0.075		0.996		0.593	
Moisture (%, wet basis)	10.4		7.5		7.8	
Ash (%, dry basis)	1.2		22.1		9.8	
Ash Analysis (% oxides)		Volatile Free		Volatile Free		Volatile Free
SiO_2	9.35	14.01	75.38	82.13	57.47	70.28
TiO_2	0.13	0.19	0.01	0.01	0.05	0.06
Al_2O_3	3.12	4.68	0.09	0.10	0.77	0.94
Fe_2O_3	1.14	1.71	0.10	0.11	0.39	0.48
MnO	1.76	2.64	0.27	0.29	0.07	0.09
MgO	4.93	7.39	1.64	1.79	1.82	2.23
CaO	32.06	48.05	1.60	1.74	2.8	3.42
Na_2O	0.39	0.58	0.14	0.15	0.8	0.98
K_2O	10.72	16.06	11.95	13.02	16.55	20.24
P_2O_5	3.13	4.69	0.61	0.66	1.05	1.28
Volatiles	27.59		7.97		14.91	
Total	94.32	100.00	99.76	100 00	96.68	100.00
SO_2	0.69		0.67		1.66	
Cl	<0.065		3.18		3.58	
CO_2	6.24		0.22		0.19	

Ultimate analyses by Hazen Research, Inc., Golden, CO, except that Cl and K determined at UCD by INA. Ashing temperature was 525 ºC. Ash composition determined at University of Aarhus, except SO_2 and CO_2 determined by Hazen and Cl determined at UCD by INAA. Volatiles is the loss-on-ignition determined from heating the ash to 950ºC.
Oxygen was estimated by difference to a ideal 100 % total.

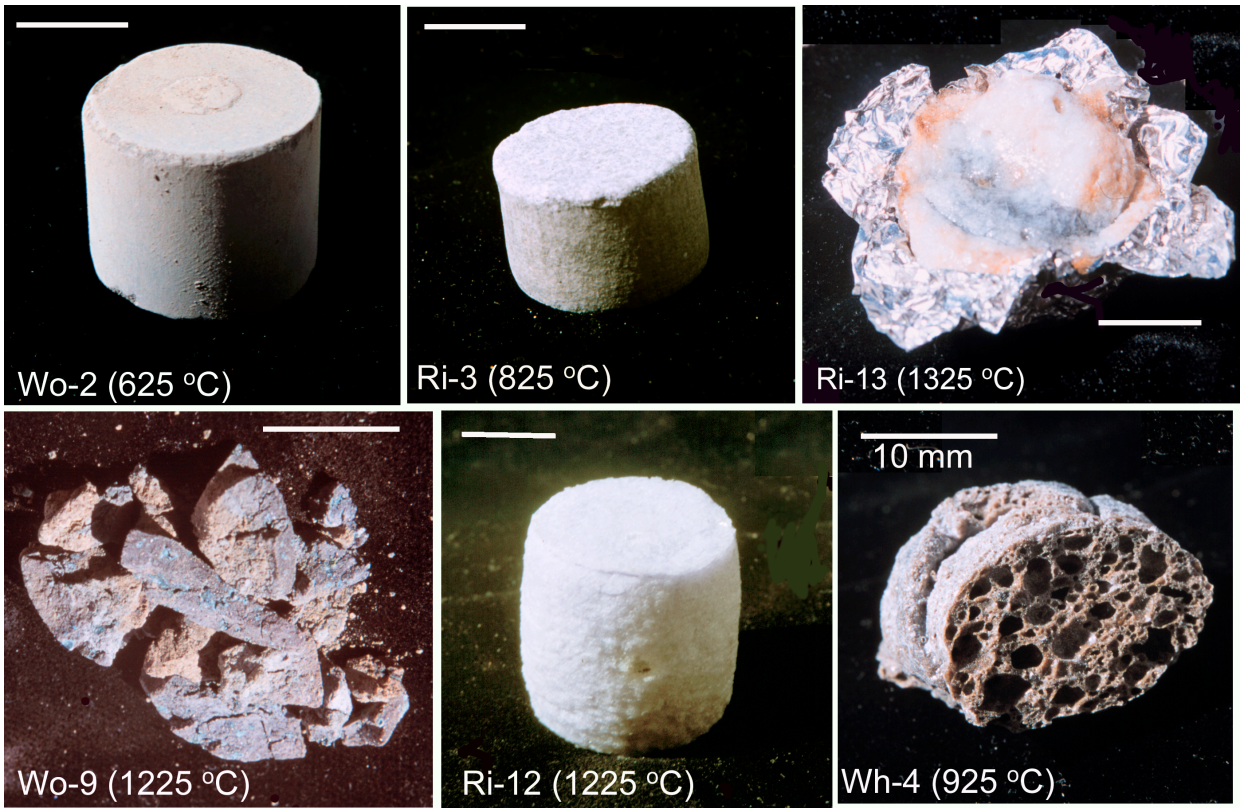

Figure 1. Typical experimental products. Wo-2, wood ash fired at 625 °C. Ri-3, rice straw ash fired at 825 °C. Ri-13, rice straw ash fired at 1325 °C. Melt is retained by platinum foil. Wo-9, wood ash fired at 1225 °C. Pellet is broken up in smaller pieces. Ri-12, rice straw ash fired at 1225 °C. Wh-4 wheat straw ash fired at 925 °C within the melting interval showing exsolved gas vesicles.

2.2 Experimental Techniques

For each experiment, about 20 g of powder was pressed into a pellet at up to 3000 psi pressure. The pellets were placed in a bottom-fed, Kanthal furnace at a temperature between the original ashing temperature of 525 °C and their respective melting temperatures in intervals of about 50 °C for straws and 100 °C for wood. The pellets were raised into the hot zone of the furnace and kept there for 2 hours for straw ashes or 3 hours for wood ash. The furnace and sample temperatures were monitored by an S-type thermocouple near the pellet inserted through the top of the furnace. The furnace set point temperature was corrected to experimental temperature by the equation $T_{exp} = 12.402 + 0.97377 \times T_{setpoint}$ (in °C) as determined using the inserted thermocouple. Typically, the sample heated to the maximum at 20 °C/min. Lowering the furnace

bottom cooled the pellet to ambient temperature and terminated the experiment. Pellets were placed on platinum foil to avoid reaction with the alumina bottom plate.

Table 2. Summary of Experiments and Principal Results

Experimental ID	T (oC)	Loss %	Ash Color		
			L* Lightness	a* red/green	b* yellow/blue
Wood					
WO-8	1525		52.28	-2.80	4.28
WO-10	1425	36.2	45.93	3.36	11.25
WO-7	1325	32.6	47.94	1.48	8.57
WO-9	1225		51.02	0.44	8.17
WO-6	1125	27.5	46.51	0.50	7.23
WO-1	1011	27.3	49.65	1.36	10.34
WO-5	913	25.2	49.30	0.20	9.13
WO-4	816	21.9	45.83	2.29	6.60
WO-3	718	9.9	53.10	1.04	5.02
WO-2	621	4.2	57.82	0.84	7.86
WO-S	524		62.45	1.23	11.63
Wheat Straw					
WH-5	962	18.5	69.01	1.66	10.02
WH-4	913	16.3	66.36	1.45	9.39
WH-6	864	15.5	63.42	0.78	7.91
WH-3	816	14.5	61.26	0.34	5.35
WH-7	767	13.8	57.12	0.07	2.82
WH-2	718	13.9	54.25	0.57	2.12
WH-8	670	12.5	50.64	0.67	1.74
WH-1	621	12.1	52.74	0.27	-0.24
WH-9	572	10.5	54.95	0.37	-0.09
WH-S	524		50.79	-0.09	0.00
Rice Straw					
R-13	1325		49.83	0.23	1.25
R-12	1225	14.6	85.34	2.76	0.21
R-11	1125	14.0	84.56	3.54	-0.79
R-10	1011	10.6	82.02	3.21	-0.44
R-5	962	9.6	82.15	2.55	1.37
R-4	913	8.7	80.34	2.37	2.03
R-6	864	8.1	79.60	1.80	2.67
R-3	816	7.7	74.42	1.21	2.11
R-7	767	7.3	65.85	1.03	1.66
R-2	718	7.0	62.74	1.14	0.16
R-8	670	6.1	60.06	0.64	-0.05
R-1	621	5.7	57.68	0.30	0.10
R-9	572	5.5	53.59	0.76	0.09
R-S	524		48.16	0.08	-0.26

Temperature in oC . Sample weight loss in percentages (Loss %).
Ash color measured using the BYK-Gardner Colour Guide 6805.
See text for details.

The experimental temperatures together with some principal results (weight loss during firing and the measured ash color) are summarized in Table 2. The experimental products were powdered in an agate mortar or if required using a SPEX wolfram carbide mill for about 2

minutes. The color of the powder was measured by using a BYK-Gardner Colour Guide 6805 (L* lightness; a* red/green, b* yellow/blue). Color standards were measured concurrently with the powders and gave satisfactory results (green, white, black). The color variations of the powdered ashes or slag are illustrated in Figures 2 to 4.

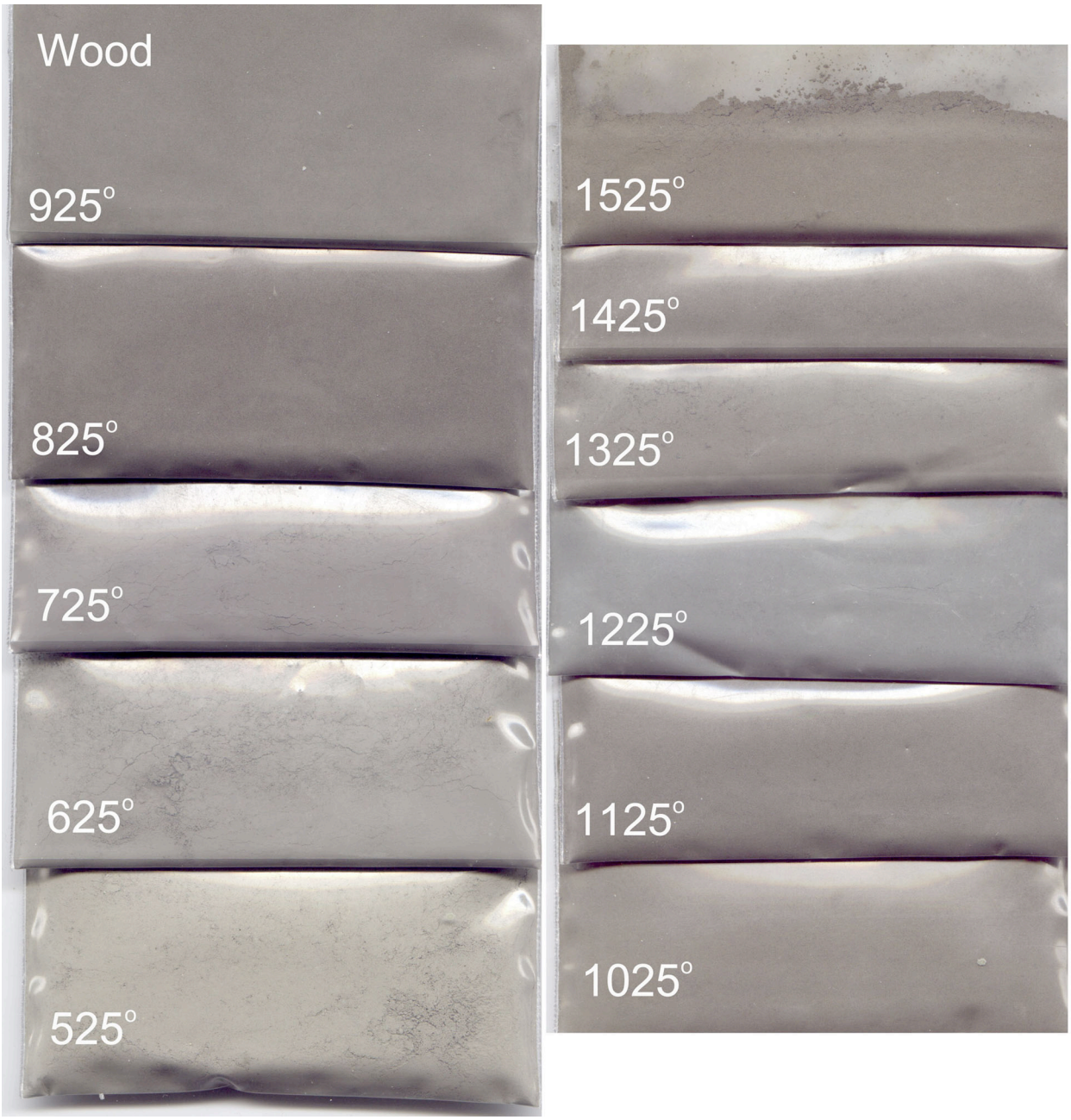

Figure 2. Color variation of powdered experimental ashes and slag of wood. Experimental temperature is given in degrees Celsius and is the uncorrected set point values. The powdered ashes and slag are contained in plastic bags. Color variation is given in Table 2.

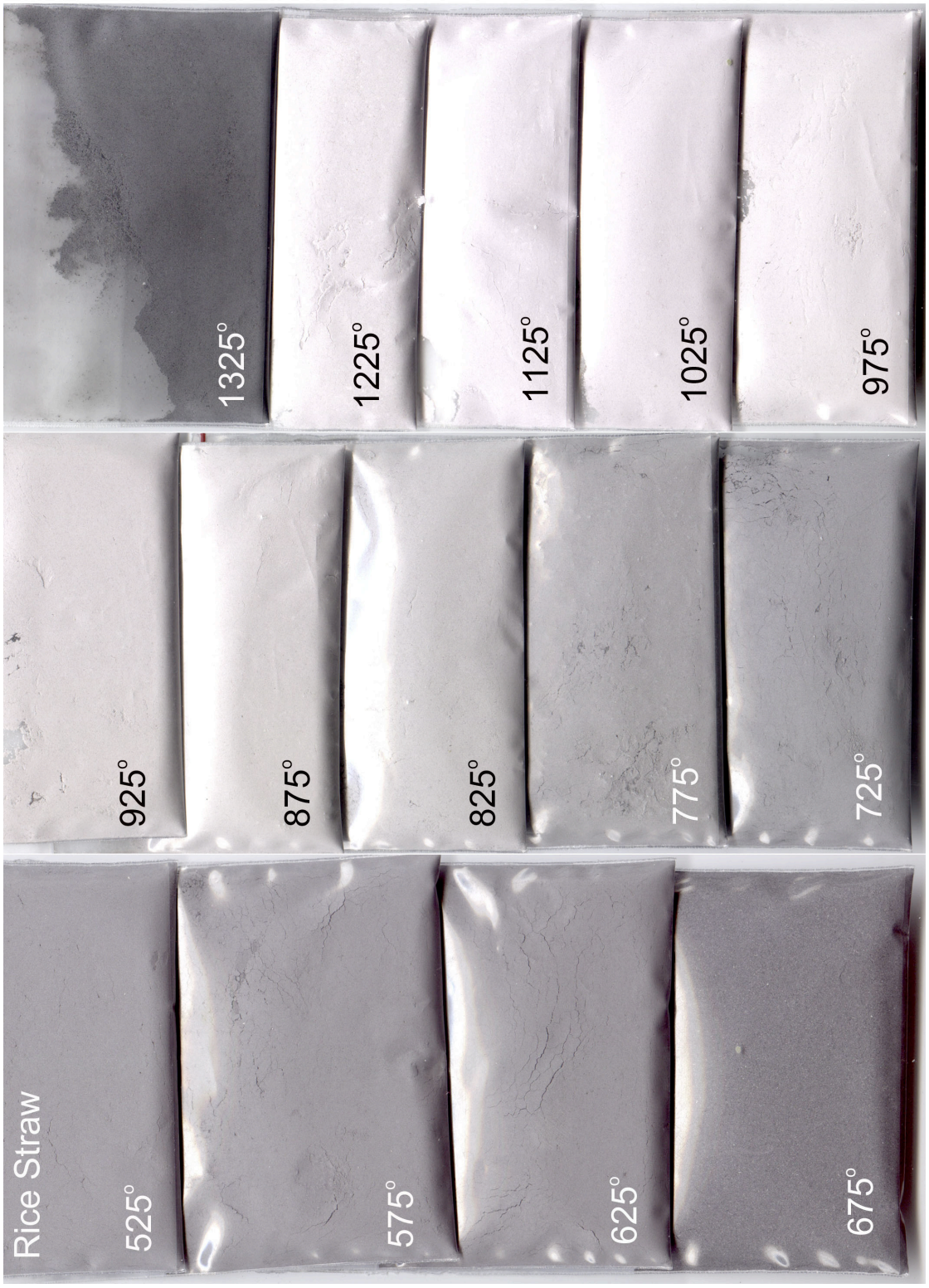

Figure 3. Color variation of powdered experimental ashes and slag of rice straw. Experimental temperature is given in degrees Celsius and is the uncorrected set point values. The powdered ashes and slag are contained in plastic bags. Color variation is given in Table 2.

Figure 4. Color variation of powdered experimental ashes and slag from wheat straw. Experimental temperature is given in degrees Celsius and is the uncorrected set point values. The powdered ashes and slag are contained in plastic bags. Color variation is given in Table 2.

3. Experimental Fly Ashes

In addition to the directly experimentally produced ashes from common biomass fuel types, we have also used fly ash from previous fluidized bed combustion experiments. Ashes were selected from two sets of experiments both based on controlled biomass fuel intakes and both supported by the California Energy Commission (Jenkins et al. 1999; Thy et al., 2004).

Table 3. Additional Ashes and Fly Ashes

Identification	Description	Ashing Temperature	Source
HEL-A	Rice straw ash	575 °C	Jenkins et al. 2003
EER	Rice straw ash	575 °C	Meister et al. 2005
Urban Wood	Urban wood ash	525 °C	Thy et al. 2000
CFM	California feed lot cattle manure ash	525 °C	Thy and Jenkins, unpublished
LR-S	Leached rice straw ash	525 °C	Leached straw from Table 2 (R-S)
Wood17.40	Fly ash from commercial plant in California (wood stack baseline, 8/10/98, 17:40)		Jenkins et al. 1999
Wood15.52	Fly ash from commercial plant in California (wood stack baseline, 8/10/98, 15:52)		Jenkins et al. 1999
Straw12.35	Fly ash from commercial plant in California (straw blend, 8/11/98, 12:35)		Jenkins et al. 1999
Straw14.30	Fly ash from commercial plant in California (straw blend, 8/11/98, 14:30)		Jenkins et al. 1999
Flyash2000	Fly ash collected March 11, 2000, from commercial biomass plant in California		
CycFBC6	Cyclone ash March 26, 2003 (FBC-6, leached rice blend)		Thy et al. 2004
CycFBC5	Cyclone ash March 15, 2003 (FBC-5, wood)		Thy et al. 2004
CycFBC3	Cyclone ash March 2, 2003 (FBC-3, raw rice blend)		Thy et al. 2004

3.1. Commercial Biomass Power Plant Experiment with Leached Rice Straw Fuel

Jenkins et al. (1999) conducted tests of leached rice straw during fuel intake-controlled experiments in commercial biomass boilers. Ash samples from that earlier testing were used here. The power plant sampled is a conventional superheated Rankine-cycle design with a total net generating capacity of 25 MWe (Figure 5). A variety of urban wood and agricultural residues were typically used (in 1998 as well as today) as primary fuel, with urban wood residues representing the majority of the fuel fraction throughout the year. Combustion takes place in a circulating fluidized bed boiler that employs two cyclones to separate bed media and larger ash particles from the flue gas. The separated material is re-circulated back to the furnace. Flue gas exiting the cyclone passes through a convection pass that consists of tertiary, secondary, and primary superheaters, followed by additional generating bank and economizers. Stack gas

particulate matter emission control consists of a multiclone followed by a baghouse. Normal superheater outlet steam temperature is 454 ^{o}C and pressure is 6.2 MPa. Regular furnace exit gas temperature is in the 900-920 ^{o}C (before the cyclones) and approximately 870 ^{o}C at the start of the convection pass (i.e., tertiary superheaters). During normal operation, soot blowers are used at regular intervals to blow deposits from the heat exchanger units at different locations in the convection pass. These blowers were not operated during the experiments from which fly ash was obtained and used in the present study.

Table 4. Compositions of Fuel Blends Used at Commercial Plant in 1998

	Baseline Wood Fuel (1)	Straw Test Fuel (2)
Ultimate Analysis (% dry matter)		
Carbon	49.79	46.78
Hydrogen	5.65	5.28
Nitrogen	0.33	0.48
Sulfur	0.11	0.13
Ash	5.54	11.44
Chlorine	0.03	0.03
Ash Content (wt. % oxides)		
SiO_2	41.55	66.43
TiO_2	0.83	0.53
Al_2O_3	12.41	9.13
Fe_2O_3	6.93	4.37
MnO		
MgO	2.93	1.56
CaO	15.56	6.82
Na_2O	2.67	1.68
K_2O	3.86	2.59
P_2O_5	1.73	1.06
SO_3	3.98	2.05
CO_2	5.24	1.98
Cl	0.19	0.09

1. Baseline wood fuel made from blending orchard pruning wirth urban wood fuel in a 1/6 ratio (dry fuel basis). From Jenkins et al. (1999, table 2.26).
2. Straw test fuel made by blending leached rice straw and baseline wood fuel in the 1/3 ratio (dry fuel basis). From Jenkins et al. (1999, table 2.26).

The test carried out on August 11, 1998, used 40 metric tons of leached rice straw that was blended with wood representative of the fuel normally used at the facility. This wood consisted of a mixture of urban wood fuel and orchard prunings blended at a 6/1 ratio (wood/pruning). The leached straw fuel was hammermilled and mixed with the wood fuel a day prior to the test in a 1/3 ratio (straw/wood fuel) and fed to the furnace as described by Jenkins et al. (1999). The two

fly ash samples obtained for the present study were from the August 11, 1998, experiment as detailed in Table 3. A similar set of fly ash samples were obtained on August 10, 1998, during which the boiler was operated using the 'baseline' wood fuel also used for the straw addition experiment. An additional fly ash sample (Table 3) from the same facility was obtained during March 2000 and is likewise included. The commercial fly ashes used in the present study are summarized in Table 3 and identified by fuel type and date and time of collection. The ultimate and ash compositions of the source fuel blends are given in Table 4 modified from Jenkins et al. (1999).

Figure 5A. The central boiler stack of the commercial biomass plant used by Jenkins et al. (1999) for controlled fuel intake experiments. Fly ash produced as part of this experiment was used in the present study.

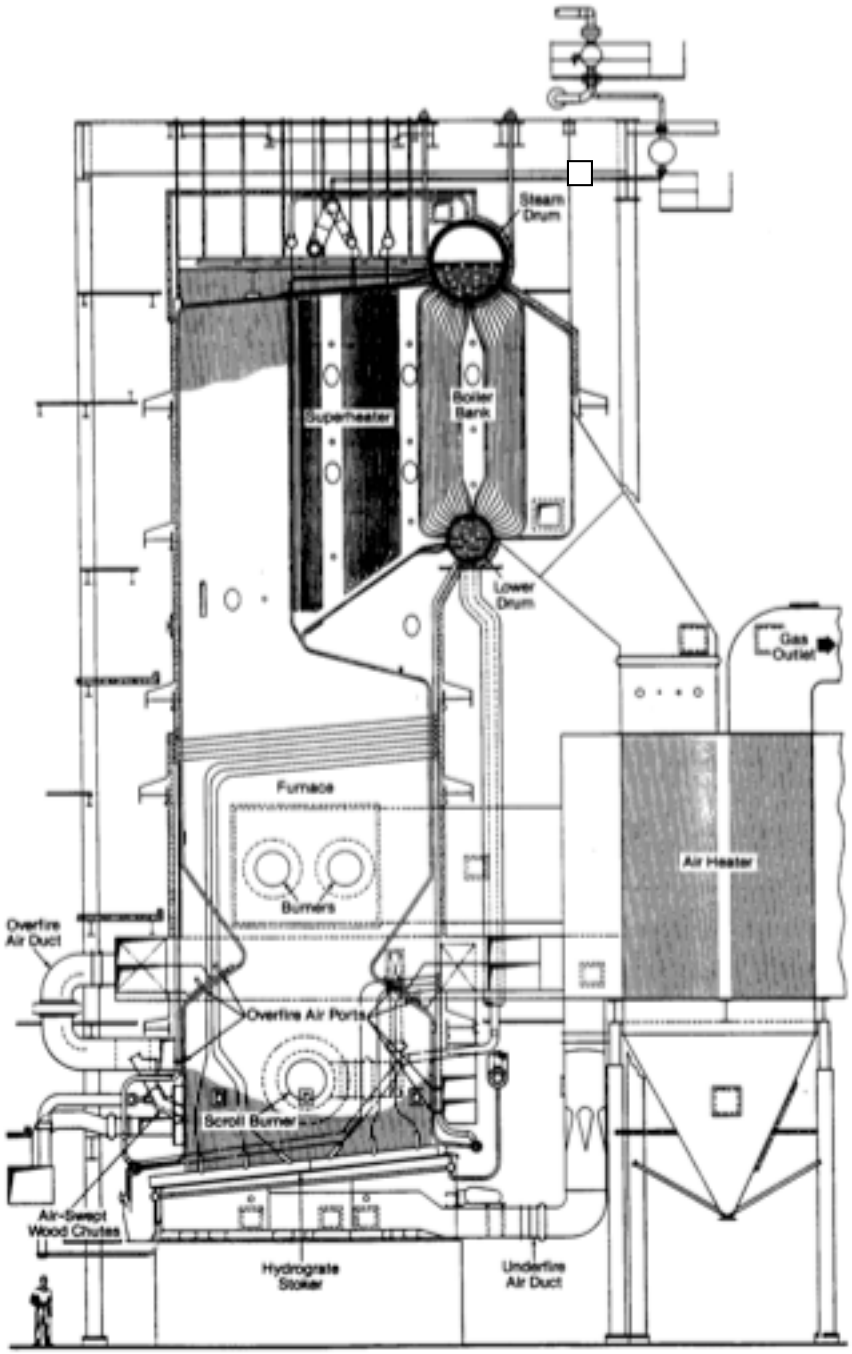

Figure 5B. Schematic central boiler stack of commercial biomass traveling grate plant.

3.2. University of California Fluidized Bed Combustor Experiments

Combustion tests using wood and rice straw blends were conducted in an atmospheric laboratory scale fluidized bed combustor (FBC) (Figure 6). The main combustor consists of a stainless cylindrical reactor tube surrounded by an insulated electric heater utilized for preheating. A distributor nozzle at the base of the reactor supplies electrically preheated air and fluidizes the bed. The bed material is refractory mullite sand. Fuel is supplied to the bed near the bottom of the reactor through a high-speed auger and a variable speed belt. The reactor tube is connected to a disengagement zone for internal recirculation of bed material. Connected to the disengagement zone is a horizontal pass that is equipped with an ash dropout. Another ash dropout trap is placed down-stream after passing through a cyclone for separation of larger fly ash particles.

Figure 6A. The laboratory scale fluidized bed combustor at University of California, Davis. This combustor was used by Thy et al. (2004) for controlled experiments that provided fly ash samples for the present study.

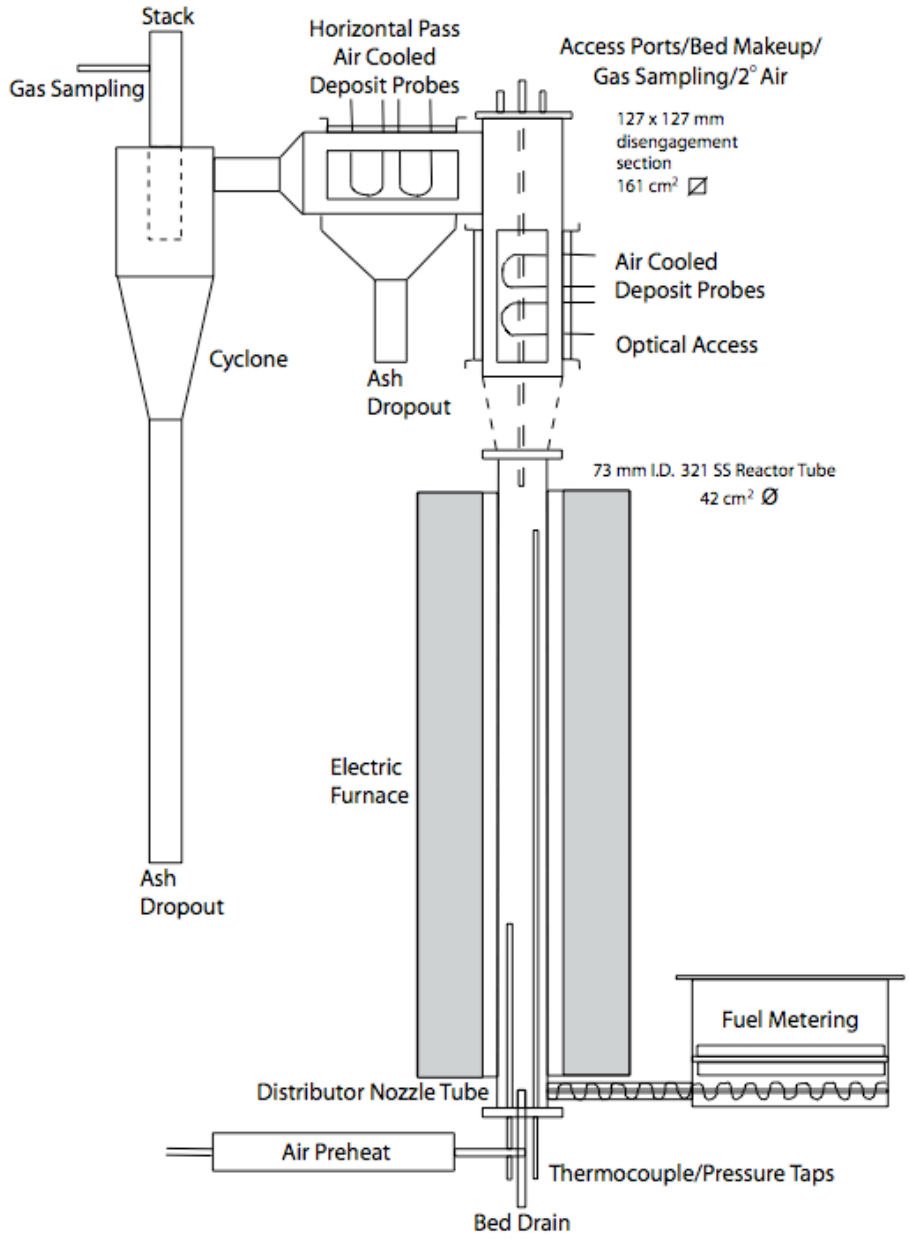

Figure 6B. Technical drawing of the laboratory scale fluidized bed combustor at University of California, Davis. (see Figure 6A).

The FBC experiments that supplied fly ash for the present study (Table 3) were conducted using either a 2.4 % rice straw and 97.6 % mixed conifer (FBC-3), 100 % mixed conifer (FBC-5), or 10.7 % leached rice straw and 89.3 % mixed conifer (FBC-6) blends (all wet fuel proportions). A 1000 ^{o}C target wall temperature controlled the combustion. Experimental duration varied between 4 and 6 hours. All fly ash was collected after the cyclone pass. A summary of the fuel compositions is given in Table 5. The basic fuel types (wood, rice straw, and leached rice straw)

are included in the present study and in part similar to the fuels and ashes used in the main experimental part of this study (Table 1).

Table 5. Fuels Used in Fluidized Bed Combustor Experiments in 2003

	Wood	Rice Straw	Leached Rice Straw*	2.4 % Rice Straw	9.6 % Rice Straw	10.7 % Leached Rice Straw
Ultimate Analysis (%, dry basis)				Calculated	Calculated	Calculated
Carbon	53.0	38.5	38.0	52.7	51.6	51.4
Hydrogen	5.7	3.6	4.7	5.6	5.5	5.6
Nitrogen	0.1	0.6	0.6	0.1	0.1	0.1
Sulfur	0.0	0.1	0.1	0.0	0.0	0.0
Ash (%, dry basis)	1.2	22.1	22.0	1.7	3.2	3.4
Chlorine	0.01	0.65	0.00	0.03	0.07	0.01
Ash Analysis (% oxides, volatile free)						
SiO_2	14.01	82.13	85.27	15.64	20.55	21.63
TiO_2	0.19	0.01	0.26	0.19	0.17	0.20
Al_2O_3	4.68	0.10	4.51	4.57	4.24	4.66
Fe_2O_3	1.71	0.11	2.51	1.67	1.56	1.80
MnO**	2.64	0.29	*0.30*	2.58	2.41	2.39
MgO	7.39	1.79	1.70	7.26	6.85	6.78
CaO	48.05	1.74	2.55	46.94	43.60	43.18
Na_2O	0.58	0.15	0.03	0.57	0.54	0.52
K_2O	16.06	13.02	2.06	15.99	15.77	14.56
P_2O_5	4.69	0.66	0.81	4.59	4.30	4.27
Total	100.00	100.00	100.00	100.00	100.00	100.00

The ash analyses were done on ash produced at 525°C. Ash composition determined at University of Aarhus by XRF. The wood and rice straw compositions are from Table 1.
* From Bakker et al. (2002, table 1). Ash content was determined at 575°C.
** MnO has when given in italics been estimated based on the present data.

3.3. Additional Utilized Ashes

A few fuel ashes (Table 3) that were not part of the experimental ashing study were also included in the present study of trace element compositions principally because their major element and physical characteristics are well known from previous studies (Urban Wood, HEL-A, and EER; Table 6). The 'Urban Wood' ash was used by Thy et al. (1999) in a study of high temperature phase relations and potassium volatilization. This relatively pure wood fuel was obtained in 1994 from the same operating biomass power plant as used for the commercial plant experiment discussed above. The

'HEL-A' rice straw ash represents a California medium-grain (M-202) rice variety and was studied by Jenkins et al. (2003). The 'EER' rice straw ash were included in a gasification experiment by Meister et al. (2005; their sample 'RSF') and were from Sutter County, California. The ash identified as 'CFM' represents a typical Californian feed lot cattle manure and is likewise included despite not having previously been extensively studied. The existing ultimate analyses of these fuels are summarized in Table 6.

Table 6. Compositions of Additional Fuels and Ashes

	Urban Wood (1)	HEL-A (2) Rice Straw	ERR (3) Rice Straw
Ultimate Analysis (% dry matter)			
Carbon		41.95	38.5
Hydrogen		4.18	3.56
Nitrogen		0.69	0.55
Sulfur		0.11	0.06
Ash		16.1	21.03
Chlorine		0.63	0.58
Ash Content (wt. % oxides)			
SiO_2	30.18	69.72	76.36
TiO_2	0.72	0.04	0.05
Al_2O3	7.47	0.61	0.99
Fe_2O_3	4.68	0.41	0.31
MnO	0.26		
MgO	4.97	2.58	1.71
CaO	19.23	3.15	2.17
Na_2O	3.58	1.55	0.3
K_2O	5.9	16.55	11.9
P_2O_5	2.42	2.48	1.55
SO_3	3.26	0.88	0.67
CO_2		0.35	0.22
Cl	0.74	2.98	2.39

1. Urban Wood fuel obtained from Woodland Biomass in 1994. The ash was used by Thy et al. (1999).
2. Medium-grain California rice straw fuel. From Jenkins et al. (2003).
3. Sutter County, California, rice staw. From Meister et al. (2005). Referred to in the original paper as 'RSF.'

4. Analytical Techniques

Representative samples were taken from the powders prepared from the ashes and slag as listed in Tables 2 and 3. The major and minor elements were analyzed using X-ray fluorescence at the University of Aarhus, Denmark. The trace elements were analyzed at the University of California, Davis and its affiliated McClellan Nuclear Radiation Center using instrumental neutron activation and inductively coupled plasma mass spectroscopy. This section briefly reviews analytical procedures together with precision and accuracy.

4.1. X-Ray Fluorescence Spectroscopy

Loss on ignition was determined by heating the powder in air in a muffle furnace at 950 °C for 3 hours. Fused glasses were prepared by mixing an amount of unheated powder equivalent to 0.75 g of ignited sample with 3.75 g of Fluore-X65 HP (a commercial flux from Socachim Fine Chemicals consisting of 66 wt. % $Li_2B_4O_7$ and 34 wt. % $LiBO_2$) in a 30 ml 95Pt-5Au crucible. The crucible was transferred to a muffle furnace and the contents melted 5 minutes twice at 1150 °C with swirling of the crucible between melting. After fusion, the melt was poured into a red-hot, 32 mm 95Pt-5Au mould and quenched with air to produce a flat glass disc.

The analyses were performed on a PANalytical PW2400 X-ray spectrometer using SuperQ software. A 3 kW Rh-tube was used operating at 50 kV and 55 mA along with PX-1 multilayer for Na and Mg, PE crystal for Al and Si, Ge crystal for P, LiF(200) crystal for K, Ca and Ti and LiF(220) crystal for Mn and Fe. The detector was a gas flow proportional counter using P10 (10% methane in Ar) gas. For Mn and Fe, this detector was used in tandem with a sealed Xe detector.

A total of 44 international silicate rock reference materials, with compositions ranging from basaltic to rhyolitic, were used for the calibrations (Govindaraju, 1994, 1995; Jochum et al., 2005). Fly ash NIST 1633a (Rasberry, 1985) was prepared and analyzed in the same way as the

unknown ashes. The results are given in Table 7 together with the recommended values from Jochum et al. (2005). Typical uncertainties for wood and straws are also given in Table 7.

Table 7. X-Ray Fluorescence Spectroscopy: Analytical Results and Uncertainties

Oxide	NIST 1633a Wt. %	NIST 1633a Recommended	NIST 1633b Recommended	Wood Ash	Wheat Straw Ash	Rice Straw Ash
SiO_2	50.24	48.78	49.24			
TiO_2	1.40	1.33	1.32			
Al_2O_3	27.97	27.02	28.44			
Fe_2O_3	14.10	13.44	11.12			
MnO	0.023	0.023	0.017			
MgO	0.82	0.75	0.80			
CaO	1.60	1.55	2.11			
Na_2O	0.22	0.23	0.27			
K_2O	2.31	2.26	2.35			
P_2O_5	0.40	0.38	0.527			
Total	99.10	95.76	96.19			
Standard Deviation						
SiO_2	0.18			0.09	0.21	0.23
TiO_2	0.028			0.009	0.006	0.003
Al_2O_3	0.18			0.07	0.03	0.011
Fe_2O_3	0.14			0.05	0.03	0.010
MnO	0.001			0.012	0.002	0.005
MgO	0.03			0.08	0.04	0.04
CaO	0.03			0.17	0.05	0.04
Na_2O	0.02			0.03	0.04	0.02
K_2O	0.03			0.05	0.07	0.05
P_2O_5	0.012			0.037	0.020	0.015

Uncertainty calculated from standard calibration curves.
NIST 1633a (Cali, 1975; Rasberry, 1985) and 1633b (Gills, 1993) recommended values compiled by Jochum et al. (2005) and taken from http://georem.mpch-mainz.gwdg.de/.

4.2. Instrumental Neutron Activation Analysis

Instrumental Neutron Activation Analysis (INAA) was performed using a TRIGA-type nuclear reactor at UC Davis' McClellan Nuclear Radiation Center. About 50 to 250 mg of sample powder was heat-sealed in a 1.8 mL polyethylene vial. Standard Reference Materials NIST 1633b (coal fly ash), 278 (obsidian), and 688 (basalt) together with reagent grade KCl were also prepared in the same manner as the unknown samples. Unknowns and standards were first

irradiated with a thermal neutron flux of ~ 8×10^{12} n cm^{-2} s^{-1} for 10 seconds (Table 8, Short). During the decay period of 20 to 60 min, delayed gamma ray was counted for 2000 seconds using a Genie-2000/Apex gamma-ray spectroscopy system from Canberra Industries Inc. (Meriden, CT). Four detectors of the system were all co-axial, high-purity germanium detectors, whose energy resolution ranged between 1.8 and 2.4 keV for ^{60}Co peak at 1332 keV. Gamma-ray spectra of this acquisition included short-lived isotopes such as ^{24}Na, ^{38}Cl, ^{42}K, ^{56}Mn, ^{87m}Sr, ^{139}Ba, and ^{165}Dy.

Following complete decay after the first irradiation, unknowns and standards were again irradiated with a thermal neutron flux of ~ 4×10^{11} n cm^{-2} s^{-1} for 8 hours (Table 8, Long). During this irradiation, pure Ni wire, as an additional standard, was attached to the outside of the vials for standard NIST 688. Gamma ray assay was carried out twice (i.e., 2000 seconds acquisition during a decay period of 4.8 to 6.8 days and 8 to 12 hours acquisition during a decay period of 12 to 28 days) to detect long-lived isotopes such as ^{46}Sc, ^{51}Cr, ^{58}Co (to determine Ni), ^{59}Fe, ^{60}Co, ^{65}Zn, ^{85}Sr, ^{86}Rb, ^{95}Zr, ^{131}Ba, ^{134}Cs, ^{140}La, ^{141}Ce, ^{153}Sm, ^{152}Eu, ^{147}Nd, ^{160}Tb, ^{169}Yb, ^{175}Yb, ^{177}Lu, ^{181}Hf, ^{182}Ta, ^{233}Pa (to determine Th), and ^{239}Np (to determine U). The half-life of ^{233}Th and ^{239}U are 22.3 min and 23.5 min, respectively, so that almost all ^{233}Th and ^{239}U formed by irradiation are considered to have decayed into ^{233}Pa and ^{239}Np before counting started.

A summary of analyzed elements together with principal techniques (nuclide and short or long irradiation) and typical uncertainties for straw and wood ashes is given in Table 8. In short and long irradiations, unknowns and each standard material were irradiated at four and three vertical levels, respectively. For quantification, unknowns and standards irradiated at the same level were compared to cancel out the vertical gradient in neutron flux. To calculate the slope of the calibration curve, decay corrected activity of a reference material that has the highest concentration of an analyte element was adopted because of the lowest uncertainty. The activity of the other references was used to evaluate the result of calibration. The concentration data for NIST reference standards were taken from Roelandts and Gladney (1998). Table 9 summarizes the result of the evaluation, in which the results are average of four or three irradiation levels, depending on irradiation length.

For unknowns, elements that typically could be detected are the major and minor elements Na, K, Fe, and Cl (wt.%) with uncertainties mostly below 3 %; transition elements Sc, Cr, Mn, and Co (ppm) with uncertainties below 8 %; and alkali elements and metals Rb, Cs, and Ba (ppm) with uncertainties below 13 %. The elements Ta and Th were occasionally present, but were detected with uncertainties above 8 %. Other elements were either undetected or had relative standard deviation above 15 % also considered undetected despite that peaks could be seen. The undetected elements included most of the rare earth elements (except for some of the wood ashes). Other elements not detected include Ni, Sr (except for wood ash), and U.

Table 8. Instrumental Neutron Activation Analyses: Uncertainties

Z	Symbol	Irraditation Duration	Nuclide	Energy (keV)	Unit for Concentration	Rice Straw Ash RSD %	Wheat Straw Ash RSD %	Wood Ash RSD %
11	Na	Short	Na-24	1368.6	%	3.07	1.02	2.77
17	Cl	Short	Cl-38	1642.7	%	2.1	0.79	nd
19	K	Short	K-42	1524.7	%	2.28	1.51	4.69
21	Sc	Long	Sc-46	889.3	ppm	4.47	1.65	1.35
24	Cr	Long	Cr-51	320.1	ppm	6.79	4.77	2.68
25	Mn	Short	Mn-56	1810.7	ppm	0.83	1.20	0.67
26	Fe	Long	Fe-59	1099.2	%	7.86	3.48	2.52
27	Ni	Long	Co-58	810.8	ppm	nd	nd	nd
27	Co	Long	Co-60	1332.5	ppm	4.89	4.29	4.21
37	Rb	Long	Rb-86	1076.6	ppm	6.38	8.55	6.30
38	Sr	Short	Sr-87m	388.4	ppm	nd	nd	12.05
55	Cs	Long	Cs-134	795.9	ppm	11.53	12.60	7.90
56	Ba	Long	Ba-131	496.3	ppm	12.09	7.39	4.15
57	La	Long	La-140	1596.5	ppm	nd	11.71	7.87
58	Ce	Long	Ce-141	145.4	ppm	nd	nd	8.33
60	Nd	Long	Nd147	91.1	ppm	nd	nd	nd
62	Sm	Long	Sm153	103.2	ppm	nd	12.72	7.42
63	Eu	Long	Eu-152	1408.0	ppm	nd	nd	5.13
65	Tb	Long	Tb-160	879.4	ppm	nd	nd	nd
66	Dy	Short	Dy-165	94.7	ppm	nd	nd	nd
70	Yb	Long	Yb-169	177.2	ppm	nd	nd	nd
71	Lu	Long	Lu-177	208.4	ppm	nd	nd	6.83
72	Hf	Long	Hf-181	482.2	ppm	nd	nd	1.42
73	Ta	Long	Ta-182	1221.4	ppm	9.07	13.30	8.09
90	Th	Long	Pa-233	312.0	ppm	nd	14.67	8.30
92	U	Long	Np-239	277.6	ppm	nd	nd	nd

RSD %, relative standard deviation.
nd, not detected or with uncertanty above 15 %.

Table 9. Comparison of Results of NIST Standard Reference Materials.

Symbol	Unit for Conc.	NIST 1633b			NIST 278			NIST 688			Alternative Standard Material
		Reported value	This Analysis conc.	This Analysis s.d.	Reported Value	This Analysis conc.	This Analysis s.d.	Reported Value	This Analysis conc.	This Analysis s.d.	
Na	%	0.201	0.21	0.01	3.59	> STD		1.58	1.60	0.04	
Cl	%	0.06	not detected		---	not detected		---	not detected		KCl
K	%	1.95	2.39	0.04	3.46	4.15	0.18	0.175	not detected		KCl
Sc	ppm	41	> STD		4.9	5.30	0.09	36.4	37.61	0.52	
Cr	ppm	198.2	197.48	3.66	6.4	8.83	0.69	321	> STD		
Mn	ppm	131.8	134.49	2.58	396	375.44	6.55	1250	> STD		
Fe	%	7.78	> STD		1.45	1.49	0.04	7.2	7.27	0.09	
Ni	ppm	120.6	not detected		7	not detected		150	not detected / POND		Ni wire
Co	ppm	49	> STD		1.76	1.70	0.13	48	49.14	0.95	
Rb	ppm	142	> STD		130	133.92	12.99	2.7	not detected		
Sr	ppm	1041	> STD		63	not detected		169	not detected		
Cs	ppm	10.6	> STD		5.2	5.23	0.60	0.2	not detected		
Ba	ppm	709	733.03	79.41	960	> STD		191	not detected / POND		
La	ppm	90	> STD		32	31.96	0.92	5.2	5.21	0.37	
Ce	ppm	188	> STD		62	66.61	1.23	12.1	12.56	1.30	
Nd	ppm	84	> STD		29	31.06	2.35	8.1		POND	
Sm	ppm	19	> STD		5.9	6.09	0.11	2.37	2.43	0.09	
Eu	ppm	4.0	> STD		0.78	0.87	0.06	0.99	1.02	0.02	
Tb	ppm	2.6	> STD		1.02	1.01	0.18	0.5	not detected / POND		
Dy	ppm	16.6	> STD		6.2	6.40	0.39	3.2	3.35	0.21	
Yb	ppm	7.5	> STD		4.7	4.68	0.34	2.02	1.98	0.45	
Lu	ppm	1.1	> STD		0.76	0.74	0.02	0.316	0.35	0.09	
Hf	ppm	6.8	6.89	0.42	8.4	> STD		1.54	1.65	0.29	
Ta	ppm	1.8	> STD		1.3	1.46	0.08	0.275	not detected / POND		
Pa	ppm	25.7	> STD		12.4	13.09	0.37	0.31	not detected / POND		
Np	ppm	8.79	> STD		4.56	not detected / POND		0.32	not detected		

Results by short and long irradiations are the average of four and three values, respectively.
Reported values were taken from Roelandts and Gladney (1998).
POND stands for peak observed, but not determined.

4.3. Inductively Coupled Plasma Mass Spectroscopy

Trace elements were determined using an inductively coupled plasma mass spectrometer (ICP-MS) at the Interdisciplinary Center of Plasma Mass Spectrometry at University of California, Davis. About 500 mg of homogenized powdered samples was dried in an oven overnight at 105 ^{o}C. Unknown samples and working standard were digested using a slightly modified procedure described by CEM microwave sample preparation note # OS-6 for coal fly ash (http://www.cem.com/analytical/refpapers_dig.asp). Nearly 250 mg of each powder was weighted and transferred to a microwave digestion vessel containing 7mL of reagent grade nitric, 1.0 mL of hydrochloric acid, and 1.5 mL hydrofluoric acid. Each batch for analysis used a total of 12 vessels: one vessel was used for a blank, one for the working standard, and ten for unknown samples.

The solutions were microwaved three times, each of 25-minutes at 55 % power, using a CEM 205 microwave digestion system. At the end of the third run, each vessel received 7.5 mL of boric acid and was microwaved again for 10 minutes at 55 % power. Once the samples cooled, the solutions were transferred into 125 mL vessels and diluted 500 fold using Milli-Q deionized water. An aliquot of each solution was spiked with 1 mL of an internal standard containing Sc, Ge, Y, In, and Bi, which was used to monitor instrumental drift.

Solutions were analyzed using an Agilent 7500a quadrupole ICP-MS. Daily tuning ensured the highest sensitivity and lowest variability (RSD > 2%) using a 10 ppb solution that contains Li, Cr, Y, Ce, and Tl. The production of ionized oxides (mass ratio 156/140) and doubly charged ions (mass ratio 70/140) were reduced to less than 1% and ~2%, respectively. External calibration was completed using ICP-MS multi-element standards (Fisher brand SPEX standards: https://www1.fishersci.com/Search?t=r&key=ICPMS+calibration+SPEX), which were diluted in a series from 0.5 to 1000 parts per billion (ppb). Calibration curves were always linear (r = 0.9995 or better) and instrument detection limits were based on the calibration blank (3 times the standard deviation of the count at the zero concentration level).

The NIST 1633a fly ash standard material (Cali, 1975; Newberry, 1985) was the appropriate working standard and was repeatedly analyzed as an unknown (n=8). The precision and accuracy for this working standard is listed in Table 10. The recommended values for this standard were complied by Jochum et al (2005) and were retrieved from GeoReM (2006). The recovery for NIST 1633a was found to be reasonable for all elements except for Ag. Also given in Table 10 is the relative standard deviations obtained for the main groups of ashes analyzed in this study (rice straw, wheat straw, and wood).

Table 10. Inductively Coupled Plasma Mass Spectroscopy: Accuracy and Precision.

Z	Element	Nuclide	Blank Average (N=6) ppm	Blank RSD %	Detection Limit ppb	NIST 1663a Average (N=8) ppm	NIST 1663a RSD %	NIST 1663a Accepted	NIST 1663a Recovery %	Wood Ash RSD %	Wheat Straw Ash RSD %	Rice Starw Ash RSD %
4	Be	9	0.23	23.56%	0.034	11.17	2.16%	12	93%	13.73%	16.65%	28.94%
23	V	51	0.35	2.85%	0.013	300.16	1.83%	297	101%	3.33%	3.54%	2.35%
24	Cr	53	0.76	4.01%	0.150	185.22	1.38%	196	94%	2.82%	2.97%	2.13%
25	Mn	55	0.10	5.14%	0.053	184.80	1.40%	179	103%	3.07%	3.35%	2.56%
27	Co	59	-0.03	25.38%	0.014	43.71	1.56%	46	95%	3.71%	3.04%	2.86%
28	Ni	60	0.14	10.85%	0.013	120.51	1.46%	127	95%	2.76%	3.44%	1.97%
29	Cu	63	0.08	6.94%	0.213	114.79	1.19%	118	97%	2.78%	3.07%	2.17%
30	Zn	66	1.11	5.54%	0.064	224.49	1.57%	220	102%	2.70%	3.47%	1.98%
33	As	75	0.65	6.31%	0.024	147.01	1.29%	145	101%	4.17%	5.23%	2.07%
34	Se	82	0.02	2.41%	0.615	12.24	2.85%	10.1	121%	10.67%	6.75%	7.38%
37	Rb	85	0.00	3.14%	0.026	141.33	1.23%	131	108%	2.62%	3.39%	2.48%
38	Sr	88	0.03	12.73%	0.021	919.53	2.79%	830	111%	2.24%	3.11%	2.61%
40	Zr	90	0.08	24.32%	0.003	256.11	1.84%	310	83%	2.99%	2.65%	10.69%
47	Ag	107	0.01	20.99%	0.023	0.61	2.02%	0.076	802%	4.62%	6.13%	8.96%
48	Cd	111	0.01	2.75%	0.042	1.07	2.47%	1.0	107%	2.38%	4.55%	7.63%
50	Sn	118	0.06	13.89%	0.071	7.45	1.66%	9	83%	3.26%	4.45%	6.70%
51	Sb	121	0.03	16.53%	0.014	7.56	2.33%	6.8	111%	3.84%	3.14%	4.52%
55	Cs	133	0.00	13.29%	0.029	12.78	2.65%			4.76%	2.62%	3.94%
56	Ba	137	0.12	2.55%	0.056	1541.50	1.28%	1500	103%	2.14%	2.64%	2.07%
57	La	139	-0.06	6.88%	0.001	80.12	1.63%	83	97%	3.27%	2.50%	2.79%
58	Ce	140	-0.06	14.91%	0.002	186.64	1.74%	170	110%	2.94%	2.78%	2.34%
59	Pr	141	-0.05	22.56%	0.001	22.69	1.56%			4.19%	3.58%	4.24%
60	Nd	146	0.05	23.89%	0.006	91.69	1.56%	77	119%	3.80%	2.80%	5.74%
62	Sm	147	0.03	23.06%	0.003	19.50	2.23%	16.7	117%	7.28%	4.52%	10.02%
63	Eu	153	-0.10	22.61%	0.002	3.46	1.64%	3	115%	4.85%	5.09%	8.76%
64	Gd	157	0.00	31.52%	0.006	17.37	2.18%	16	109%	22.55%	5.18%	12.14%
65	Tb	159	-0.03	25.50%	0.001	2.47	1.94%	2.4	103%	9.41%	5.87%	12.67%
66	Dy	163	-0.01	29.05%	0.007	16.10	1.95%	15.3	105%	6.88%	4.37%	10.05%
67	Ho	165	-0.10	27.48%	0.001	2.82	1.72%	2.8	101%	9.57%	5.40%	10.24%
68	Er	166	0.02	30.34%	0.002	11.36	2.01%			8.12%	4.55%	8.92%
69	Tm	169	0.01	20.56%	0.001	1.60	1.92%	1.8	89%	12.80%	8.30%	12.93%
70	Yb	172	-0.02	35.49%	0.004	7.86	2.09%	7.6	103%	7.43%	4.74%	9.12%
71	Lu	175	-0.01	22.99%	0.001	1.22	2.30%	1.12	109%	15.00%	6.58%	14.12%
72	Hf	178	0.08	41.13%	0.005	6.90	1.52%	8	86%	4.24%	5.00%	10.25%
73	Ta	181	0.15	20.04%	0.002	2.18	1.64%			4.10%	3.68%	4.38%
74	W	182	0.01	36.24%	0.002	6.45	1.51%	6	108%	2.42%	4.22%	4.38%
81	Tl	205	-0.01	30.31%	0.014	5.21	1.83%	5.7	93%	10.08%	16.07%	17.99%
82	Pb	208	0.00	18.17%	0.042	66.91	3.61%	72.4	92%	2.63%	3.04%	1.94%
90	Th	232	-0.07	11.34%	0.002	25.16	2.16%	24.7	102%	8.49%	3.73%	6.62%
92	U	238	0.00	10.72%	0.027	8.98	1.84%	10.2	88%	9.45%	4.31%	3.67%

RSD % - Relative standard deviation in percentages.
ppm - parts per million weight basis.
ppb - parts per billion weight basis.

Table 11. XRF Analyses of Ash Heated to 950 oC (wt. % Oxides)

ID	T (oC)	Loss %	SiO2 XRF	TiO2 XRF	Al2O3 XRF	Fe2O3 XRF	MnO XRF	MgO XRF	CaO XRF	Na2O XRF	K2O XRF	P2O5 XRF	LOI	Cl INA	K2O INA	Na2O INA	Fe2O3 INA	Sum	Sum O=Cl
Wood																			
WO-8	1525		12.90	0.15	4.28	1.51	2.36	7.73	47.82	0.53	5.51	4.50	9.33	nd	8.20	0.332	1.379	99.30	99.30
WO-10	1425	36.2	13.82	0.17	4.66	1.63	2.58	7.83	49.71	0.52	5.09	4.95	6.39	nd	6.91	0.368	1.527	99.18	99.18
WO-7	1325	32.6	13.56	0.17	4.48	1.59	2.47	7.48	48.04	0.60	5.65	4.74	8.24	nd	7.56	0.373	1.548	98.93	98.93
WO-9	1225		12.19	0.16	4.23	1.52	2.42	7.03	45.52	0.61	9.19	4.51	8.74	nd	10.59	0.389	1.322	97.52	97.52
WO-6	1125	27.5	12.36	0.15	3.95	1.46	2.26	6.54	42.33	0.64	11.00	4.21	11.42	nd	14.56	0.519	1.372	99.87	99.87
WO-1	1011	27.3	12.65	0.16	3.99	1.46	2.15	6.20	40.30	0.72	10.93	4.00	13.67	nd	11.57	0.357	1.161	96.87	96.87
WO-5	913	25.2	13.38	0.15	3.84	1.40	2.12	6.09	39.95	0.66	11.28	3.99	13.33	nd	12.89	0.379	1.233	97.80	97.80
WO-4	816	21.9	14.42	0.15	3.81	1.34	2.07	6.04	39.41	0.68	10.97	3.87	13.94	nd	14.76	0.400	1.112	100.49	100.49
WO-3	718	9.9	10.77	0.13	3.45	1.23	1.95	5.67	36.37	0.62	10.06	3.58	22.94	nd	13.25	0.382	1.151	99.96	99.96
WO-2	621	4.2	10.05	0.12	3.28	1.19	1.85	5.44	34.77	0.58	9.41	3.42	26.73	nd	12.79	0.380	1.156	100.22	100.22
WO-S	524		10.48	0.12	3.21	1.35	1.82	5.33	34.14	0.56	9.14	3.37	27.59	nd	13.54	0.394	1.293	101.50	101.50
Wheat Straw																			
WH-5	962	18.5	68.65	0.06	1.00	0.52	0.08	2.19	3.27	1.13	14.98	1.19	4.75	2.82	19.63	0.917	0.503	102.47	101.84
WH-4	913	16.3	68.47	0.05	0.94	0.47	0.08	2.17	3.26	1.11	14.84	1.17	5.27	3.39	20.60	0.835	0.472	103.59	102.83
WH-6	864	15.5	68.50	0.06	1.05	0.51	0.08	2.14	3.20	1.15	14.61	1.12	5.25	3.55	19.83	0.827	0.541	102.88	102.08
WH-3	816	14.5	67.56	0.06	0.97	0.49	0.08	2.16	3.22	1.28	15.44	1.17	4.92	4.01	20.97	0.828	0.499	102.88	101.97
WH-7	767	13.8	68.28	0.06	0.97	0.48	0.08	2.12	3.19	1.29	15.63	1.12	3.51	4.28	20.84	0.799	0.494	101.93	100.97
WH-2	718	13.9	66.84	0.05	0.84	0.44	0.08	2.11	3.21	1.36	16.58	1.16	3.32	4.34	20.83	0.819	0.403	100.24	99.26
WH-8	670	12.5	68.00	0.06	0.98	0.50	0.08	2.10	3.20	1.35	15.23	1.10	4.17	4.32	20.55	0.807	0.486	102.08	101.11
WH-1	621	12.1	65.55	0.05	0.82	0.41	0.07	2.07	3.11	1.26	15.41	1.12	6.94	4.30	20.53	0.797	0.366	101.94	100.97
WH-9	572	10.5	65.89	0.06	0.96	0.50	0.07	2.00	3.04	1.27	14.57	1.05	7.26	4.09	19.17	0.785	0.421	101.27	100.34
WH-S	524		60.25	0.05	0.80	0.43	0.07	1.91	2.92	1.30	13.49	1.09	14.91	3.72	18.31	0.693	0.375	102.04	101.20
Rice Straw																			
R-13	1325		84.44	0.01	0.32	0.12	0.39	2.02	2.35	0.51	8.58	0.49	0.59	0.34	10.80	0.175	0.137	102.03	101.96
R-12	1225	14.6	84.30	0.02	0.31	0.12	0.39	2.02	2.36	0.52	8.84	0.65	0.28	nd	11.38	0.156	0.115	102.35	102.35
R-11	1125	14.0	83.56	0.01	0.17	0.11	0.39	2.02	2.35	0.44	9.15	0.68	0.71	0.04	10.78	0.165	0.069	101.22	101.21
R-10	1011	10.6	80.69	0.02	0.12	0.13	0.37	1.95	2.24	0.54	9.01	0.67	2.85	1.77	13.58	0.201	0.096	103.16	102.76
R-5	962	9.6	79.78	0.02	0.13	0.12	0.37	1.93	2.21	0.55	8.93	0.66	3.98	2.28	12.25	0.189	0.091	102.00	101.49
R-4	913	8.7	78.93	0.02	0.13	0.10	0.37	1.91	2.20	0.57	8.89	0.66	4.65	2.85	13.84	0.165	0.088	103.39	102.74
R-6	864	8.1	78.70	0.02	0.12	0.10	0.37	1.90	2.20	0.57	9.01	0.65	4.82	2.97	14.00	0.173	0.109	103.45	102.78
R-3	816	7.7	78.35	0.02	0.13	0.10	0.36	1.89	2.19	0.54	8.88	0.65	5.35	3.14	14.47	0.181	0.111	104.05	103.34
R-7	767	7.3	77.73	0.02	0.12	0.11	0.37	1.88	2.16	0.53	9.01	0.65	5.85	3.32	14.68	0.173	0.100	104.10	103.35
R-2	718	7.0	77.28	0.02	0.13	0.10	0.36	1.85	2.16	0.54	8.94	0.64	6.59	3.38	13.99	0.164	0.090	103.66	102.90
R-8	670	6.1	76.67	0.02	0.11	0.09	0.36	1.84	2.12	0.56	8.89	0.64	7.18	3.25	12.84	0.167	0.071	102.43	101.69
R-1	621	5.7	76.31	0.02	0.12	0.10	0.35	1.82	2.09	0.51	9.20	0.63	7.18	3.46	13.54	0.151	0.081	102.67	101.89
R-9	572	5.5	75.51	0.02	0.12	0.10	0.35	1.82	2.13	0.54	9.01	0.64	7.95	3.43	13.67	0.161	0.089	102.85	102.08
R-S	524		73.30	0.02	0.11	0.10	0.34	1.76	2.02	0.52	8.57	0.61	10.94	3.20	13.17	0.144	0.186	102.89	102.17

Oxides given as weight %, Chloride in atomic weight %. Oxides are determined by X-ray fluorescence (XRF) or instrumental neutron activation (INA). Cl was only determined by XRF.
Loss % is the percentage weight loss during firing. All iron is calculated as Fe2O3. LOI is the weight loss of ignition at 950 oC.
Sum is calculated using K2O determined by INA. Sum (O=Cl) is the sum corrected for oxygen equivalent of chlorine.

5. Ash and Slag Results

This section presents the ash compositions using existing information together with the new analytical results. All analytical data are summarized in tables keyed to the relevant text, however, the complete results are included as Excel spreadsheets available from http://www.geology.ucdavis.edu/~thy/ or by contacting the senior author.

The analytical results are all reported on a weight percentage basis. The major and minor elements are reported as the oxides SiO_2, TiO_2, Al_2O_3, Fe_2O_3, MnO, MgO, CaO, Na_2O, K_2O, and P_2O_5. Iron is assumed to exist exclusively as Fe_2O_3. The loss-on-ignition was determined as the weight loss from firing at 950 ^oC and has not been corrected for possible oxidation of iron. However, the assumption that all iron exists as ferric iron appears reasonable considering that the ashes and slag were produced in air. Chloride is reported as percentages on an elemental basis. The trace elements are reported as parts per million (ppm) also on an elemental basis.

The sum of the individual components measured in an ash is often used as a measure of the completeness and quality of an analysis by assuming that the sum of all analyzed elements should total to 100 %. For reporting purposes, the ash or slag is assumed to be composed of silicates, oxides, carbonates, and sulfates where the electropositive elements are directly bonded to oxygen (or chlorite, if present). This way oxygen is taken into account without being directly analyzed. The ash compositions are therefore conveniently expressed as oxides and the total as the sum of the individual oxides (i.e., grams per 100 grams of ash). Because chlorine is present in substantial amounts in some ashes, the totals must be corrected for the excess oxygen used to balance the positive charged elements. The other volatile components C-S-H (or CO_2, SO_2, H_2O) were not directly analyzed, but their sum is assumed to be represented by the loss-on-ignition. Because the inorganic oxides were determined on ash that was heated to 950 ^oC and also that the loss-on-ignition were determined at 950 ^oC, the analyses do not strictly represent the ashes produced at temperatures below 950 ^oC, or above.

The general analytical errors and precisions of the analyses can be evaluated from the results on NIST 1633a or 1633b fly ash standards given in Table 7 for X-ray fluorescence analyses, in

Table 9 for instrumental neutron activation analyses, and in Table 10 for inductively coupled plasma mass spectroscopy analyses.

5.1. Experimental Ashes and Slag

The compositional variation of the experimental ashes and slag as a function of temperature are examined from 524 ^{o}C to 962 ^{o}C for wheat straw, to 1325 ^{o}C for rice straw, and to 1525 ^{o}C for wood. A corresponding set of major and minor element compositions of the same ashes and slag was discussed at some length by Thy et al. (2006). The dataset utilized in this report includes major and minor elements produced by conventional X-ray fluorescence spectroscopy on a set of ashes fired at 950 ^{o}C to determine the loss-on-ignition. The discussion of Thy et al. (2006) was based on a comparative set of data also produced by X-ray fluorescence, but without firing at 950 ^{o}C. The effects on particularly potassium from whether or not the ashes were fired at 950 ^{o}C prior to analysis were discussed by Thy et al. (2005). The present discussion further utilizes new data on potassium and chloride for all ashes produced by instrumental neutron activation analysis instead of the previous available results for potassium produced by X-ray fluorescence. New neutron activation results for Na_2O and Fe_2O_3 are also available, but are not utilized for the present analyses.

The firing of the fuels was conducted in two steps. All fuels were first fired at 524 ^{o}C to eliminate most, if not all, volatile C-H-S-N components. The second step used these ashes as reactants and additionally heated them to the desired final temperatures. The elemental losses endured from ambient temperature to the basic ashing temperature of 524 ^{o}C are therefore not known. This issue was discussed at length by Thy et al. (2006) using part of the same analytical results and concluding that the elemental loss during initial ashing was minimal. They showed that potassium losses were below detection limits for both straws and the wood. Only for chloride was a small loss (~20 %) detected for wheat straw.

5.2. Mineralogical Variation

It is expected that there will be a correlation between the mineralogical contents of the ashes and their major and trace element compositions. In this section, the mineralogical compositions as a function of temperature as determined by X-ray diffraction by Thy et al. (2006b) are reviewed. The mineralogical variation is summarized in stacked X-ray diffraction diagrams with characteristic measured d-values in Ångstrom used to identify specific minerals in Figures 7 to 9.

5.2.1. Wood

The wood ash was fired at temperatures from 621 to 1425 ^{o}C without extensively melting. The experimental products are grayish brown to brown and largely unconsolidated. An unidentified bluish-green pigmentation on the surface is sometimes associated with vesicle channels and thus presumably the release of volatiles from the interior of the pellets.

The mineralogical changes as a function of temperature are summarized in Figure 7. Calcite is present to 718 ^{o}C, easily identified by the 3.017 Å diffraction peak. Larnite can be identified in products from 718 ^{o}C by a group of three diffraction peaks probably representing a larnitic phase (d=2.606, 2.696, and 2.811). Pericline can be identified in products from 816 ^{o}C by the 2.094 Å and the 1.489 Å diffraction peaks. The intensities of the larnite peaks increase with increasing temperature until 1425 ^{o}C reflecting increased recrystallized volume, while pericline peaks at 1225 ^{o}C.

These results can be compared with the high temperature melting experiments of Thy et al. (2004, 2006a) that on the same wood ash by extrapolation indicating a solidus temperature between 1347 and 1390 ^{o}C. A phosphor-containing larnite mineral and pericline coexisting with quenched melt was found in melting experiments between 1405 and 1541 ^{o}C. These experiments were unable to reach the liquidus that was estimated to be above 2000 ^{o}C. The present results suggest that the appearances of larnite and pericline commence at temperatures well below the solidus within the subsolidus range. Additional phases were not detected at or below the solidus.

Modeling using the FactSage thermochemical database (Bale et al., 2002) confirms the high liquidus temperatures of 1900-2000 ^{o}C. Carbonates break down over a wide temperature range from 500 ^{o}C and are completely eliminated at 1100 ^{o}C due to the stabilization of Na-K carbonates at high temperature. Monoxide minerals (pericline or lime) are variably stable to the liquidus. The modeling, however, fails to predict the formation of phosphor-bearing larnite that is seen in the experiments and also suggests that release of potassium is restricted to temperatures near or above the liquidus in contrast to the low temperature release observed in the experiments.

5.2.2. Rice Straw

The rice straw ash was fired at temperatures from 572 to 1325 ^{o}C well into its melting interval. Significant hardening and sintering of the pellets occurs from the starting temperature of 572 ^{o}C. Large-scale melting is apparent at 1325 ^{o}C with abundant bubble formation and pellet expansion.

The mineralogical changes as a function of temperature are summarized in Figure 8. Sylvite is conspicuously present until 1125 ^{o}C and can easily be identified by the 3.146 Å and the 2.225 Å diffraction peaks. Cristobalite appears at 767 ^{o} C identified by the 4.040 Å diffraction peak. Tridymite appears to replace cristobalite from above 1125 ^{o} C. The transformation of cristobalite into tridymite is observed by the development of the 4.328 Å and the 3.818 Å diffraction peaks. The original 4.040 Å cristobalite diffraction peak shifts toward 4.107 Å. Additional silicate phases were not detected at or below the solidus.

The same rice straw ash was melted at high temperature by Thy et al. (2004, 2006a). The melting behavior was interpreted to be strongly affected by loss of potassium. This resulted in a progressive raise in the liquidus and the coexistence of tridymite with liquid to temperatures well above the high-K_2O liquidus. Thy et al. (2000) determined the liquidus temperature for a relatively similar rice straw ash at 1074 ^{o}C again with tridymite on the liquidus.

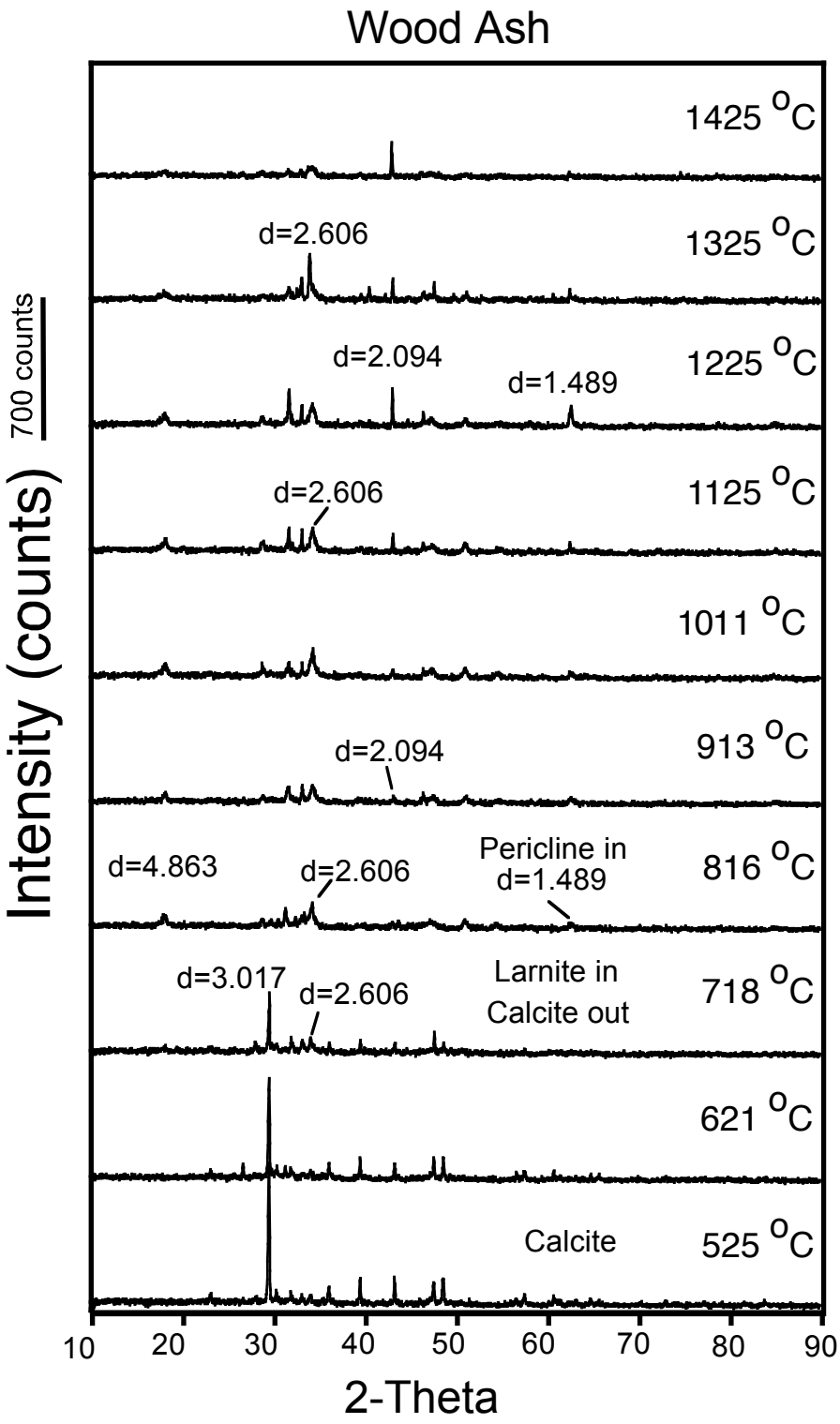

Figure 7. Summary of XRD patterns (Cu K_{α} radiation) for the wood ashes. Characteristic measured d-values in Ångstrom used to identify specific minerals (from Thy et al., 2006b).

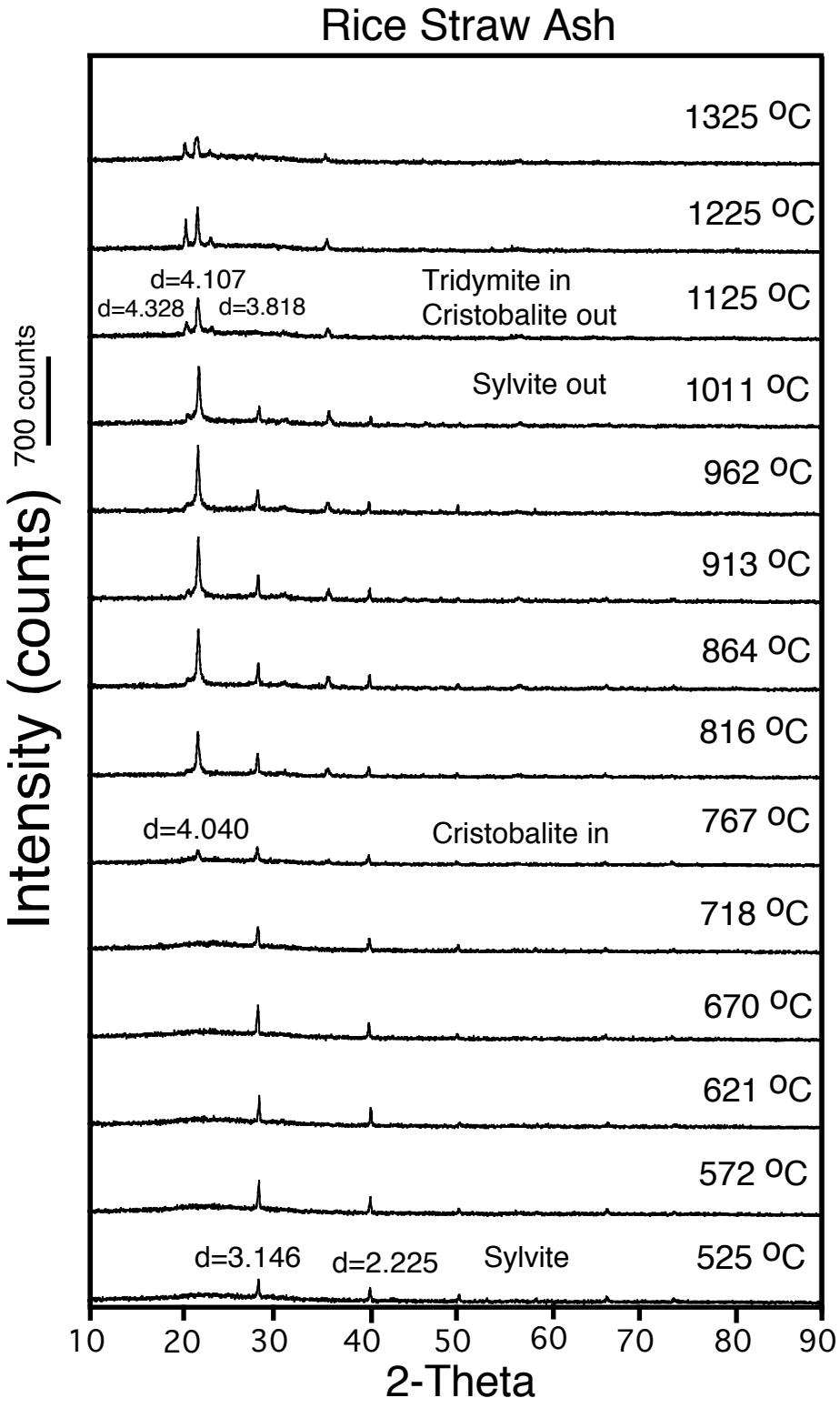

Figure 8. Summary of XRD patterns (Cu K_{α} radiation) for the rice straw ashes. Characteristic measured d-values in Ångstrom used to identify specific minerals (from Thy et al., 2006b).

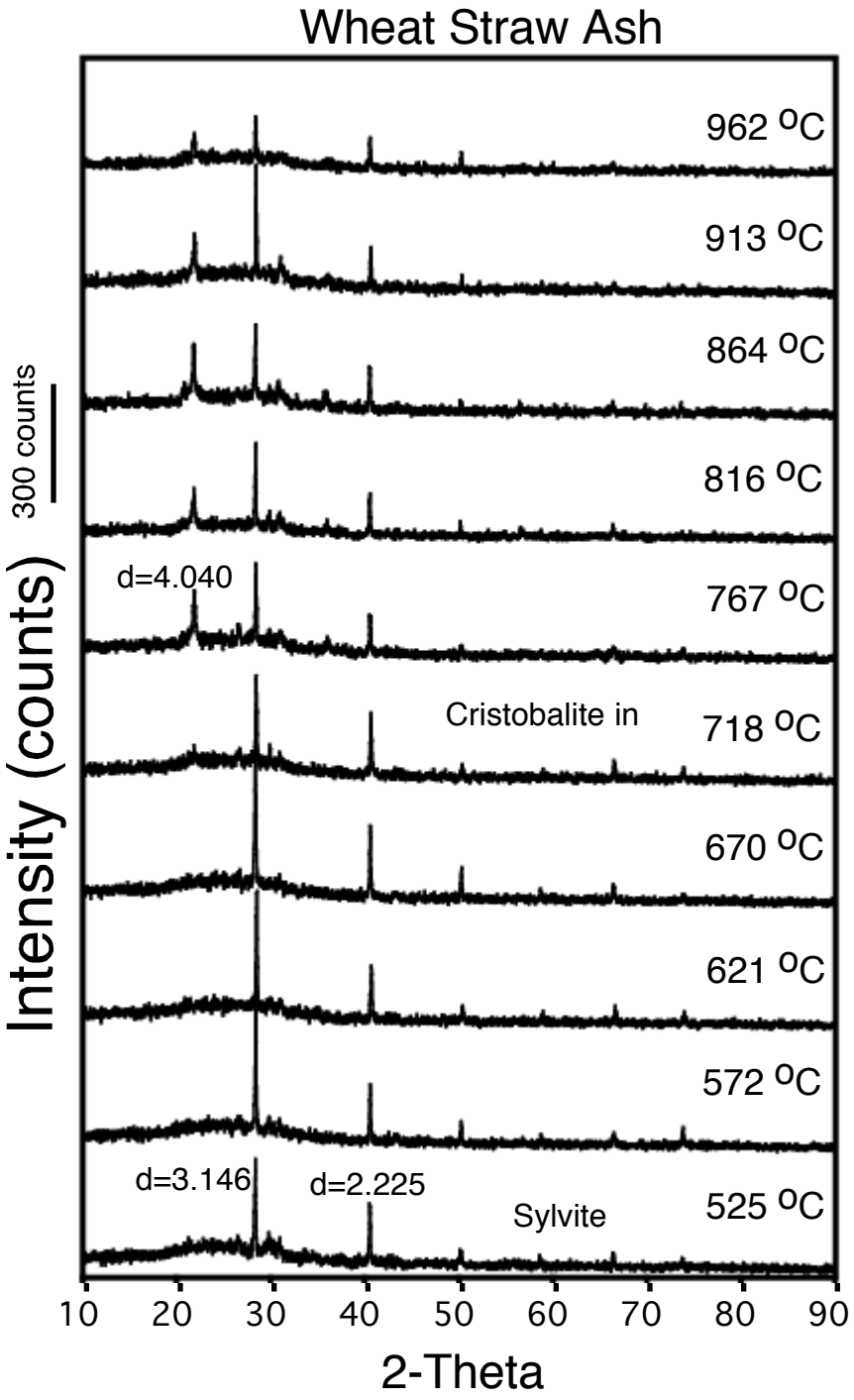

Figure 9. Summary of XRD patterns (Cu K_{α} radiation) for the wheat straw ashes. Characteristic measured d-values in Ångstrom used to identify specific minerals (from Thy et al., 2006b).

Modeling using the FactSage thermochemical database (Bale et al., 2002) reproduced some of the essential features of the experiments. Melting is initiated between 600 and 700 ^{o}C and the liquidus is reached at 1500 ^{o}C, well above the experimental predictions. The dominant mineral predicted is a silica phase with the high-quartz to tridymite transition between 800-900 ^{o}C. This modeling result contrasts with the experiments that show a cristobalite to tridymite transition much higher at about 1125 ^{o}C. This finding may be due to the effect of release of K_2O from the ash. Potassium is in the model results released above 1000 ^{o}C mainly as KCl by the breakdown of sylvite.

5.2.3. Wheat Straw

The wheat straw ash was fired at temperatures from 572 to 962 ^{o}C well into its melting interval. Significant hardening and sintering of the pellets occurs from 572 ^{o}C. Large-scale melting is apparent at 816 ^{o}C with abundant bubble formation and pellet expansion.

The mineralogical changes as a function of temperature are similar to those observed for rice straw ash (Figure 9). Sylvite is present throughout the investigated temperatures into the melting interval. Cristobalite appears at 718 ^{o} C. Tridymite does not appear because of the relatively low melting temperature. Additional phases were not detected despite that the experiments bracketed the solidus temperature.

Modeling using the FactSage database suggests very low initial melting temperature and a liquidus at 1300-1400 ^{o}C, unrealistically high compared to the experimental results. A high-quartz to tridymite transformation is modeled at 800-900 ^{o}C, although not observed in the experiments that contain cristobalite as the only stable SiO_2 polymorph. The modeling further suggests that the liquidus minerals are pyroxenes and that tridymite melts 1100-1200 ^{o}C. As observed for rice straw, sylvite breaks down from 1000 ^{o}C to release potassium as KCl.

5.3. Ash Color Variation

The wood ash color becomes systematically darker until about 800 ^{o}C, after which the color is relatively unchanged (Figure 10). This change in color may be due to the breakdown of calcite and the appearance of larnite and pericline in the temperature range of 700-800 ^{o}C. The rice ash color in contrast becomes systematically lighter with increasing temperature and changes from gray to whitish gray at 816 ^{o}C and finally pinkish white at 975 ^{o}C (Figure 10). The wheat ash color similarly becomes systematically lighter with a yellowish tint from about 700-800 ^{o}C (L* and b*, Figure 10 and Table 2). The variation in the color of the straw ashes is mainly due to the removal of carbon.

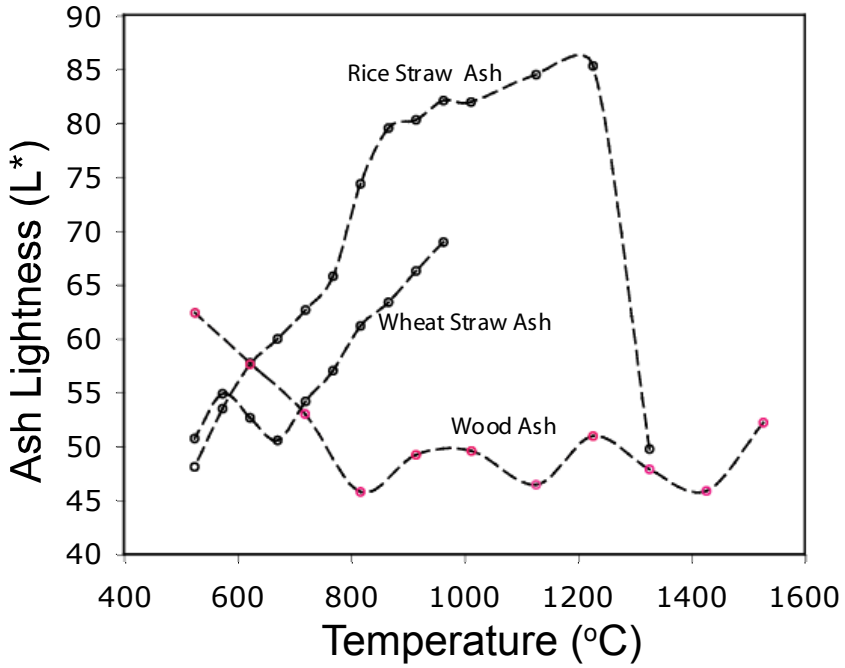

Figure 10. Ash lightness (L*) as a function of firing temperature (Table 2),

5.4. Weight Loss During Firing and Loss-on-Ignition

The change in weight as a function of heating temperature principally reflects the breakdown of organic components (C-H-S-O) and the efficiency of their removal from the products. The interpretation of weight loss is, however, complicated by several factors. Combustion may be

incomplete from having been conducted at low oxygen activity leaving inorganic carbon (graphite) in the products. Further, the breakdown of organic components during combustion often stabilize inorganic minerals like hydrates, hydroxides, carbonates, and sulfates in the ashing products that thus may retain some volatile components to the much higher temperatures of breakdown (e.g., carbonates) or even to decomposition temperatures well above melting (e.g., sulfates). Halogen salts are also stable in some biomass materials to relatively high temperatures (e.g., halite). As shown in previous work (Thy et al., 2006a,b), potassium (and possibly other alkali elements) may completely or in part be released during heating at high temperatures above typical ashing.

Two measurements were made that reflect on the efficiency of removal of the organic component. First, the weight loss during heating were measured for the specific ashing temperature (Table 2). Second, the loss-on-ignition (LOI) at 950 ^{o}C were measured for all experimental products (Table 11). These variables are graphically illustrated in Figure 10. One would expect that the loss-on-ignition is very low for products fired at 950 ^{o}C or above. The fact that this is not the case suggests that the combustion was incomplete and that organic (relict fuel fragments) and inorganic carbon (graphite) may be retained in some of the products.

The weight loss during combustion of wood increases with temperature from 4 % to about 36 % (Figure 10A). The corresponding losses-on-ignition determined at 950 ^{o}C vary inversely with the weight losses from ashing (Figures 10B and 10C) suggesting that the efficiency of removal increases with firing temperature.

If the two loss determinations are added, the results for ashing above 950 ^{o}C are fairly similar to the weight loss measured for the high-temperature melting experiments of Thy et al. (2004) (39-42 %). This suggests that complete removal of the volatile components was not achieved during ashing and that a carbonate compound as indicated by the XRD analysis was preserved in the experimental high temperatures products (Thy et al., 2004).

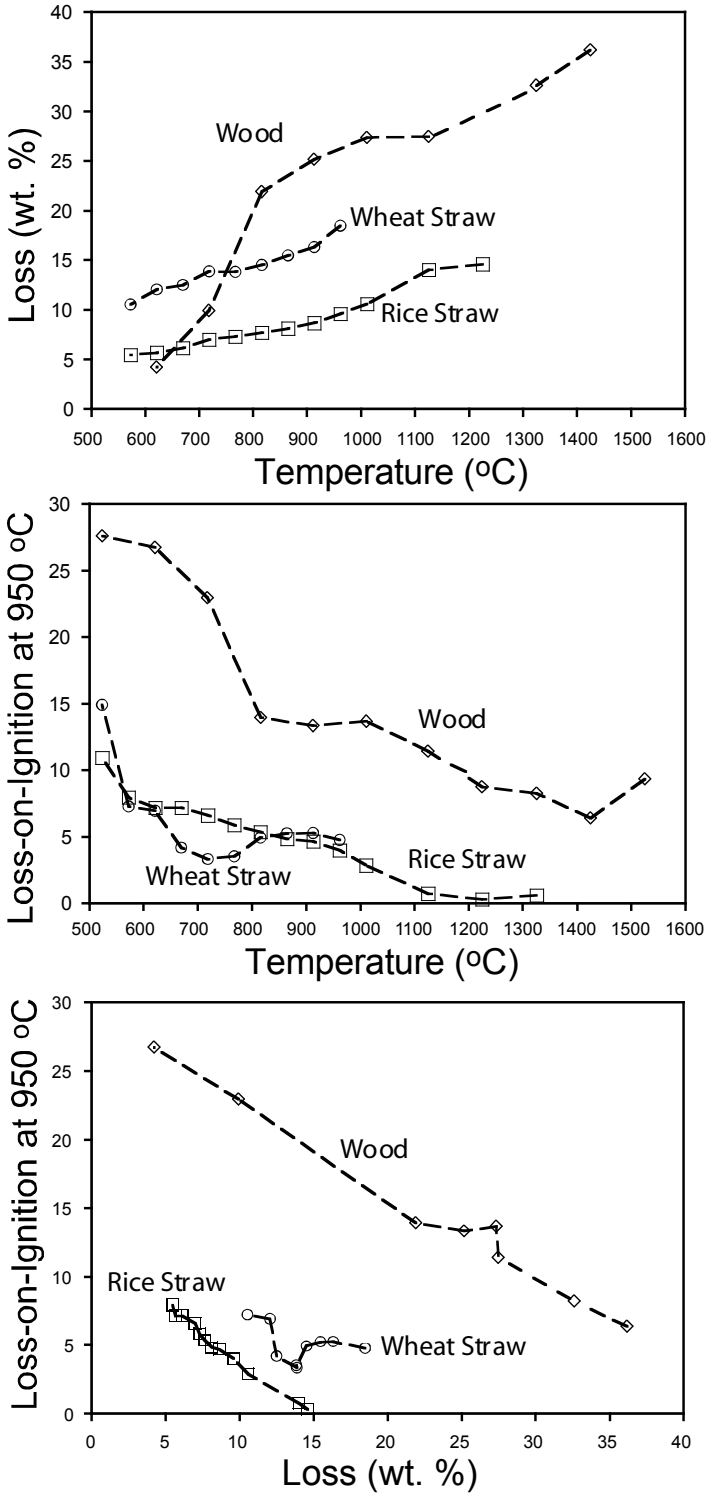

Figure 11. Correlations between loss during firing (wt.%), temperature (°C), and loss-on-ignition (wt. %) for the three fuel types (wood, rice straw, and wheat straw). From top to bottom: (A) Weight loss as a function firing temperature. (B) Loss-on-ignition determined at 950 °C as a function of original firing temperature. (C) Loss-on-ignition as a function of original loss during firing.

The weight loss from the rice straw during firing shows systematic increase from 5.5 % at 572 ^{o}C to 15 % at 1225 ^{o}C (Figure 10a). The average weight loss determined in the melting experiments on the same ash by Thy et al. (2004) was 15 %. The loss-on ignition at 950 ^{o}C is below 4 % for all experiments fired above this temperature. The sum of the volatile losses suggests that most carbon and organic components were removed from the ash at temperatures above 1000 ^{o}C.

The weight loss from the wheat straw during firing (Figure 11a) shows systematic increase from 10.5 % at 572 ^{o}C to 18.5 % at 962 ^{o}C. The loss-on ignition determined at 950 ^{o}C reached a maximum of 7 % and suggests that carbon remains in the slag even in the 962 ^{o}C products.

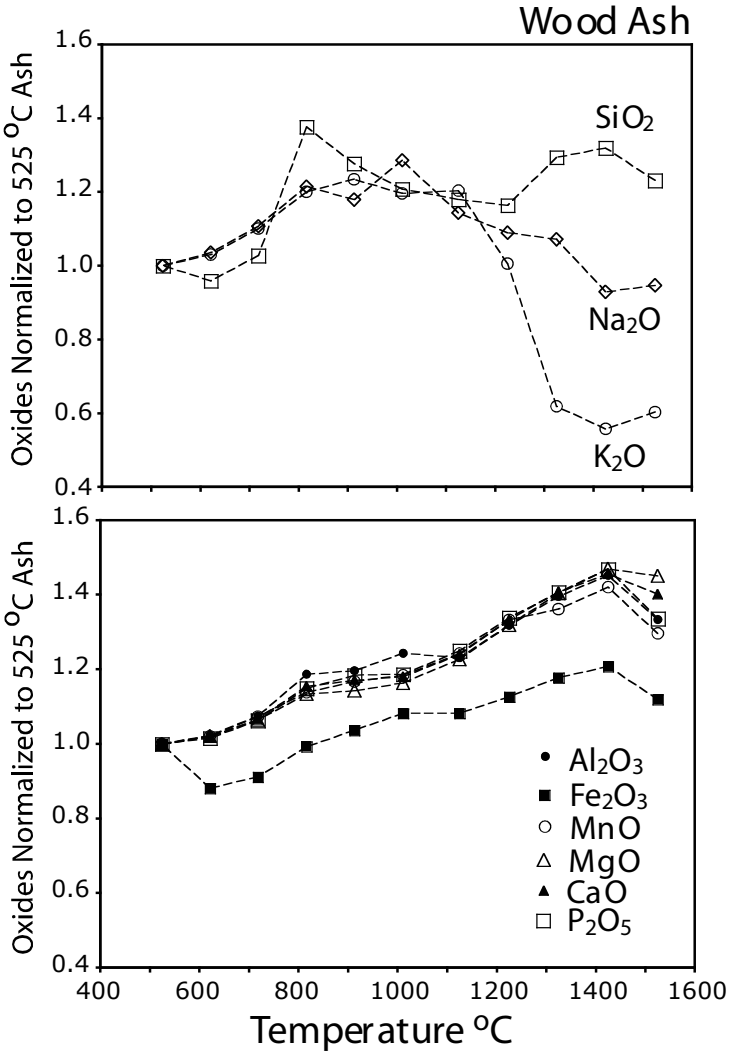

Figure 12. Major and minor oxide compositions of wood ash normalized to the 524 ^{o}C ash and shown as a function of firing temperature.

6. Major and Minor Elements

The major element results for the ashing experiments as a function of fuel type and temperature are summarized in Table 11, giving for the three groups of fuel, the experimental temperatures, firing weight losses, and composition of the ashes as determined by a combination of X-ray fluorescence spectroscopy and instrumental neutron activation. The major and minor elements of the ashes are given as wt. % oxides. The chlorine content is given as elemental wt. %. The presence of chlorine requires the sums to be corrected for the oxygen equivalent of chlorine (Table 11).

6.1. Wood

The analytical results for wood ash are summarized in Figure 11 as oxides normalized to the composition of the 524 ^{o}C ash. It is seen that most oxides steadily increase with firing temperature from ratios of about 1 to 1.5. The only exception is Na_2O and K_2O that show a systematic fall from between 1011 and 1125 ^{o}C. SiO_2 shows an irregular variation despite a general increase with firing temperature. Fe_2O_3 shows a systematic increase like most oxides despite an initial drop between 524 and 621 ^{o}C. We relate the anomalies in SiO_2 to problems either with sampling or to accurately analyzing the concentrations for this oxide. The unexpected drop in Fe_2O_3 for the whole suite of ashes may be related to the assumption of the oxidation of iron for the initial 524 ^{o}C ash. It is possible that this ash contains significant amounts of FeO in addition to Fe_2O_3. It should also be noted that the experiment at the highest temperature (1525 ^{o}C) was not completely equilibrated due to heating element failure and contained an anomalously high content of carbon (graphite).

The main observation for wood ash is of a systematic increase in most oxides (SiO_2, Al_2O_2, Fe_2O_2, MnO, MgO, CaO, Na_2O, and P_2O_2) with increasing firing temperature and a systematic decrease in the alkali oxides Na_2O and K_2O. The systematic increase in many oxides is a simple result of the removal of volatile components (see Figure 10). This is what often is referred to the 'total sum effect.' When something is removed, something else will increase, particularly detected for the high concentration oxides. If the oxide concentrations are normalized to an oxide

that has been constant throughout the investigated temperature range, this constant sum effect can be eliminated. Figure 12 shows the wood ash concentrations normalized to the CaO concentrations (all wt. %) that is thought to be constant and independent on temperature (cf., Thy et al. 2000). The main compositional variation can now be seen to be a marked decrease in K_2O initiated at about 900 ^oC. SiO_2 shows a decrease between 1000-1200 ^oC and MgO may show a slight increase from 1000 ^oC. The remaining major and minor oxides (TiO_2, Na_2O, MnO, Al_2O_3, P_2O_5) show small or no variations. It is unclear whether the variation in SiO_2 is real or perhaps due to a breakdown in the assumption that CaO is constant. A study of an urban wood ash above its liquidus temperature at 1300 ^oC by Thy et al. (2000) suggests that CaO is independent of duration at superliquidus conditions.

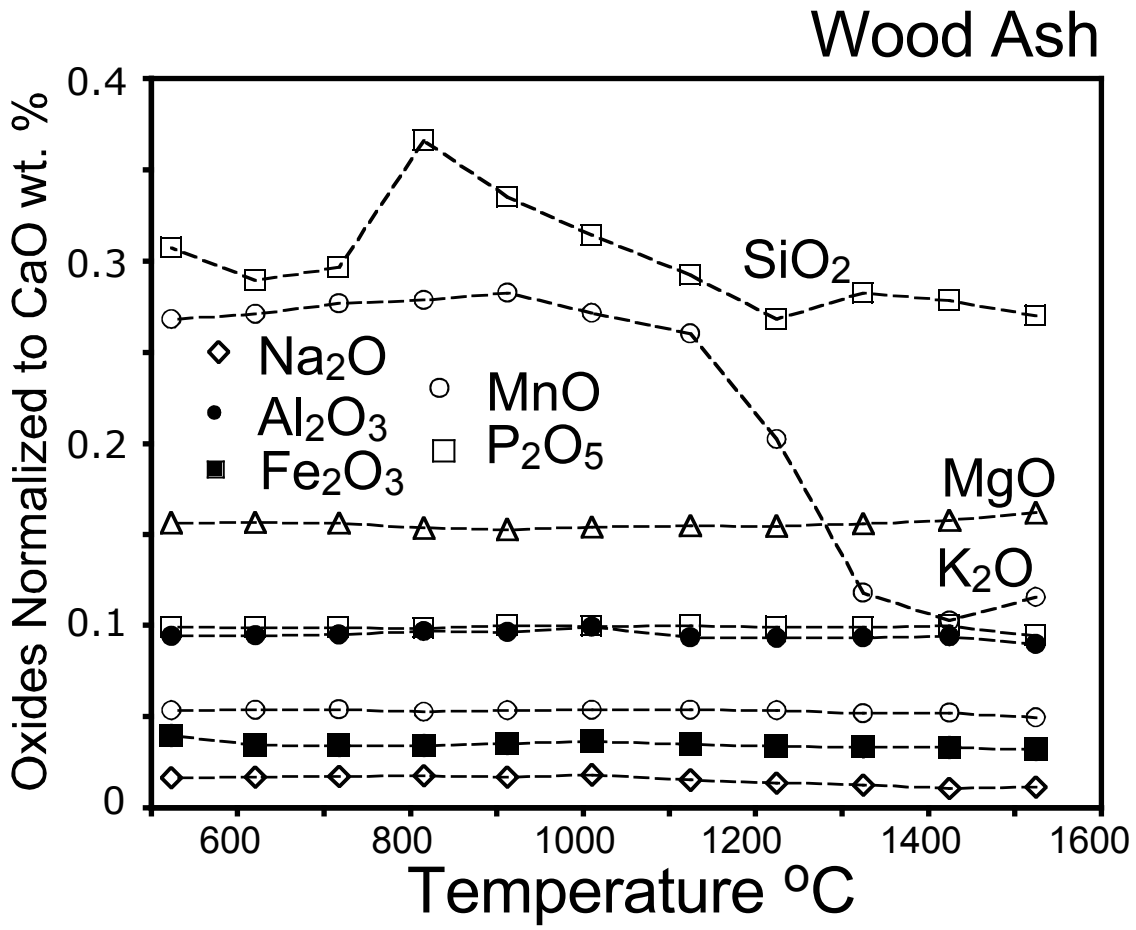

Figure 13. Major and minor oxide compositions of wood ash normalized to CaO and shown as a function of firing temperature.

6.2. Rice Straw

The analytical results for rice straw ash are summarized in Figure 14 as oxides normalized to the composition of the 525 ^{o}C ash. SiO_2 displays a systematic increase, while K_2O and P_2O_5 show systematic decreases from about 1100 ^{o}C. Na_2O shows irregularity, but in general appears to decrease similarly to K_2O. Figure 15 shows that K_2O normalized to the SiO_2 concentration markedly decreases after 1225 ^{o}C. Chloride dramatically drops from about 700 ^{o}C and is completely removed from the ash at temperatures above 1100 ^{o}C. Other oxides occur in low concentrations and record no detectable variation with temperature.

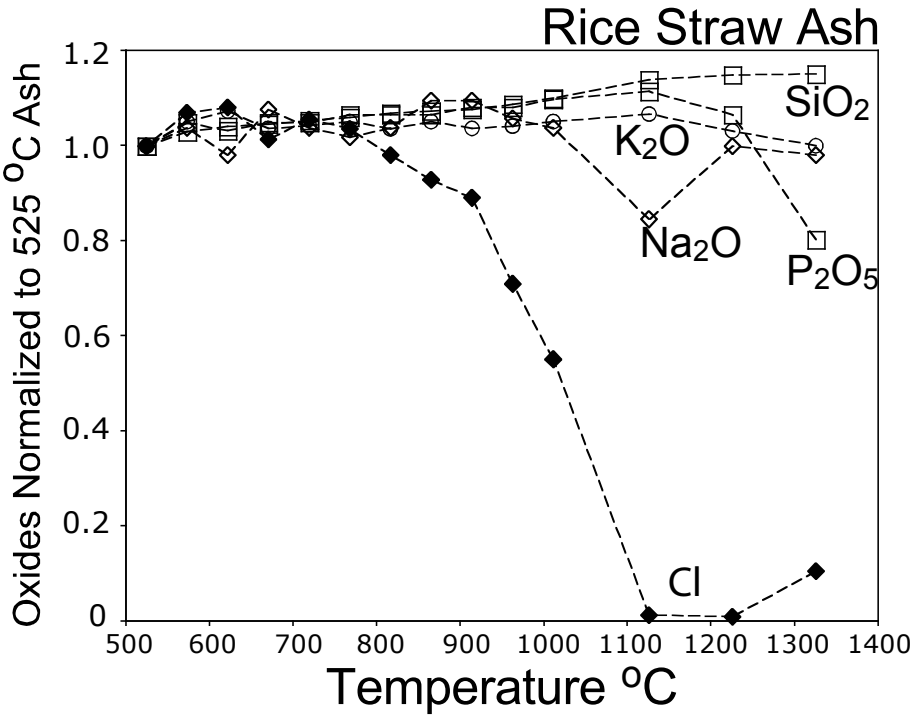

Figure 14. Major and minor oxide compositions of rice straw ash normalized to the 524 ^{o}C ash and shown as a function of firing temperature.

6.3. Wheat Straw

The analytical results for wheat straw ash are summarized in Figure 16 normalized to the composition of the 525 ^{o}C ashes. The variation shows trends very similar to those observed for rice straw ash (Figure 14). SiO_2 initially increases to about 600 ^{o}C and there after appears

relatively constant or increases. K_2O and Na_2O similarly increase until about 700 ^oC and thereafter decreases. Na_2O shows an initial drop that may reflect an analytical problem. Similar to rice straw ash, chloride shows a marked drop from 700 ^oC. These variations are as for wood and rice straw ashes related to a combination of the loss of volatile components (mainly C) and losses of K_2O and Cl. P_2O_5 does not show the same drop at high temperatures as observer for rice straw. The reason is likely that the firing temperatures for wheat straw ash did not reach the same high temperatures as for rice straw ash.

Figure 15 shows K_2O normalized to the SiO_2 concentration and assuming that SiO_2 remains unchanged throughout the investigated temperature interval. Similar to the rice straw ash results, most of the oxides occur in low concentrations that record no detectable variation with temperature. The normalized concentrations of K_2O vary significantly, but without any marked drop as for rice straw ash at high temperature.

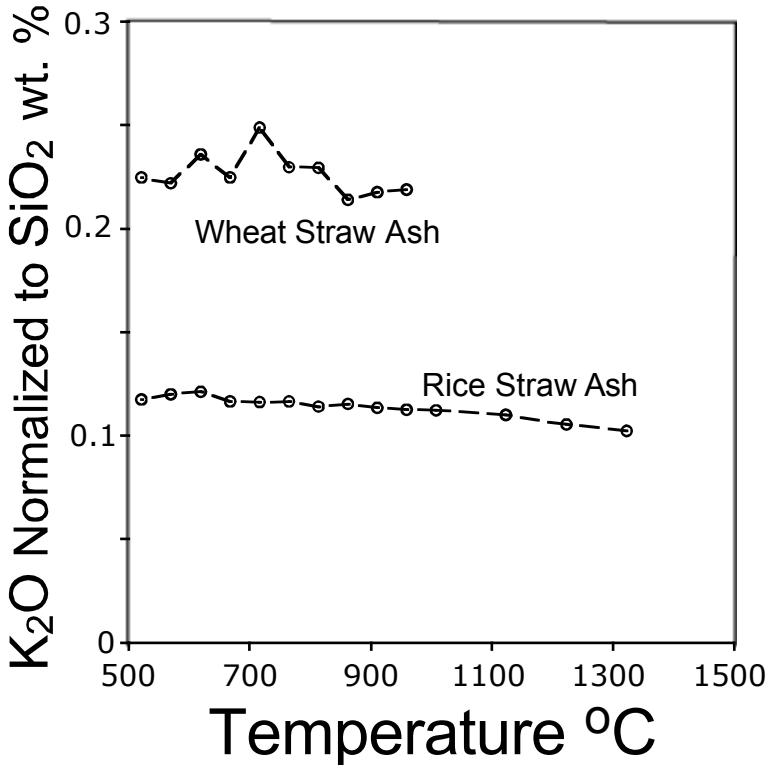

Figure 15. Major and minor oxide compositions of straw ashes normalized to SiO_2 and shown as a function of firing temperature.

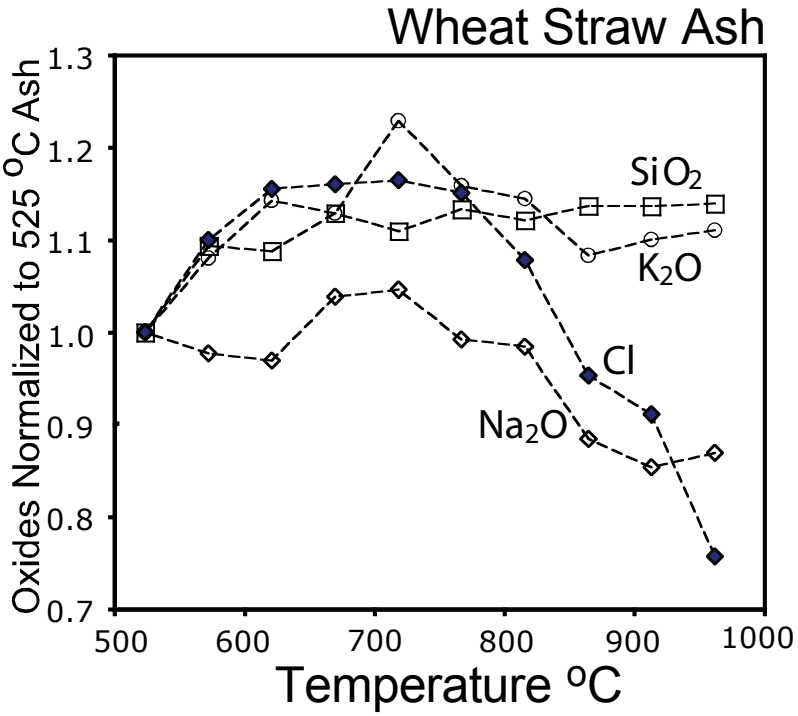

Figure 16. Major and minor oxide compositions of rice straw ash normalized to the 524 °C ash and shown as a function of firing temperature.

6.4. Cl-K Variation

Chlorine concentrations for the straw ashes show systematic variation with temperature (Figure 17). Until temperatures of about 767 °C, the concentrations steadily rise due to the removal of volatile components (Figure 16). For temperatures above 767 °C, chlorine concentrations decrease, eventually leading to strong depletion in the rice straw ash. The wheat straw ash was not heated above 962 °C and, therefore, does not show the same strong depletion as does the rice straw ash, where temperatures of 1325 °C are reached at which point 11 % of the original chlorine remains in the sample. This change in behavior is taken to reflect the breakdown of sylvite and the loss of Cl to the furnace atmosphere.

There is a strong co-variation between Cl and K calculated on an atomic basis (Figure 17). The rice straw ash with the strongest depletion in Cl shows a linear correlation between Cl and K (R^2=0.971). The wheat straw ash shows a similar, but less-well defined variation. Extrapolation to Cl=0 suggests that a maximum of about 15 % of K is lost to breakdown of sylvite (25 % on a weight oxide basis). If the slope were controlled by breakdown of sylvite alone and the release of

both K and Cl to the furnace atmosphere, the slope of the lines in Figure 12 would have been 0.5 as opposed to the observed slopes of 1.8. This suggests that not all K released from breakdown of sylvite is lost from the ash and that 50 % is retained.

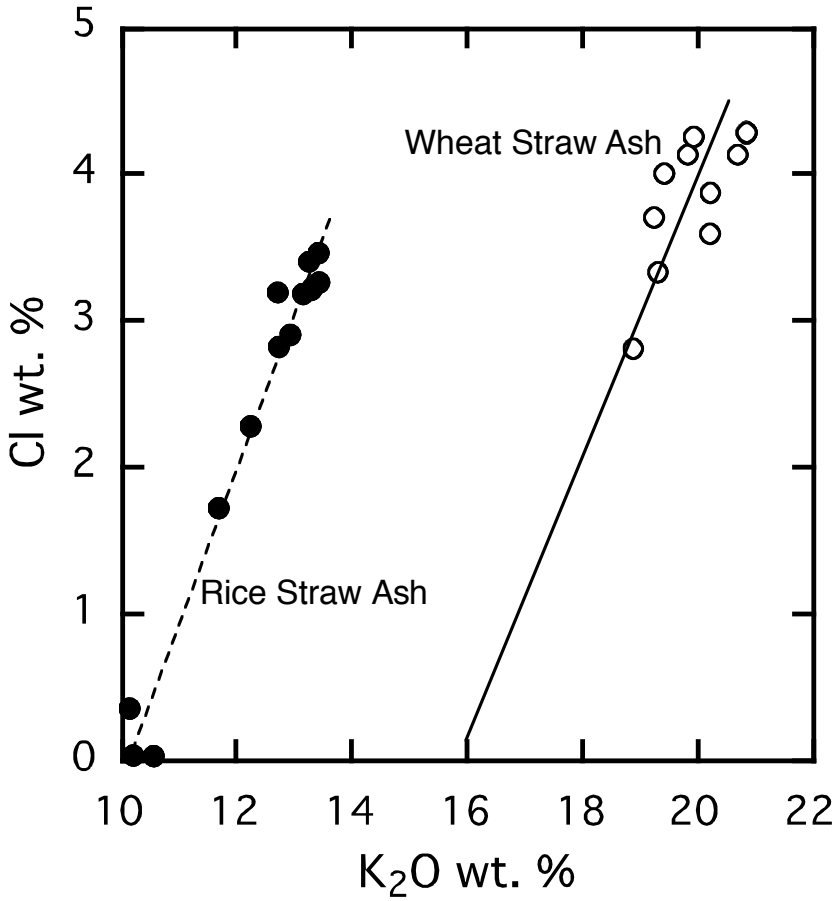

Figure 17. Cl concentrations (atomic %) as a function of K content (atomic %). Linear correlation for rice straw ash is Cl = -23.237 + 1.8675 x K (R^2=0.9711).

6.5. Elemental Losses During Initial Ashing

The initial losses of potassium and chloride during initial ashing at 524 ^{o}C cannot be evaluated based on the present results. Thy et al. (2006b) were able to determine the K and Cl contents of the same raw fuels used in this study by a non-destructive analytical method (INAA). They concluded that 36 % of the original K_2O was lost during ashing of the wood, but were unable to detect K_2O losses from the straw fuels. Chlorine was detected lost only from wheat straw (20 %) with the highest original Cl content.

Table 13. Summary of ICPMS Results (ppm)

ID	T (oC)	Be	V	Cr	Mn	Co	Ni	Cu	Zn	As	Se	Rb	Sr	Zr	Ag	Cd	Sn	Sb	Cs	Ba
Wood																				
WO-8	1525	1.1	37.1	128	23562	13	100.6	193	1086	18.3	0.9	98	2178	14.4	0.5	6.2	1.6	0.78	0.24	2324
WO-10	1425	1.2	36.1	91	26451	14	99.0	215	1112	10.7	0.4	76	2692	9.3	0.3	4.5	1.6	0.79	0.38	2476
WO-7	1325	1.1	40.9	111	26039	14	103.5	201	1172	17.8	0.9	33	2450	14.8	0.2	2.1	1.6	0.82		2604
WO-9	1225	1.0	35.2	137	22215	10	85.1	183	997	17.5	1.0	94	2263	16.9	0.7	7.1	1.4	0.92		2390
WO-6	1125	1.0	30.2	127	19745	9	71.2	166	870	13.6	1.2	131	2116	13.7	1.5	7.5	1.2	0.78	0.02	1811
WO-1	1011	1.0	30.5	166	17799	9	92.0	162	806	16.5	1.1	126	2128	22.2	2.0	7.5	1.1	0.66	0.20	2201
WO-5	913	1.1	35.8	142	22063	10	72.8	197	992	19.4	1.3	193	2382	19.8	2.7	8.9	1.3	0.71	0.94	2380
WO-4	816	1.1	32.3	108	19581	9	61.5	176	968	17.8	1.0	139	2110	9.9	2.5	8.4	1.1	0.67	0.94	2098
WO-3	718	1.0	32.5	118	17937	9	64.3	171	875	18.6	1.2	142	2086	20.6	2.3	7.8	1.2	0.60	1.04	2219
WO-2	621	1.0	30.8	106	17731	8	59.6	160	812	17.6	0.7	139	2095	14.1	2.3	7.5	1.1	0.57	0.89	2210
WO-S	524	1.0	21.1	66	13298	6	43.1	117	603	9.6		152	1844	16.1	1.7	5.9	0.9	1.27	0.73	1731
Wheat Straw																				
WH-5	962	0.9	12.8	23	752	2	14.3	38	65	3.8	3.0	47	248	6.3	0.1	1.4	0.4	0.36	0.30	684
WH-4	913	0.9	16.8	44	896	6	31.5	68	94	4.4	0.8	46	286	8.5	0.3	1.9	2.0	0.42	0.34	786
WH-6	864	1.0	18.6	42	915	7	23.5	56	98	4.6	0.9	51	283	9.5	0.1	1.8	0.9	0.45	0.40	826
WH-3	816	0.9	15.3	36	842	5	22.3	50	80	4.5	1.1	48	264	8.1	0.2	1.6	1.2	0.36	0.31	741
WH-7	767	0.9	16.6	35	851	9	20.5	48	77	4.5	1.5	52	267	7.9	0.1	1.7	0.9	0.39	0.40	800
WH-2	718	0.9	17.0	32	892	6	19.1	52	85	5.0	1.7	52	278	7.8	0.2	2.0	20.6	0.47	0.38	783
WH-8	670	0.9	16.5	31	822	3	19.6	52	77	4.3	2.7	50	258	8.1	0.1	1.4	20.7	2.66	0.41	750
WH-1	621	0.9	14.6	28	811	17	17.1	76	94	5.6	2.7	50	263	6.7	0.1	1.8	0.6	0.69	0.32	711
WH-9	572	0.9	15.4	28	779	2	17.6	42	70	4.1	2.7	47	239	7.8	0.1	1.4	0.7	0.37	0.34	699
WH-S	524	0.9	17.7	62	732	2	19.0	32	61	11.8	2.5	42	235	7.4	0.1	1.2	0.4	0.29	0.30	647
Rice Straw																				
R-13	1325	1.1	4.0	16	4348	7	9.9	20	162	3.1		69	121	2.4	0.0	0.2	0.4	0.22	0.32	131
R-12	1225	1.1	3.3	12	3899	7	10.4	29	184	2.8	0.1	45	110	1.9	0.1	0.1	0.8	0.26	0.30	118
R-11	1125	1.1	4.1	15	4127	7	11.8	26	192	4.0	0.1	59	120	2.1	0.1	0.3	0.5	0.28	0.31	129
R-10	1011	1.1	3.6	21	3726	6	16.7	24	185	6.0		50	105	1.5	0.1	0.3	0.4	0.25	0.33	118
R-5	962	0.8	3.4	21	4054	7	13.0	41	201	6.6	0.1	63	79	1.3	0.1	0.3	0.4	0.21		113
R-4	913	0.9	3.4	12	4201	6	7.0	55	218	6.9		65	78	1.3	0.1	0.3	0.4	0.20		118
R-6	864	0.8	2.8	13	3559	5	7.9	37	175	5.6		59	71	1.1	0.1	0.5	0.3	0.17		98
R-3	816	0.9	3.4	11	4175	6	7.0	32	201	6.7		67	81	1.4	0.0	1.0	0.5	0.33		114
R-7	767	0.8	3.1	14	3798	4	12.6	32	187	6.0		60	71	1.5	0.0	0.3	0.3	0.20		107
R-2	718	0.8	3.3	13	3921	2	8.6	60	213	6.5		69	76	1.2	0.0	0.4	0.4	0.23		109
R-8	670	0.9	3.2	14	4001	1	8.6	32	197	6.4		67	75	1.2	0.0	0.3	0.3	0.21		114
R-1	621	0.8	3.2	20	3879	1	11.1	54	211	6.2		69	75	1.2	0.0	0.2	0.4	0.18		104
R-9	572	0.9	2.8	12	3557	1	7.1	33	172	5.8		64	71	1.2	0.0	0.3	0.3	0.18		102
R-S	524	0.9	3.3	8	3675	1	5.5	15	161	6.1		68	74	1.2	0.0	0.2	0.3	0.18		96

Blank means that the element was not detected.
Eu and Ho were not detected in any of the ashes.

Table 13. Continued.

ID	T (oC)	La	Ce	Pr	Nd	Sm	Gd	Tb	Dy	Er	Tm	Yb	Lu	Hf	Ta	W	Tl	Pb	Th	U
Wood																				
WO-8	1525	1.06	1.51		1.23	0.28	0.27	0.03	0.19	0.23	0.02	0.04	0.02	0.42	0.40	29.53		5.7		0.33
WO-10	1425	2.67	1.83	0.34	1.56	0.43	0.18			0.11	0.02			0.48	0.39	32.09		2.9		0.39
WO-7	1325	1.04	1.59		1.29	0.29	0.28	0.03	0.17	0.22	0.02	0.02	0.02	0.45	0.42	29.33		0.3		0.36
WO-9	1225	3.54	2.08	0.01	1.56	0.35	0.32	0.04	0.22	0.26	0.03	0.06	0.02	0.48	0.24	2.08		1.8	0.04	0.30
WO-6	1125	1.18	1.80		1.35	0.31	0.24	0.03	0.18	0.20	0.02	0.03	0.02	0.38	0.20	1.00		4.9		0.28
WO-1	1011	1.80	2.73	0.10	2.01	0.43	0.40	0.05	0.28	0.28	0.03	0.07	0.02	0.64	0.25	1.02	0.13	9.5	0.00	0.29
WO-5	913	2.00	2.99	0.12	2.06	0.45	0.44	0.06	0.32	0.34	0.04	0.11	0.03	0.54	0.27	1.02	0.24	12.2	0.19	0.31
WO-4	816	0.94	1.49		1.24	0.28	0.25	0.03	0.15	0.19	0.02	0.01	0.01	0.33	0.22	0.89	0.25	10.3		0.26
WO-3	718	2.24	3.45	0.18	2.30	0.48	0.45	0.06	0.33	0.34	0.04	0.11	0.03	0.56	0.27	18.50	0.27	11.3	0.15	0.27
WO-2	621	1.64	2.38	0.06	1.83	0.38	0.35	0.04	0.23	0.24	0.03	0.04	0.02	0.45	0.22	4.15	0.27	10.7		0.25
WO-S	524	2.10	3.32	0.14	2.14	0.47	0.46	0.06	0.36	0.31	0.04	0.14	0.03	0.47	0.20	0.71	0.33	8.6	0.30	0.26
Wheat Straw																				
WH-5	962	0.45	1.31		0.96	0.25	0.18	0.02	0.15	0.20	0.02	0.02	0.01	0.24	0.09	0.31		3.1		0.09
WH-4	913	0.67	1.85		1.24	0.30	0.23	0.03	0.20	0.25	0.03	0.04	0.02	0.30	0.48	32.09		10.8		0.11
WH-6	864	1.11	1.95		1.29	0.33	0.25	0.04	0.22	0.28	0.03	0.05	0.02	3.72	0.60	44.63		5.7		0.12
WH-3	816	0.55	1.59		1.09	0.28	0.21	0.03	0.18	0.23	0.02	0.03	0.01	0.29	0.48	31.68		6.2		0.10
WH-7	767	0.60	1.71		1.16	0.30	0.22	0.03	0.20	0.26	0.03	0.04	0.02	0.29	0.82	61.03		7.6		0.11
WH-2	718	0.62	1.75		1.19	0.30	0.22	0.03	0.19	0.25	0.03	0.03	0.02	0.31	0.62	40.17		17.1		0.11
WH-8	670	0.61	1.70		1.15	0.30	0.21	0.03	0.20	0.25	0.03	0.04	0.02	0.30	0.10	0.46		414		0.11
WH-1	621	0.49	1.44		1.04	0.27	0.20	0.03	0.16	0.22	0.02	0.02	0.01	0.26	1.52	101.32		5.0		0.10
WH-9	572	0.58	1.64		1.09	0.27	0.19	0.03	0.16	0.23	0.02	0.02	0.01	0.29	0.05	0.41		4.3		0.09
WH-S	524	0.44	1.35		1.01	0.26	0.20	0.03	0.16	0.21	0.02	0.02	0.01	0.27	0.11	0.23		2.8		0.09
Rice Straw																				
R-13	1325	0.27	0.61	0.09	0.48	0.26	0.02			0.04	0.02			0.22	1.31	81.36	0.01	2.2		0.04
R-12	1225	0.27	0.52	0.07	0.43	0.23	0.01			0.02	0.01			0.37	1.76	92.92	0.00	46		0.03
R-11	1125	0.38	0.85	0.11	0.55	0.27	0.02			0.03	0.02			0.25	1.28	74.73	0.01	2.8		0.04
R-10	1011	0.26	0.60	0.09	0.45	0.25	0.02			0.03	0.02			0.20	0.60	53.41	0.01	3.3		0.03
R-5	962				0.32	0.11	0.04	0.01	0.03	0.09				0.13	0.63	63.82		5.2		0.02
R-4	913				0.32	0.11	0.04	0.01	0.03	0.09				0.13	0.51	56.88		5.6		0.01
R-6	864				0.30	0.11	0.03	0.01	0.03	0.08				0.12	0.38	42.10		4.4		0.01
R-3	816				0.36	0.12	0.04	0.01	0.03	0.09				0.17	0.40	42.01		3.8		0.01
R-7	767				0.30	0.11	0.03		0.03	0.08				0.14	0.29	24.71		4.3		0.01
R-2	718				0.32	0.11	0.04		0.03	0.08				0.13	0.09	3.37		5.3		0.01
R-8	670				0.33	0.11	0.04	0.01	0.03	0.09				0.14	0.05	0.27		5.3		0.01
R-1	621				0.30	0.10	0.03	0.01	0.03	0.08				0.14	0.04	0.23		4.4		0.01
R-9	572				0.31	0.11	0.03		0.03	0.09				0.13	0.06	0.23		3.2		0.01
R-S	524				0.31	0.11	0.04		0.03	0.08				0.18	0.03	0.10		2.2		0.01

7. Trace Element Concentrations

The trace element concentrations in the experimental ashes are summarized in this section. Table 12 gives the instrumental neutron activation analyses (INAA) results, while Table 13 gives the inductively coupled plasma mass spectroscopy (ICPMS) results. The analytical uncertainty is summarized in Table 8 for the INA results and in Table 10 for the ICP-MS results. All analyses are given as parts-per-million (ppm) on a weight basis (µg/g). The following discussion is based on the ICPMS data, unless otherwise specified, and mostly shown in simple variation diagrams with firing temperature as the abscissa.

*7.1. Alkali Metals (*Na, K*, **Rb, Cs)*

The alkali metals Na and K were analyzed as major elements and show systematic decrease in concentrations with increasing firing temperature. It was thus expected that other alkali metals likewise would show concentration decreases with increasing firing temperature. The alkali metals Rb and Cs were analyzed as trace elements; Rb determined by both INA and ICPMS and Cs only detected by ICPMS. There is a reasonable correspondence between Rb determined by the two methods despite some systematic deviation from the expected 1:1 correlation (Figure 18).

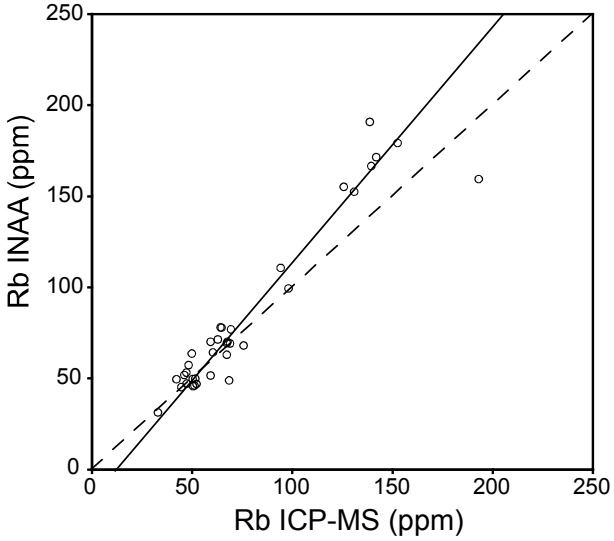

Figure 18. Correlation of Rb (ppm) determined by INA and ICP-MS. Dashed line is the 1:1 correlation.

The concentrations as a function of temperature for the three experimental ash and slag groups are illustrated in Figure 19. The wood ash contains averages of 120 ppm Rb and 0.6 ppm Cs that both show systematic decrease with increasing firing temperature. For the ICPMS analyses, the relative standard deviations (Tables 8 and 10) are for Rb about 3 % (or ±5 ppm) and for Cs about 3 % for straw and 5 % for wood (or ±0.05 ppm and ±0.01 ppm, respectively). The relative standard deviation for the INAA determination of Rb is about 6 % (or ±10 ppm). The straw ashes contain about 50-60 ppm Rb and about 0.3 ppm Cs and do not show systematic dependency on firing temperature (Figure 19). If the Rb data obtained by INAA is plotted in a similar fashion (Figure 19), a systematic decrease in Rb can likewise be observed from above 900 ^{o}C.

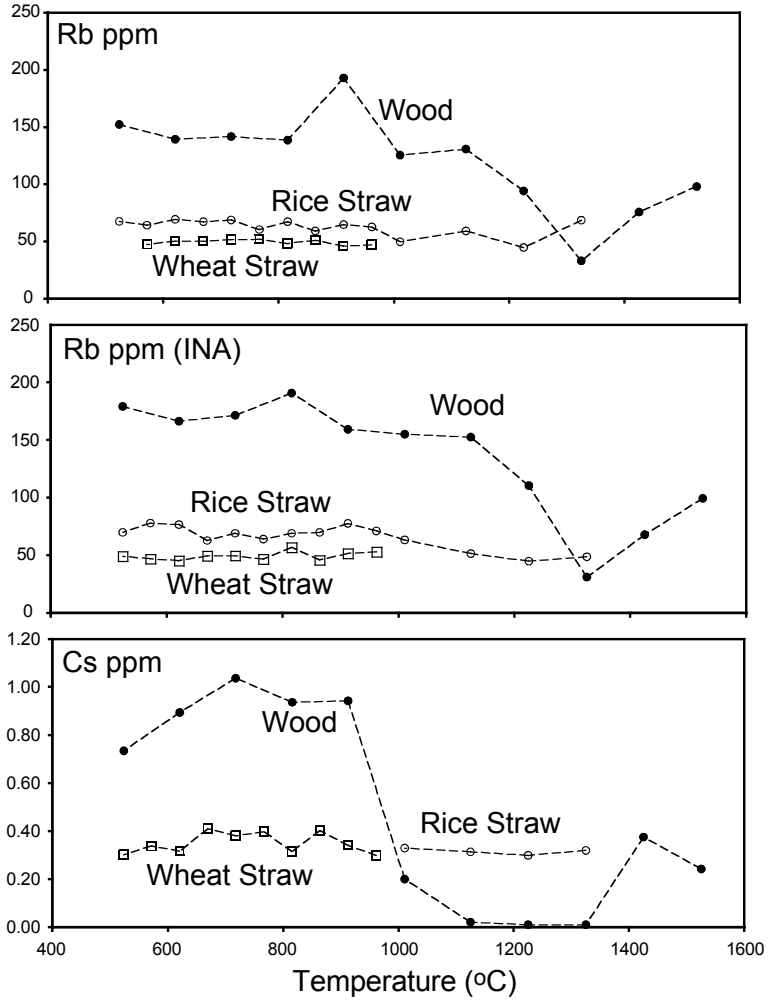

Figure 19. Variations of Rb and Cs as a function of firing temperature.

7.2. Alkali Earth Metals (Be, Mg, Ca, ***Sr, Ba)***

The alkali earth metals Mg and Ca were analyzed as major elements and show no detectable variation in concentrations with firing temperature. The elements Be, Sr, and Ba were analyzed as trace elements; Be and Sr were determined only by ICPMS and Ba detected both by ICPMS and INAA. There is a reasonable correspondence between Ba determined by the two methods despite some systematic deviation from the expected 1:1 correlation (Figure 20) and that Ba only was detected in a few ashes by INA.

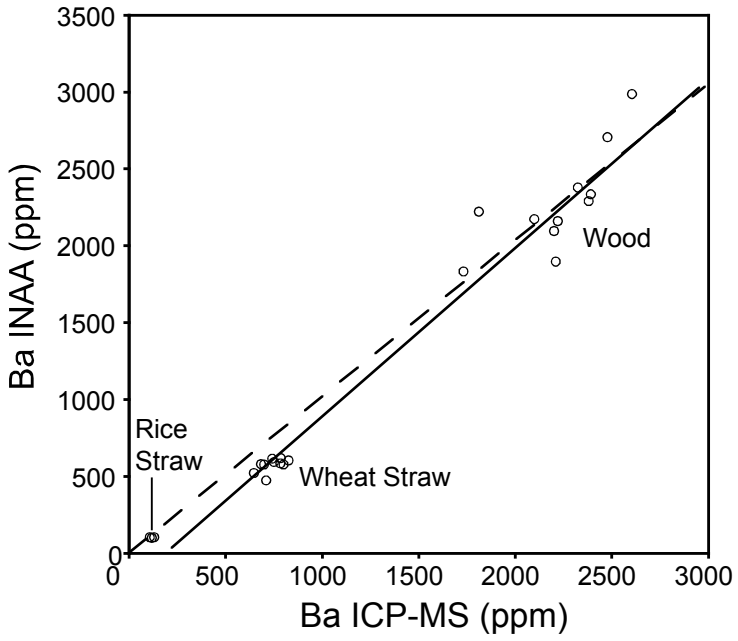

Figure 20. Correlation of Rb (ppm) determined by INA and ICPMS. For only a few rice straw ashes was Ba detected with INA. Dashed line is the 1:1 correlation.

The concentrations as a function of temperature for the three experimental ash and slag groups are illustrated in Figure 21. For the ICPMS analyses, the relative standard deviations (Table 10) for Be are high in the range of 15-30 % (or ±0.15-0.30 ppm), for Sr about 3 % (or ±60 ppm for wood and ±4-8 ppm for the straws), and for Ba about 2.5 % (or ±55 ppm for wood and ±18 ppm for wheat, and ±3 ppm for rice). The relative standard deviation for the INA determination (Table 8) of Ba is 4, 7, and 12 %, respectively for wood, wheat, and rice, and significantly larger than for the ICPMS analyses.

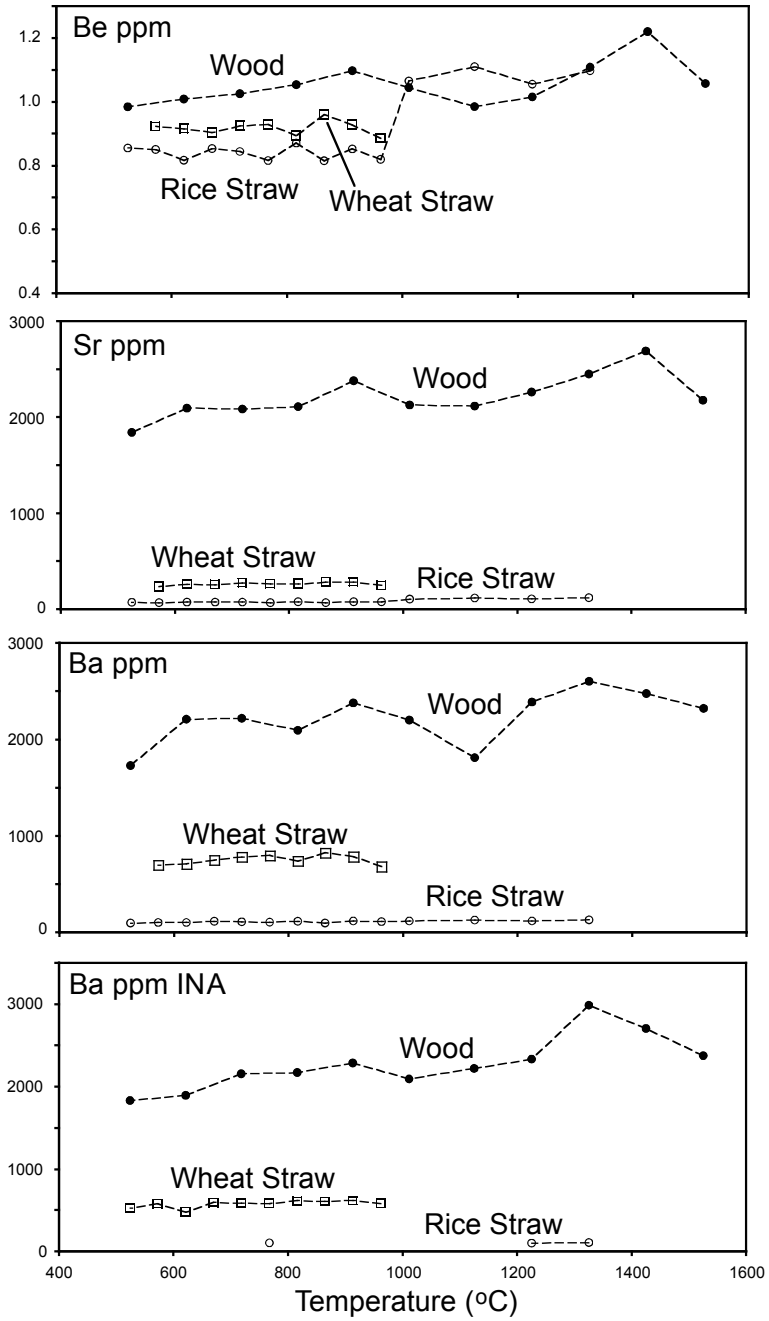

Figure 21. Variations of Be, Sr, and Ba as a function of firing temperature.

The ashes contain averages of about 1 ppm Be with little differences between the three groups of ashes as well as no systematic variation as a function of firing temperature considering the analytical error of 0.15-0.30 ppm. Sr shows large differences between the three fuel groups with an average of 2200 ppm for wood, 260 ppm for wheat straw, and 90 ppm for rice straw ashes. Ba

likewise shows large differences between the three fuel groups with an average of 2200 ppm for wood, 740 ppm for wheat straw, and 110 ppm for rice straw ashes.

Table 14. Effect on Major and Trace Elements From Loss of Volatiles and Alkalies

Oxide/ Element	As Analyzed	After Loss
SiO_2	10.48	17.64
TiO_2	0.12	0.20
Al_2O_3	3.21	5.40
Fe_2O_3	1.35	2.27
MgO	5.33	8.97
CaO	34.14	57.46
Na_2O	0.56	
K_2O	13.54	
P_2O_5	3.37	5.67
LOI	27.59	
Sum	99.69	97.62
Sc	2.7	4.5
V	21	35
Cr	66	111
Mn	13298	22382
Co	6.4	10.8
Ni	43	72
Cu	117	198
Zn	603	1015
Total	101.11	100.00

Data from Tables 11, 12, and 13 (WO-S).

There seems to be a systematic increase with firing temperature in Sr and Ba concentrations for wood ash (Figure 21), exceeding the analytical error. The Sr content of the wood ashes varies from about 1800 ppm in low temperature ashes to about 2700 ppm in high temperature ashes. This is a 50 % increase and is well above the analytical error of about ±60 ppm. Similarly, the Ba content varies from 1700 ppm to 2400 ppm. This is a 40 % increase and is well above the analytical error of about ±55 ppm. The straw fuels show no systematic increase in these elements. Such an increase either can be caused by the addition (contamination) during firing or can be an effect of removal of volatile components during firing (total-sum effect). In the present case, we can exclude with confidence contamination and are thus left with the 'total sum effect' to explain the observed apparent increase. The wood ash contains about 30 % volatiles

determined as loss-on-ignition at 950 ^{o}C (mostly CO_2 bonded in carbonates) (Table 1). Experiments at higher temperatures to 1500 ^{o}C suggest a total loss of 40 % or slightly above (Thy et al., 2004, 2006b), including the loss of K_2O from the slag. Such high volatile losses will significantly affect the major oxides as well as the minor and trace elements as illustrated in Table 14 and can explain the systematic increase for wood ash as seen for many elements. The maximum increase resulting from the total-sum effect amounts to 66 % for a 40 % loss. For fuels with less volatile losses, like the straw ashes, the effect is smaller.

7.3. Transition Metals (Sc, Ti, ***V, Cr, Mn,*** Fe, ***Co, Ni, Cu, Zn)***

The transition metals Ti and Fe were analyzed as major elements and show no detectable variation in concentrations with firing temperature. The element Mn was analyzed both as a minor and as a trace element. The remaining transition metals (Sc, V, Cr, Co, Ni, Cu, Zn) were analyzed by INAA and/or ICPMS. The elements Cr, Mn, and Co were analyzed by both INA and ICPMS and Sc was only detected by INAA. There is a good correlation between the results for Cr, Mn, and Co analyzed by the two methods (Figure 22), despite some erratic results particularly for Co.

The concentrations as a function of temperature for the three experimental ash and slag groups are illustrated in Figures 23 and 24. For the ICPMS analyses, the relative standard deviations (Table 10) for the transition metals vary depending on absolute concentrations between 2 and 3.5 % or translated to ±0.1-3 ppm for V, Cr, and Ni; ±0.1-0.3 for Co; ±1-30 ppm for Cu and Zn; and ±25-600 ppm for Mn. For Sc only analyzed by INAA, the relative standard deviation is below 4.5% or ±0.03 ppm.

The absolute concentrations of the transition metals are typically high in the wood ash with particularly high Cr, Ni, Cu, and Zn (80-1000 ppm). The straw ashes contain much lower concentrations (10-200 ppm) with systematic differences between rice and wheat straw ashes.

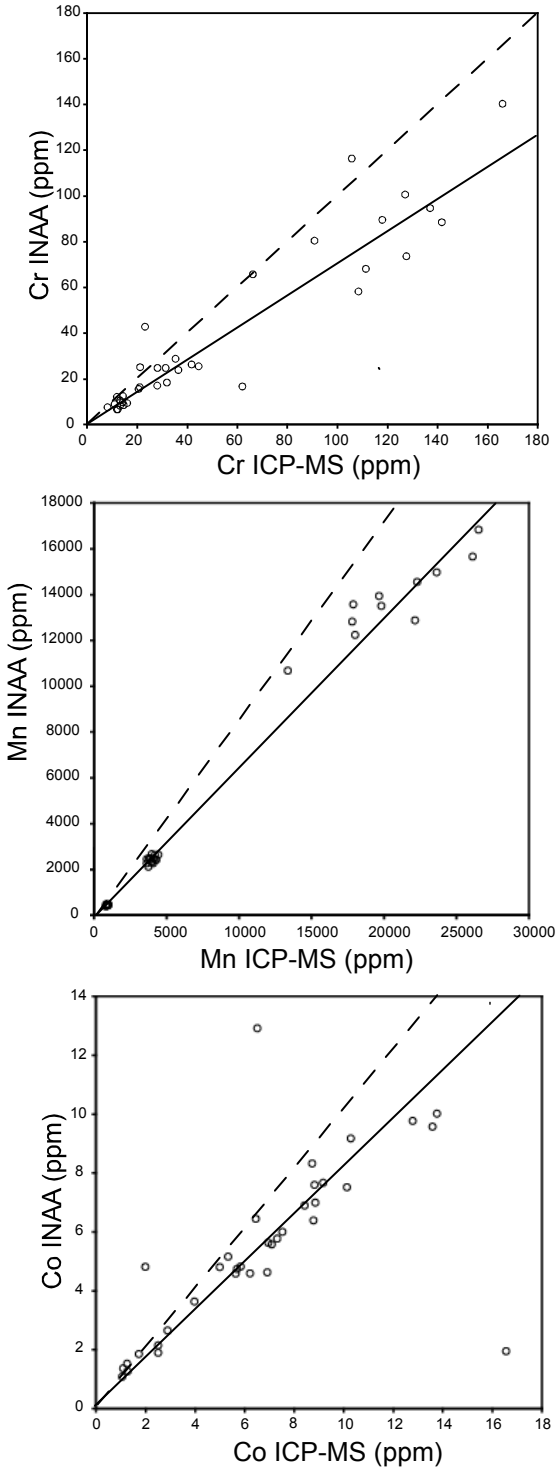

Figure 22. Correlations of Cr, Mn, and Co (ppm) determined by INAA and ICPMS. The dashed lien is the 1:1 correlation.

There is a systematic increase for most transition metals in the wood ash with increasing firing temperature for the wood ash, while little variation is observed for the straw ashes. This increase

in the wood ash concentrations can again be explained by the 'total sum effect' (Table 14). The variations in the transition elements analyzed by INAA are illustrated in Figure 25. There is in general a good correspondence between the two methods although the INAA results do not always show the same increase with temperature. Both methods result in some erratic results for Co in the straws.

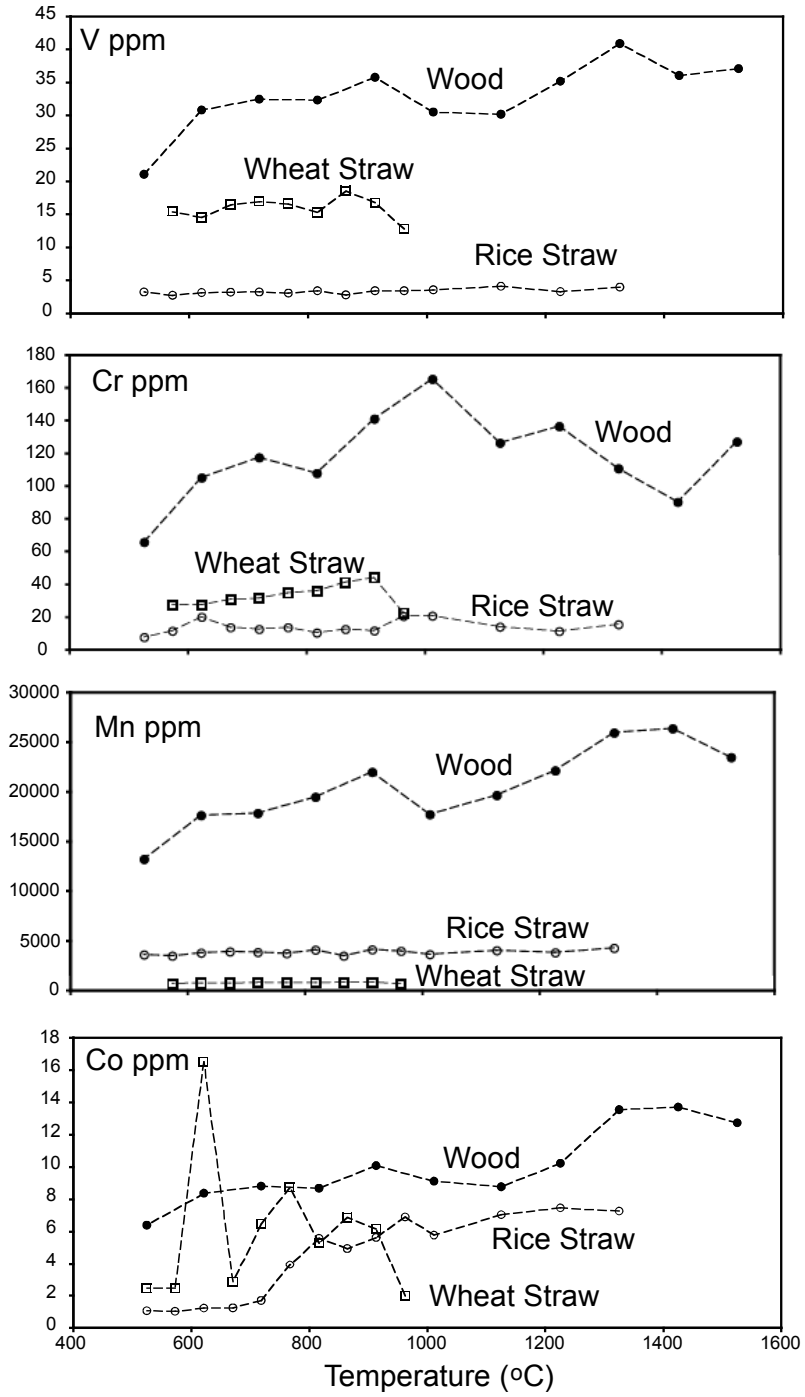

Figure 23. Variations of V, Cr, Mn, and Co as a function of firing temperature.

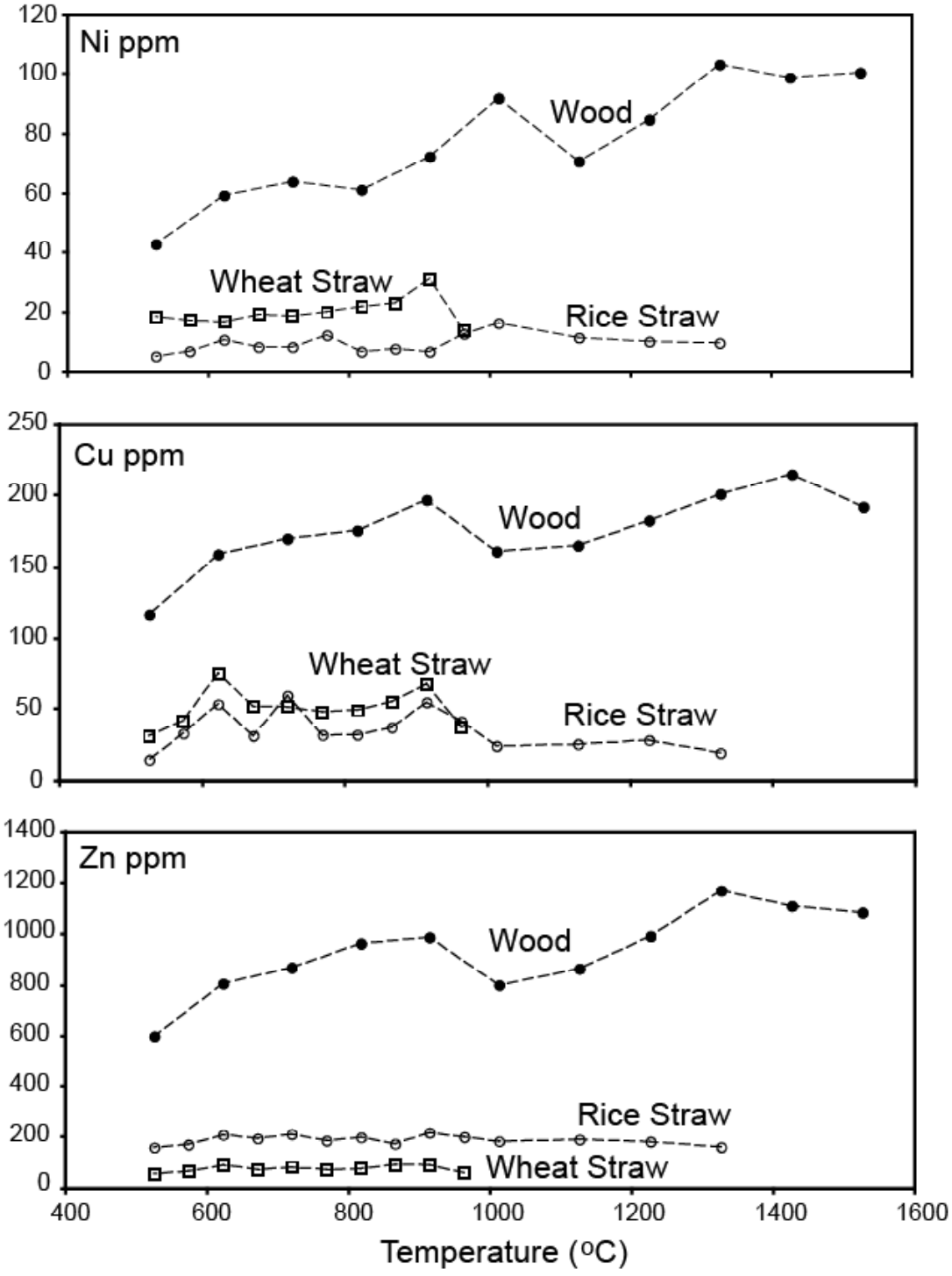

Figure 24. Variations of Ni, Cu, and Zn as a function of firing temperature.

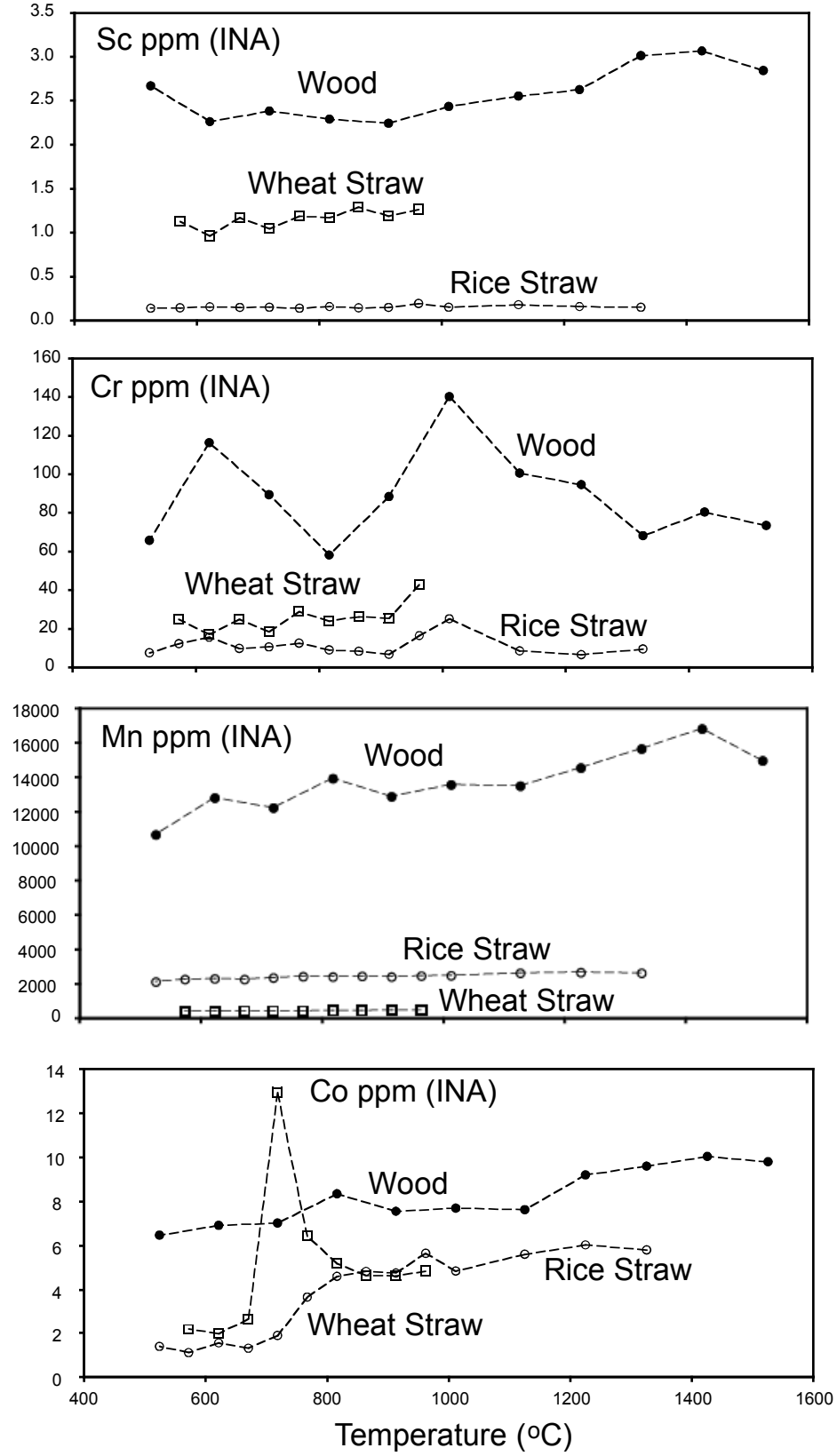

Figure 25. Variations of Sc, Cr, Mn, and Co determined by INA as a function of firing temperature.

7.4. Zr, Ag, Cd

The elements Zr, Ag, and Cd were analyzed only by ICPMS. The concentrations as a function of temperature for the three experimental ash groups are illustrated in Figure 26. The relative standard deviations (Table 10) vary depending on absolute concentrations from 3 % for wood and wheat straw ashes (or ±0.5 ppm and ±0.2 ppm, respectively) to 11 % for rice straw ash (or ±0.2 ppm). A control analysis of the NIST standard 1633 failed to reproduce the recommended value (Table 10) and the absolute values obtained for Ag may therefore be incorrect.

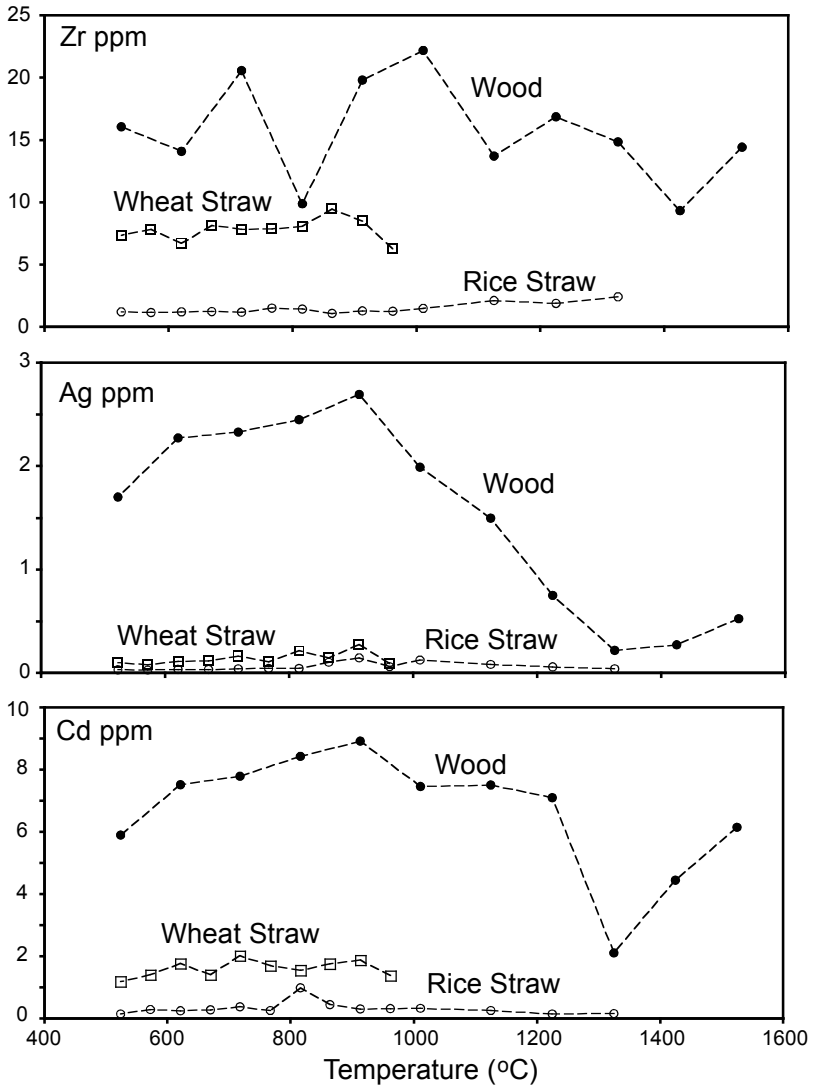

Figure 26. Variations of Zr, Ag, and Cd as a function of firing temperature.

The average concentrations of Zr in wood ash are relatively high (16 ppm) compared to the straw ashes with 8 ppm in wheat straw ash and only 2 ppm in rice straw ash. There is a systematic decrease from above 900 ^{o}C particularly for Ag and also to a certain extent for Cd in the wood ash, while little systematic variation is observed for the straw ashes. The element Zr shows no systematic variation with firing temperature for wood ash.

7.5. As, Se

The elements As and Se were only analyzed by ICPMS. The concentration of As in wood ash is on an average 16 ppm, while the straw ashes contain about 5-6 ppm. The concentrations of Se in wood ash is generally low with an average of 1 ppm in wood ash, 2 ppm in wheat straw ash, and 0.1 ppm in rice straw ash. For the rice straw ash, the results are near the lower limit of detection and detection was only possible for a few ashes.

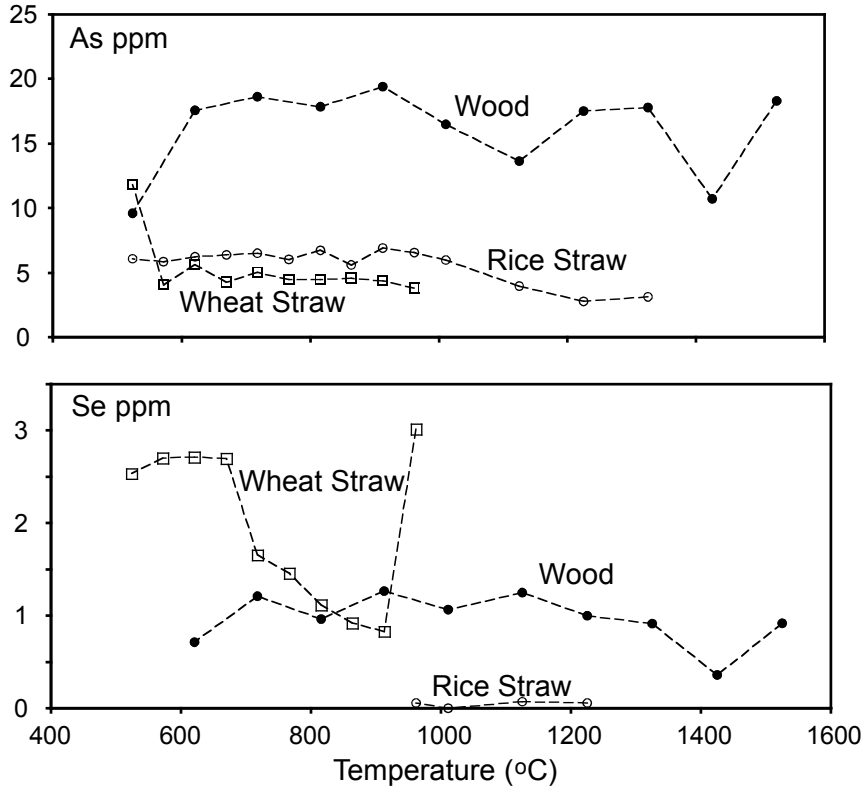

Figure 27. Variations of As and Se as a function of firing temperature.

The concentrations as a function of temperature for the three experimental ash groups are illustrated in Figure 27. The relative standard deviations (Table 10) for As vary from 4-5 % for wood and wheat straw ash (or ±1 ppm and ±0.2 ppm, respectively) to 2 % for rice straw ash (or ±0.1 ppm). The same numbers for Se are 11 % for wood (or ±0.1 ppm) and 7 % for straw ashes (or ±0.1 ppm or below).

There is no detectable systematic variation as a function of firing temperature for either of the elements, except perhaps a decrease for Se from about 700 ^{o}C discounting an anomalous high concentration for the 962 ^{o}C experiment (Figure 27).

7.6. Sn, Sb

The elements Sn and Sb were analyzed by ICPMS. The concentrations of Sn in wood and wheat straw ashes average about 1-2 ppm, while rice straw contains much less (0.5 ppm) (excluding a few anomalous high values for wheat straw). The concentrations of Sb in wood and wheat straw ashes are just below 1 ppm and again much lower for rice straw ash (0.2 ppm).

The concentrations as a function of temperature for the three experimental ash groups are illustrated in Figure 28. The relative standard deviations (Table 10) for Sn vary from 4 to 7 % translating into ±0.05-0.02 ppm. The same numbers for Sb are 3-5 % or about ±0.03-0.01 ppm.

There seems to be a systematic increase in both Sn and Sb concentrations for wood ash with firing temperature (Figure 28) as is also seen with many other trace elements. This again can be attributed to the removal of large amounts of volatile elements form the wood ash with increasing temperature. There are a few anomalous results for the wheat straw ash that have been deleted in the calculations of the averages and also from Figure 28. An unusually high concentration in Sb for the initial wood ash is also apparent and inconsistent with remaining results.

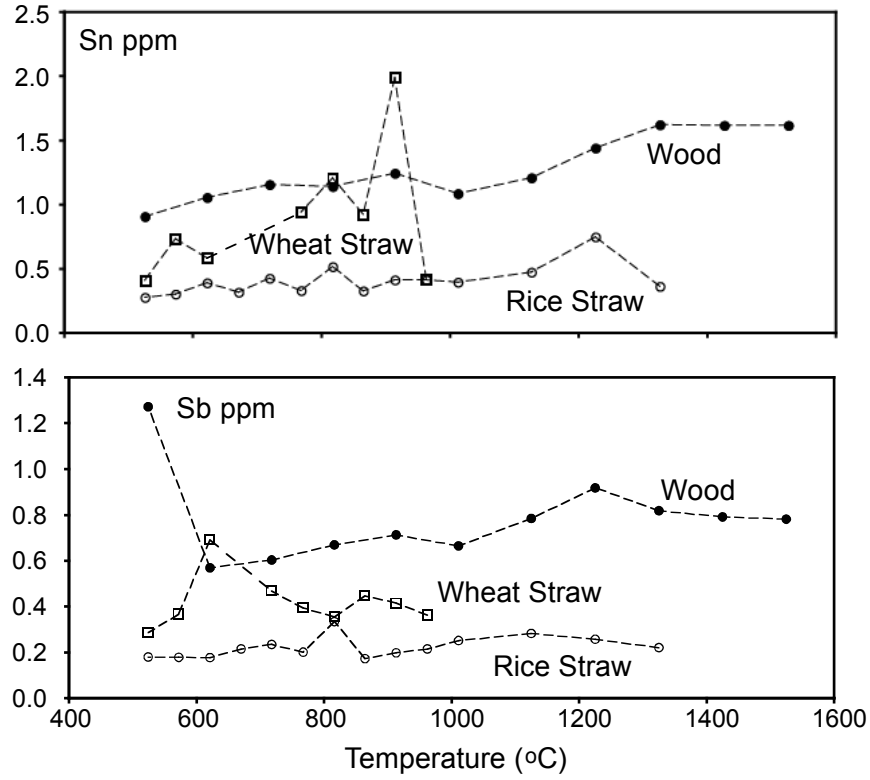

Figure 28. Variations of Sn and Sb as a function of firing temperature.

7.7. Rare Earth Elements (La, Ce, Pr, Nd, Sm, Gd, Tb, Dy, Er, Tm, Yb, Lu)

A near complete series of rare earth elements were detected by ICPMS in most ashes. Considerable efforts were made to determine the rare earth elements also with INAA; however, only sporadic results were obtained using this method (Table 12). There were also some limitations in the ICPMS results (Table 13). The rare earth elements Eu and Ho were systematically not detected, Pr could not be detected in wheat straw ash, and Tb, Yb, and Lu were not detected in rice straw ash. Other elements were only sporadic detected in rice straw ash (La, Ce, Pr, Dy, and Tm).

The absolute concentrations vary widely from 2 ppm to near the detection limits below 0.01 (Table 10). There is no systematic dependency on the firing temperature. Figure 29 shows the concentrations as a function of firing temperature for three rare earth elements (La, Sm, Er), representing the light, intermediate, and heavy rare earth elements, respectively.

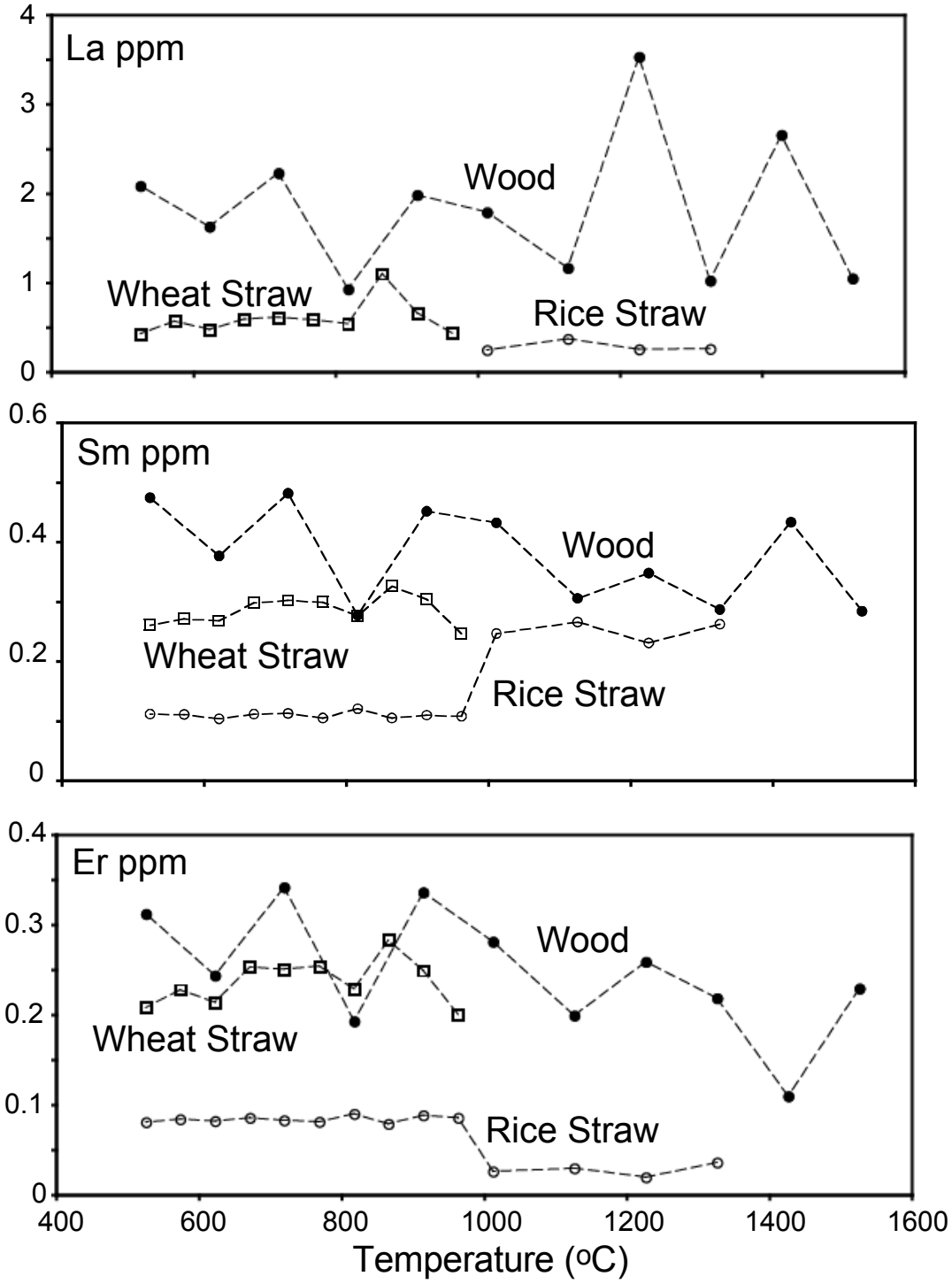

Figure 29. Variations of selected rare earth elements (La, Sm, and Er) as a function of firing temperature.

7.8. Heavy Elements (Hf, Ta, W, Tl, Pb, Th, U)

A group of heavy elements were detectable by ICPMS. These include Hf, Ta, W, Pb, and U. Only sporadic results were obtained for Tl and Th that could not be detected with confidence in the straw ashes. Attempts to analyze Hf, Ta, and Th by INA only gave sporadic results (Table 13), however, consistent with the results using ICPMS.

The concentrations as a function of temperature for the three experimental ash groups are illustrated in Figures 30 and 31. The relative standard deviations (Table 10) for all analyzed heavy elements vary from 2-10 % with the exception of Tl that reach high values and could not be detected in the straw ashes.

The absolute concentrations vary widely from 7 ppm Pb to well below 0.5 ppm for many of the remaining elements. The exception is W having average concentrations of 40 ppm with individual concentrations to above 100 ppm.

Of the heavy elements, only Pb suggests a dependency on firing temperature (Figure 30). The Pb concentration falls markedly from 12 ppm just above 900 ^{o}C to a few ppm at higher temperatures. The element U suggests in contrast a small but marked enrichment with increasing firing temperature for wood ash that results from the loss of volatiles.

The concentrations for Ta and W are highly variable with W concentrations reaching over 100 ppm (Figure 31). It is also clear that with few exceptions high W correlates with high Ta. This reflects contamination during ash preparation since some ashes were prepared in a wolfram carbide mill. The concentrations observed thus reflect the mill type and the milling duration. The true concentrations for W are revealed by the ashes that were prepared in an agate mill: 0.71-1.02 ppm for wood, 0.23-0.46 ppm for wheat straw, and 0.10-0.27 ppm for rice straw ashes. The corresponding values for Ta are 0.20-0.27 ppm, 0.05-0.11 ppm, and 0.03-0.06 ppm, respectively. This contamination with W and Ta are well known to result from use of wolfram carbide mills.

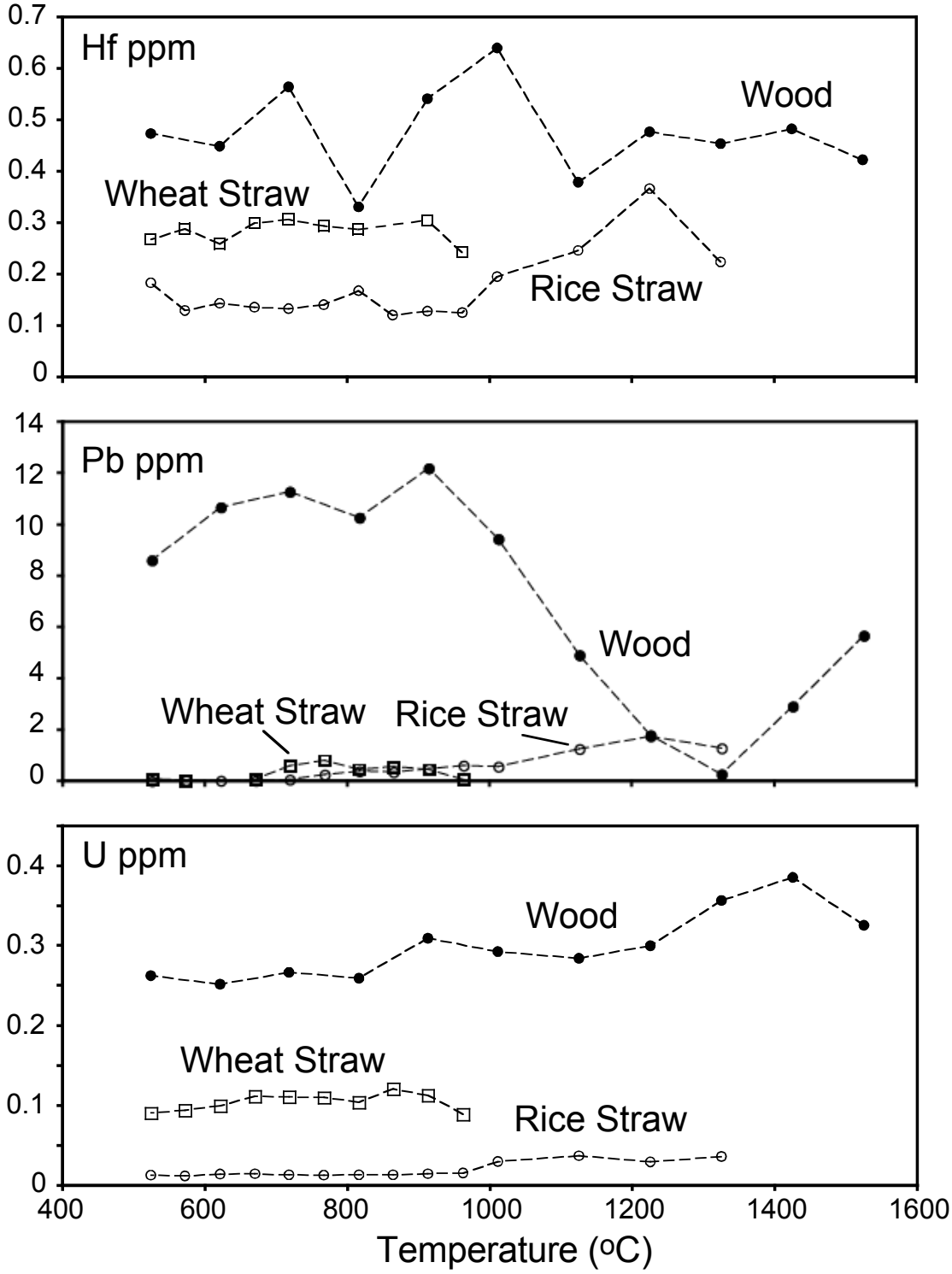

Figure 30. Variations of selected heavy elements (Hf, Pb, and U) as a function of firing temperature.

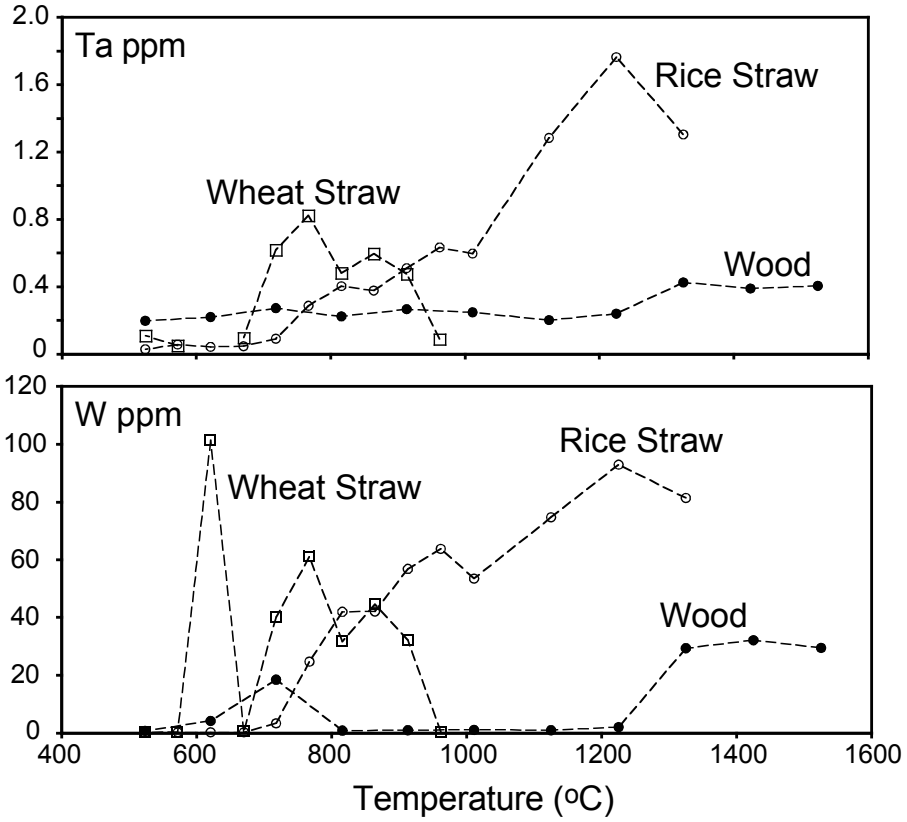

Figure 31. Variations of Ta and W as a function of firing temperature. The observed variation results from contamination from the use of a wolfram carbide mill during sample preparation.

7.9. Summary of Relative Enrichment and Depletion

Summary diagrams for each of the three fuel ashes illustrate the gain or depletion in the major, minor and trace elements (Figures 32 to 34). The concentrations have been normalized to the 524 ^{o}C ashes and are plotted on a log-scale with a color coding for the firing temperatures. The elements are ordered in the sequence of atomic number (Z) with the exception of some of the major and minor elements (Si to P) that are shown first. The elements Ti, Fe, and Mn are shown together with the other transition metals. Because they are normalized to the initial ash, elements that have not changed will plot near 1.0 in the diagram. Elements that have been depleted will plot below 1.0 and elements that have increased will plot above 1.0.

There are some good reasons to caution about the interpretation of this type of 'spider diagram.' First, the analyses used as the normalizing composition is the initial ash that may not be well

known and is certainly not better quantified than the higher temperature ashes. Therefore, the uncertainty doubles at the best. The uncertainties in the normalized values are at least 6 %, but may for some elements in low concentrations like the rare earth elements magnify to 20 % or above. Second, many of the concentrations are very low near the lower limit of detection and with high analytical uncertainties. This results in large fluctuations in the normalized concentrations. Third, some elements have not been analyzed because they occur in concentrations below the detection limits in particular for the straw ashes. Nevertheless, these 'spider-diagrams' offer a convenient tool for illustrating relative elemental concentrations. The same type of diagrams later used in this report is normalized to well-known standards or other compositions such as average continental crust and river water.

The wood ash results are summarized in Figure 32. There are some systematic features in the patterns. A group of elements indicate strong depletion. These are, as already identified: K, Rb, Ag, Cd, Cs, and Pb. Their depletion are attributed to losses as a result of firing. The rare earth elements also suggest some depletion increasing with increasing firing temperature. It is possible that Yb is lost from the slag; however, the systematic depletion may simply result from a poorly known concentration in the initial ash. Some irregularities in the concentrations (particularly Th) can be attributed to analytical problems for small concentrations (see Table 13). The remaining elements, in general, plot as expected at or above the base line. The transition metals show enrichment with the exception of Sc, Ti, and Fe. Both Ti and Fe were analyzed as major elements and their concentrations may not be sufficiently accurate to be treated as trace elements.

The wheat straw ash results are summarized in Figure 33. The majority of the elements indicate enrichments again as expected from the effect of loosing volatile components during firing (C, S, N, and Cl). The only elements that may possibly have been lost during firing are As and Se. The elements Cd, Cs, and Ba show relative depletions compared to the adjoining elements. This depletion may reflect an absolute loss considering the general enrichment due to the release of volatile C-S-N components during firing. The rare earth elements show constant ratios with curious enrichments only in La and Yb. The apparent loss seen for Cr is probably attributable to error in the concentration of this element for the initial ash.

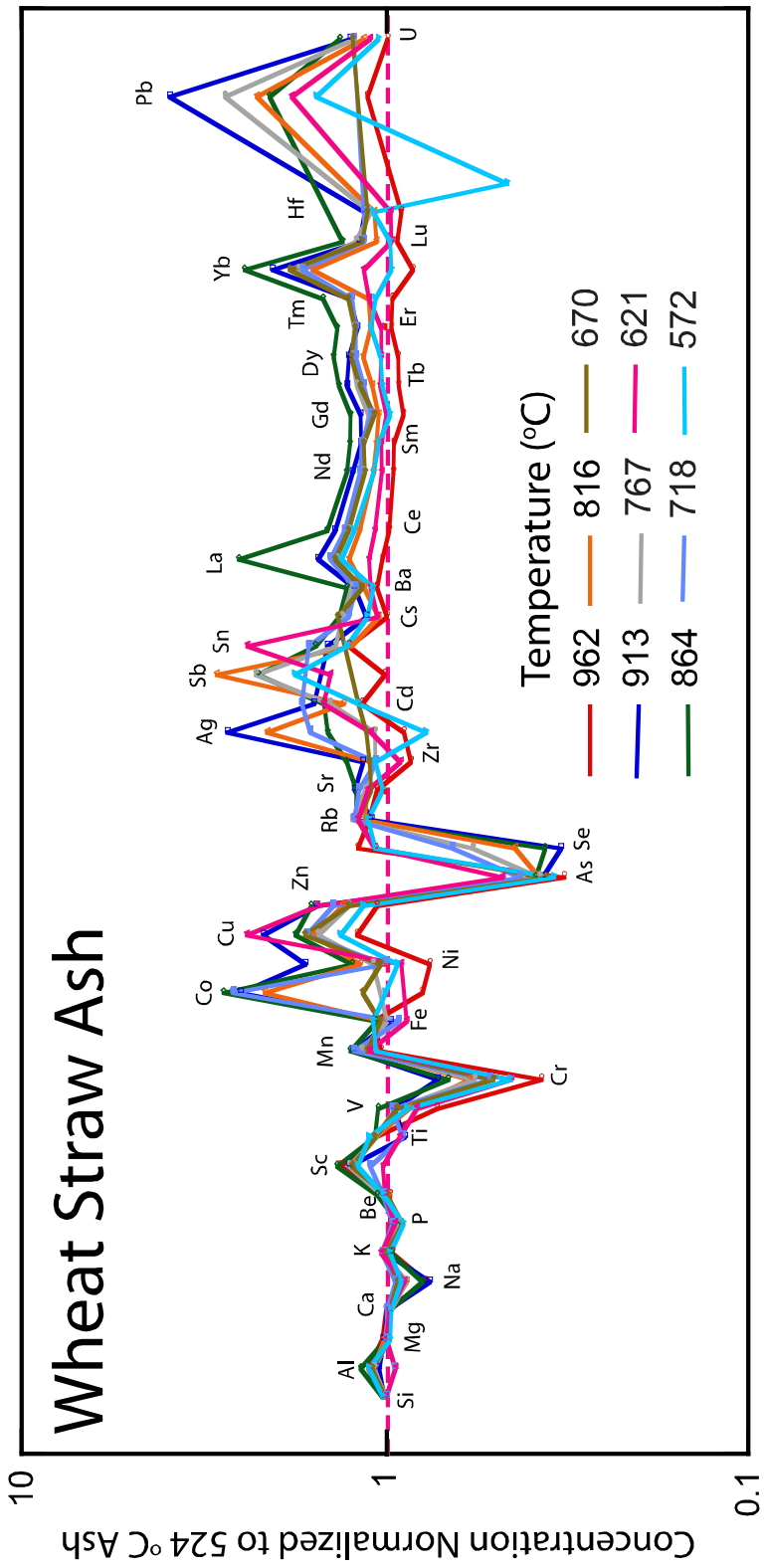

Figure 32. Normalized concentrations of major and trace elements in wood ash and slag arranged in order of increasing atomic number, with the exception that major elements are shown first in the sequence. Normalized to the 524 °C ash composition and color coded for firing temperature. Results affected by contamination (W, Ta) have been deleted together with obviously erroneous results.

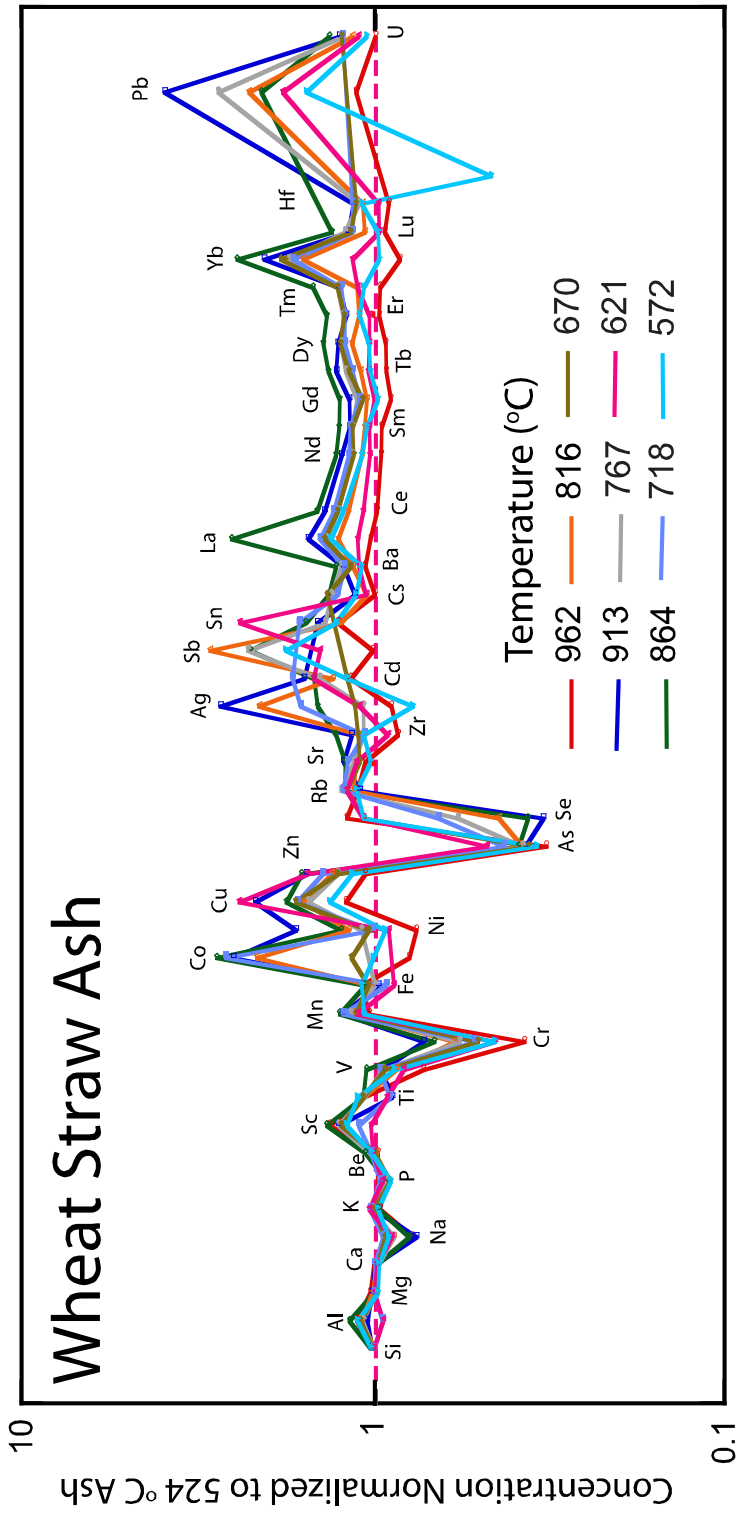

Figure 33. Normalized concentrations of major and trace elements in wheat straw ash and slag arranged in order of increasing atomic number, with the exception that major elements are shown first in the sequence. Normalized to the 524 ^{o}C ash composition and color coded for firing temperature. Results affected by contamination (W, Ta) have been deleted together with other obviously erroneous results.

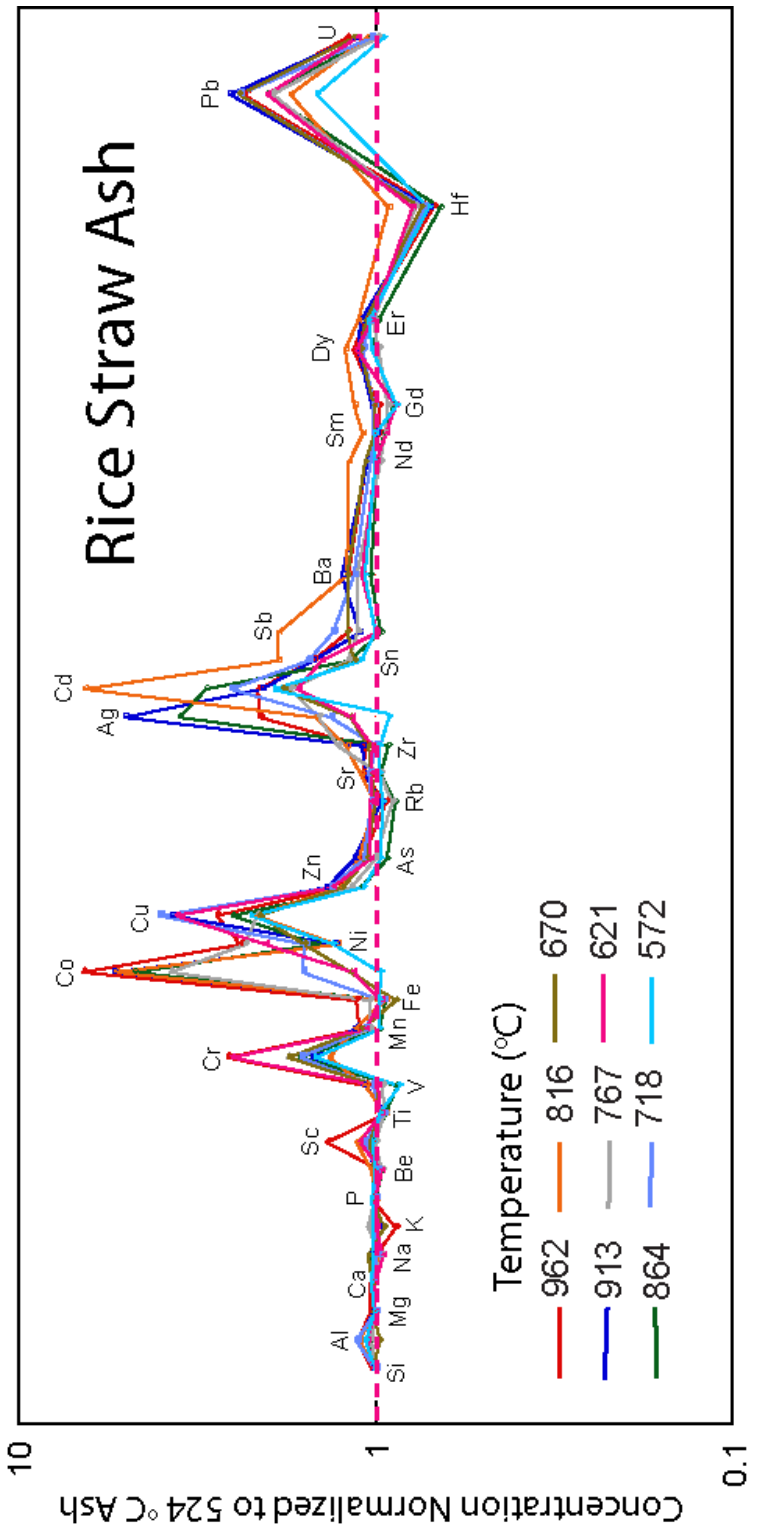

Figure 34. Normalized concentrations of major and trace elements in rice straw ash and slag arranged in order of increasing atomic number, with the exception that major elements are shown first in the sequence. Normalized to the 524 °C ash composition and color coded for firing temperature. Results affected by contamination (W, Ta) have been deleted together with other obviously erroneous results. The high temperature products above 962 °C are not shown.

The rice straw ash results are summarized in Figure 34. The high temperature ashes (1011-1325 ^{o}C) are not included on this diagram in order to simplify the presentation and also because of the need for reanalyzing these ashes (the whole data set can be seen in Tables 11 to13). The pattern observed has many of the same features as seen for the wheat straw ashes. The majority of the elements again indicate enrichments as expected from the effect of loosing volatile components during firing (C, S, N, and Cl). The majority of the major elements show little deviation from the base line, with the exception for K that may show losses and Al that may indicate enrichments. It should be noted that Al is the only element that may potentially be enriched during firing from reactive interactions with the alumina container (despite Pt lining). Such contamination is despite Pt lining particularly seen for some of the high temperature rice straw ashes (Table 11). The trace elements As and Rb may suggest relative depletions as also seen for As for the wheat straw. The nature of the apparent depletion in Hf is uncertain and may de caused by an error in the concentration of this element in the initial ash.

The normalized ratios depend on three competing processes. Enrichments may result from contaminations during ash preparation (W, Ta) or from reactions with container material during firing (Al). Analyses clearly affected by contamination (W, Ta) have been eliminated and are not shown on the various diagrams, unless otherwise specified (the full data set can be seen in Tables 11 to 13). Systematic enrichments also will result from the removal of volatile components from the system resulting in enrichments in the concentrations and ratios of the remaining elements (see Table 14). The magnitude of this enrichment increases as a function of firing temperature and may amount to as much as 60 % for the high temperature wood ashes. Finally, depletions result from the removal of certain elements (K) from the system often together with volatile gaseous components (C, S, N, and Cl). The general enrichment due to the removal of volatile components will mask depletions.

7.10. Average Concentrations

Tables 15 and 16 summarize the average concentrations of the experimental ashes and slag. The original data have been screened to eliminate concentrations resulting from contamination and other erroneous results. For each ash are given the average, standard deviation, and the number

of determinations used in the calculations. As a result, 37 trace elements in the ashes of the three fuel types were detected. Many trace elements, however, are near the lower limit of detection. Particularly, the rare earth elements were present in concentrations often too low to be detected in the straw ashes. The majority of the trace elements were detected using ICPMS techniques (Table 15). The INAA techniques proved useful for measuring particularly the transition metals, but were unable to obtain reliable results for the rare earth elements and also many of the heavier trace elements (Table 16).

Table 15. Trace Element Averages and Standard Deviations (ppm) for ICP-MS

Element	Wood			Wheat Straw			Rice Straw		
	Average	Std	N	Av	Std	N	Av	Std	N
Be	1.05	0.07	11	0.92	0.02	10	0.9	0.1	14
V	33.0	5.1	11	16.1	1.7	10	3.4	0.4	14
Cr	118	27	11	36.2	11.1	10	14.5	3.9	14
Mn	20584	3944	11	829	62	10	3923	244	14
Co	10	2	11	6	4	10	4	3	14
Ni	78	20	11	20	5	10	9.8	3.0	14
Cu	177	26	11	51	13	10	35	13	14
Zn	936	164	11	80	13	10	190	18	14
As	16.1	3.3	11	5.2	2.4	10	5.6	1.3	14
Se	1.0	0.3	10	2.0	0.9	10	0.1	0.0	3
Rb	120	43	11	49	3	10	62	7	14
Sr	2213	226	11	262	17	10	86	19	14
Zr	15.6	4.1	11	7.8	0.9	10	1.5	0.4	14
Ag	1.5	0.9	11	0.1	0.1	10	0.1	0.0	14
Cd	6.7	2.0	11	1.6	0.3	10	0.3	0.2	14
Sn	1.3	0.3	11	0.9	0.5	8	0.4	0.1	14
Sb	0.73	0.11	10	0.42	0.11	9	0.22	0.05	14
Cs	0.60	0.39	9	0.35	0.04	10	0.31	0.01	4
Ba	2222	265	10	743	57	10	112	10	14
La	1.84	0.80	11	0.61	0.19	10	0.30	0.06	4
Ce	2.29	0.73	11	1.63	0.21	10	0.64	0.14	4
Pr	0.14	0.11	9			0	0.09	0.02	4
Nd	1.69	0.40	11	1.12	0.10	10	0.36	0.08	14
Sm	0.38	0.08	11	0.29	0.02	10	0.15	0.07	14
Gd	0.33	0.10	11	0.21	0.02	10	0.03	0.01	14
Tb	0.04	0.01	10	0.03	0.00	10	0.01	0.00	6
Dy	0.24	0.07	10	0.18	0.02	10	0.03	0.00	11
Er	0.25	0.07	11	0.24	0.03	10	0.07	0.03	14
Tm	0.03	0.01	11	0.03	0.00	10	0.02	0.00	4
Yb	0.06	0.04	10	0.03	0.01	10			0
Lu	0.02	0.01	10	0.01	0.00	10			0
Hf	0.47	0.09	10	0.28	0.02	9	0.17	0.07	14
Ta	0.28	0.08	10	0.37	0.29	9	0.53	0.55	14
W	0.93	0.13	5	0.35	0.11	4	0.20	0.07	4
Tl	0.25	0.07	8			0	0.01	0.00	4
Pb	7.1	4.2	11	5.7	2.8	9	4.0	1.2	13
Th	0.17	0.11	6			0			
U	0.30	0.04	11	0.10	0.01	10	0.02	0.01	14

Av, average; Std, standard deviation; N, number of determinations.

Table 16. Trace Element Averages and Standard Deviations for INA

Element	Wood			Wheat Straw			Rice Straw		
	Av	Std	N	Av	Std	N	Av	Std	N
Sc	2.58	0.29	11	1.14	0.12	10	0.16	0.01	14
Cr	89	24	11	25.0	7.5	10	11.4	5.0	14
Mn	13834	1696	11	489	28	10	2474	154	14
Co	8.22	1.26	11	4.75	3.28	10	3.80	1.91	14
Rb	135	51	11	50	4	10	66	11	14
Sr	2413	412	4						
Cs	1.0	0.4	2	0.6		2	0.5		1
Ba	2280	332	11	574	45	10	102	3	3
La	4.6	1.4	11	0.9	0.2	5			
Ce	9.4	2.8	5						
Sm	0.7	0.1	11	0.3	0.1	7			
Eu	0.3		1						
Lu	0.2	0.2	3						
Hf	0.9	0.0	2						
Ta	8.8		1	0.6	0.4	4	0.9	0.5	3
Th	0.9	0.1	4	0.3		1			

Av, average; Std, standard deviation; N, number of determinations.

Figure 35 shows the average ash concentrations normalized to average upper continental crust after Rudnick and Gao (2004). The straw ashes show strong relative depletion in particularly Al and Na, many of the transition metals including Fe, Zr and Ag, the rare earth elements, and all heavier elements. The exceptions are K, P, and Cd that are all relatively enriched in the straw ashes. The wood ash in contrast is enriched in many elements including Mg, Ca, K, P, Mn, Cu, Zn, Sr, Cd, and Ba relative to global upper continental crust.

The same avarege concentrations are shown in Figure 36 normalized to average global river water as compiled by Gaillardet et al. (2004) and Meybeck (2004). The normalized concentrations show many similarities to the continental crust normalization of Figure 35, but also some notable differences. The elements K, P, and Al are in contrast relatively enriched compared to Mg, Ca, and Na. There is a constant plateau for the rare earth elements on both normalized diagrams indicating thate these elements are equally partitioned into the plant material during growth.

The interpretation of this type of diagram is outside scope of this report. Their usefulness depends on the identification of likely sources of trace elements that may offer better normalization compositions that those used here. It is also advantageous if the elements are arranged in an order that reflect partitioning processes plant during growth. The ‘saw blade’

pattern seen for all fuel types suggests a strong differentiation between elements and that the trace element partitioning into the plant material was not for all elements controlled by passive uptake. Some elements, such as the macronutrients K and P are actively taken up during plant growth with final concentrations on whole biomass samples dependent on partitioning among the various plant tissues and the stage of growth. Other elements are passively accumulated with other elements and reflect concentrations in soil, water, and any applied fertilizers.

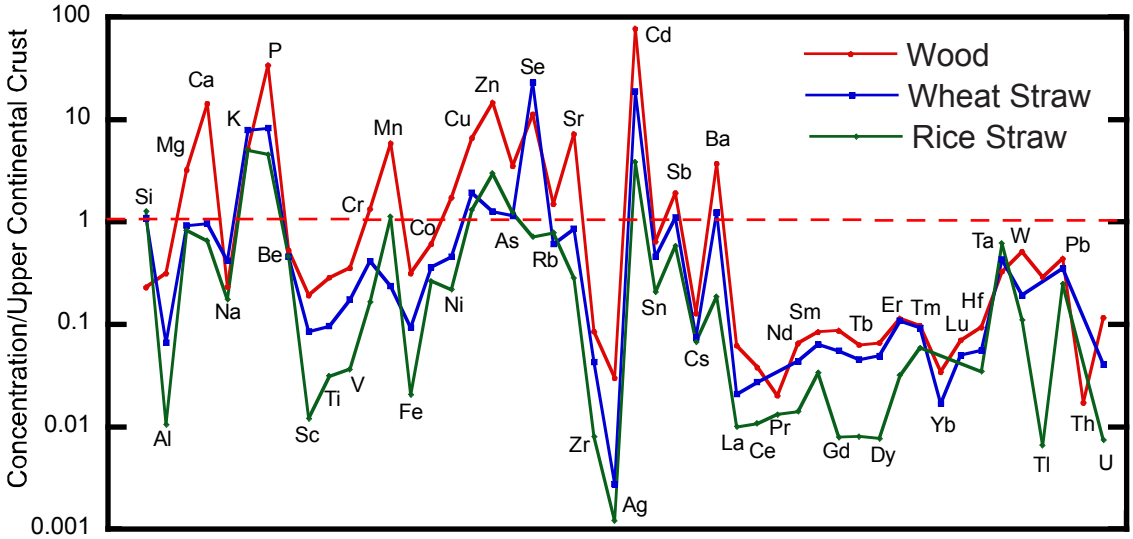

Figure 35. Normalized concentrations of average major and trace element concentrations arranged in order of increasing atomic number, with the exception that major elements are shown first in the sequence. Normalized to average continental upper crust (Rudnick and Gao, 2004). Results affected by contamination (W, Ta) have been deleted together with other obviously erroneous concentrations (see Tables 15 and 16 for the full dataset).

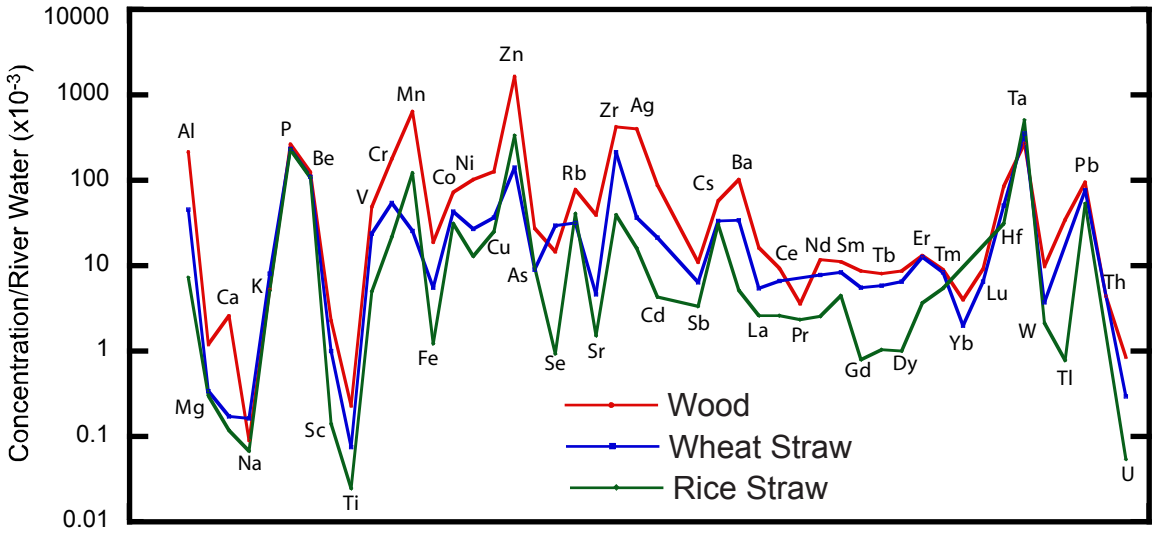

Figure 36. Normalized concentrations (x 10^{-3}) of average major and trace element concentrations arranged in order of increasing atomic number, with the exception that major elements are shown first in the sequence. Normalized to average global river water composition (Livingstone, 1963; Holland, 1978; Gaillardet et al., 2004; Meybeck, 2004). Results affected by contamination (W, Ta) have been deleted together with other obviously erroneous results (see Tables 15 and 16).

Table 17. Summary of Trace Element Concentrations in Fly Ashes and other Ashes

Element	HEL-A	EER	Urban Wood	CFM	LR-S	Wood17:40	Wood15:52	Straw12:35	Straw14:30	Flyash2000	CycFBC6	CycFBC5	CycFBC3
wt. %													
Na_2O	0.15	0.13	2.94	19.55	0.06	1.94	1.98	1.80	1.69	1.67	0.12	0.17	0.14
K_2O	17.61	13.11	9.59	11.18	3.10	4.62	4.13	3.52	3.21	4.44	2.53	2.76	2.42
Fe_2O_3	0.42	0.08	3.47	1.31	0.14	5.04	4.97	4.40	4.41	3.86	3.17	4.68	5.29
Cl	2.60	2.99	0.76	22.16	0.25	0.66	0.50	0.31	0.32	0.59	0.33	1.02	0.93
ppm													
Be	0.96	0.84	1.7	1.2	1.4	1.0	1.7	1.7	1.9	2.0	1.3	1.4	1.3
Sc	0.17	0.10	6.9	2.2	0.08	13.1	14	12	12	8.7	2.8	3.8	4.4
V	4.1	2.3	107	22	4.0	4.0	162	140	140	102	30	60	48
Cr	15	6.8	1140	47	179	13	233	195	191	188	1263	3441	2481
Mn	10131	2675	2848	1802	1783	34	1452	2592	2930	1190	3103	4131	2999
Co	9.0	1.0	20	18	3.1	0.57	23	20	22	16	22	44	62
Ni	19	3.4	100	42	126	2.7	90	78	80	92	1134	2460	2025
Cu	77	12	705	203	43	11	544	445	442	483	157	226	194
Zn	346	122	4367	2223	87	31	1048	952	932	898	147	308	282
As	8.0	4.0	603	4.9	4.1	4.0	79	59	57	56	6.9	12	11
Se	0.05		1.4	1.1	0.11		1.3	1.2	0.93	1.2	0.49	1.7	2.3
Rb	117	25	100	78	16	2.8	72	78	71	75	27	36	32
Sr	80	53	1563	506	82	104	930	814	787	822	852	1695	1015
Zr	1.5	1.1	65	8.6	1.3	3.2	46	48	46	48	11	23	22
Ag	0.13	0.19	1.1	0.14	0.10	0.07	1.2	1.0	1.1	0.96	0.77	1.6	2.3
Cd	13	2.5	3.3	1.1	2.1	0.19	5.1	3.5	4.0	3.3	2.0	5.9	8.0
Sn	0.53	0.32	11	3.0	2.6	0.61	19	12	14	18	5.4	7.5	11
Sb	0.31	0.16	15	0.96	0.29	0.45	17	10	10	13	1.1	2.1	2.8
Cs	0.13		2.1	1.4	0.42	0.38	2.2	2.5	2.4	2.8	0.63	0.89	0.80
Ba	199	101	1429	275	113	106	979	925	935	861	1366	2601	1650
La	0.14		18	3.1	0.30	1.3	15	16	15	15	5.1	9.1	7.1
Ce	0.58		37	6.0	0.68	2.4	30	33	32	31	7.8	13	12
Pr			4.2	0.77	0.12	0.32	3.6	3.9	3.8	3.6	1.1	1.8	1.5
Nd	0.51	0.28	17	3.2	0.54	1.4	15	16	16	14.7	3.9	6.7	5.7
Sm	0.20	0.11	3.3	0.83	0.32	0.42	3.2	3.4	3.4	3.1	0.85	1.3	1.2
Eu							0.08	0.03	0.05	0.05			
Gd	0.04	0.03	1.8	0.48	0.03	0.11	1.9	1.9	2.0	1.9	0.40	0.65	0.54
Dy		0.02	1.2	0.21			1.5	1.5	1.4	1.4	0.07	0.26	0.21
Er	0.07	0.08	1.1	0.33	0.06	0.11	1.4	1.4	1.4	1.4	0.26	0.44	0.38
Tm	0.01		0.16	0.08	0.05	0.03	0.21	0.21	0.21	0.23	0.06	0.09	0.08
Yb			0.49	0.05			0.65	0.62	0.64	0.70		0.08	0.06
Lu										0.01			
Hf	0.16	0.13	1.3	0.39	0.26	0.24	1.4	1.3	1.4	1.4	0.55	0.86	0.83
Ta	0.09	0.05	0.37	0.45	0.17	0.03	0.68	0.48	0.58	0.91	0.36	0.60	0.56
W	0.16	0.10	27	4.5	0.26	0.42	19	9.8	11	14	6.9	14	11
Tl			0.10	0.03	0.06	0.01	0.27	0.21	0.27	0.29	0.20	0.54	0.30
Pb	5.3	2.9	959	5.0	4.3	4.1	247	139	159	215	18	15	5.6
Th			1.9				1.5	1.8	1.7	1.3	1.7	0.67	1.3
U	0.03		1.1	0.49	0.04	0.03	1.4	1.2	1.4	1.4	0.68	0.58	0.27

Blank means that the element wes not detected.
Tb and Ho were not detected in any of the ashes.
Na_2O, Cl, K_2O, Fe_2O_3, and Sc were determined by INA.

Table 18. Analyses Used as Normalizing Values in this Report

Element/ Oxide	1633a wt. % or ppm	Wood Ash wt. % or ppm	Wheat Straw Ash wt. % or ppm	Rice Straw Ash wt. % or ppm	Average Upper Continental Crust wt. % or ppm	River Water ppb
SiO_2	*50.24*	14.68	*69.51*	*80.59*	*66.60*	
Al_2O_3	*27.97*	4.63	*0.97*	*0.15*	*15.40*	12
MgO	*0.82*	7.66	*2.18*	*1.94*	*2.48*	4100
CaO	*1.60*	49.16	*3.29*	*2.24*	*3.59*	15000
Na_2O	*0.21*	0.73	*1.30*	*0.54*	*3.27*	6300
K_2O	*2.39*	13.86	*20.94*	*13.37*	*2.80*	2300
P_2O_5	*0.40*	4.84	*1.18*	*0.65*	*0.15*	1.82
Be	11.2	1.05	0.92	0.91	2.10	0.01
Sc	197	2.58	1.14	0.16	14	1.20
TiO_2	*1.40*	0.17	*0.06*	*0.02*	*0.64*	0.49
V	300	33	16.1	3.36	97	0.71
Cr	185	118	36	14.5	92	0.70
Mn	185	20584	829	3923	3675	34
Fe_2O_3	*14.10*	1.69	*0.49*	*0.11*	*5.60*	66
Co	44	10.0	5.98	4.34	17.3	0.15
Ni	121	78	20	9.80	47	0.80
Cu	115	177	51	35	28	1.48
Zn	224	936	80	190	67	0.60
As	147	16.1	5.25	5.62	4.80	0.62
Se	12.2	0.97	1.96	0.06	0.09	0.07
Rb	141	120	49	62	84	1.63
Sr	920	2213	262	86	320	60
Zr	256	15.6	7.80	1.46	193	0.04
Ag	0.61	1.52	0.14	0.06	53	0.00
Cd	1.07	6.67	1.61	0.33	0.09	0.08
Sn	7.45	1.29	4.86	0.41	2.10	
Sb	7.56	0.78	0.64	0.22	0.40	0.07
Cs	12.8	0.60	0.35	0.31	4.90	0.01
Ba	1542	2222	743	112	628	23
La	80	1.84	0.61	0.30	31	0.12
Ce	186	2.29	1.63	0.64	63	0.26
Pr	23	0.14		0.09	7.10	0.04
Nd	92	1.69	1.12	0.36	27	0.15
Sm	19.5	0.38	0.29	0.15	4.70	0.04
Gd	17.4	0.33	0.21	0.03	4.00	0.04
Tb	2.47	0.04	0.03	0.01	0.70	0.01
Dy	16.1	0.24	0.18	0.03	3.90	0.03
Er	11.4	0.25	0.24	0.07	2.30	0.02
Tm	1.60	0.03	0.03	0.02	0.30	0.00
Yb	7.86	0.06	0.03		1.96	0.02
Lu	1.22	0.02	0.01		0.31	0.00
Hf	6.90	0.47	0.28	0.17	5.30	0.01
Ta	2.18	0.28	0.37	0.53	0.90	0.00
W	6.45	0.93	0.35	0.20	1.90	0.10
Tl	5.21	0.25		0.01	0.90	0.01
Pb	67	7.12	5.70	4.00	17.0	0.08
Th	25	0.17			10.5	0.04
U	8.98	0.30	0.10	0.02	2.70	0.37

See text for sources. Values in italic are as wt. % oxides.

8. Fly Ash Compositions

Several fly ashes produced under controlled fuel intake experiments were also analyzed as part of this study. The details of the ashes and the fuel blends used in the experiments are given in Chapter 3 (see Table 3 for a summary) and the analytical results summarized in Table 17. The concentrations of Na_2O, K_2O, Fe_2O_3, Cl, and Sc were determined by INAA, while the remaining elements were determined by ICPMS.

The first was a set of fly ashes collected during a fluidized bed experiment using the wood fuel examined in this study as the base for the combustion fuels. The results are shown in Figure 37 normalized to the base wood fuel ash (see Table 18). The three fly ashes (CycFBC6, CycFBC5, and CycFBC3) show remarkably similar patterns with strong depletions in many of the alkali elements (Na, K, Rb, Cd, Ba) and apparently also in Mn and Zn. Enrichments are seen for Se, Th, and some of the light rare earth elements. Conspicuous increases in Cr and Ni (and probably W) are likely related to contamination from boiler materials (steel). The CycFBC5 fly ash was produced from the pure wood fuel and would thus be expected to plot at the base line (1.00) when normalized as in Figure 37. The strong deviation from the base line for many elements is due to differentiation during combustion. Either preferential removal with the flue gas, deposition on furnace walls or bed material, contamination from boiler material, or preferential partitioning into particulate matter and aerosols, including fly ash, may cause this differentiation. The ashes CycFBC6 and CycFBC3 were produced from wood-rice straw blends with respectively 10.7 and 2.4 wt. % rice straw. The CycFBC6 experiment in addition utilized a leached rice straw that is reflected in the low concentrations of many elements in this ash, compared to the ashes from the pure wood fuel and the unleached rice straw blended experiments. The low abundances for many trace elements seen for CycFBC6 probably mostly reflect the high straw content for this experiment (see discussion below on straw ash abundances).

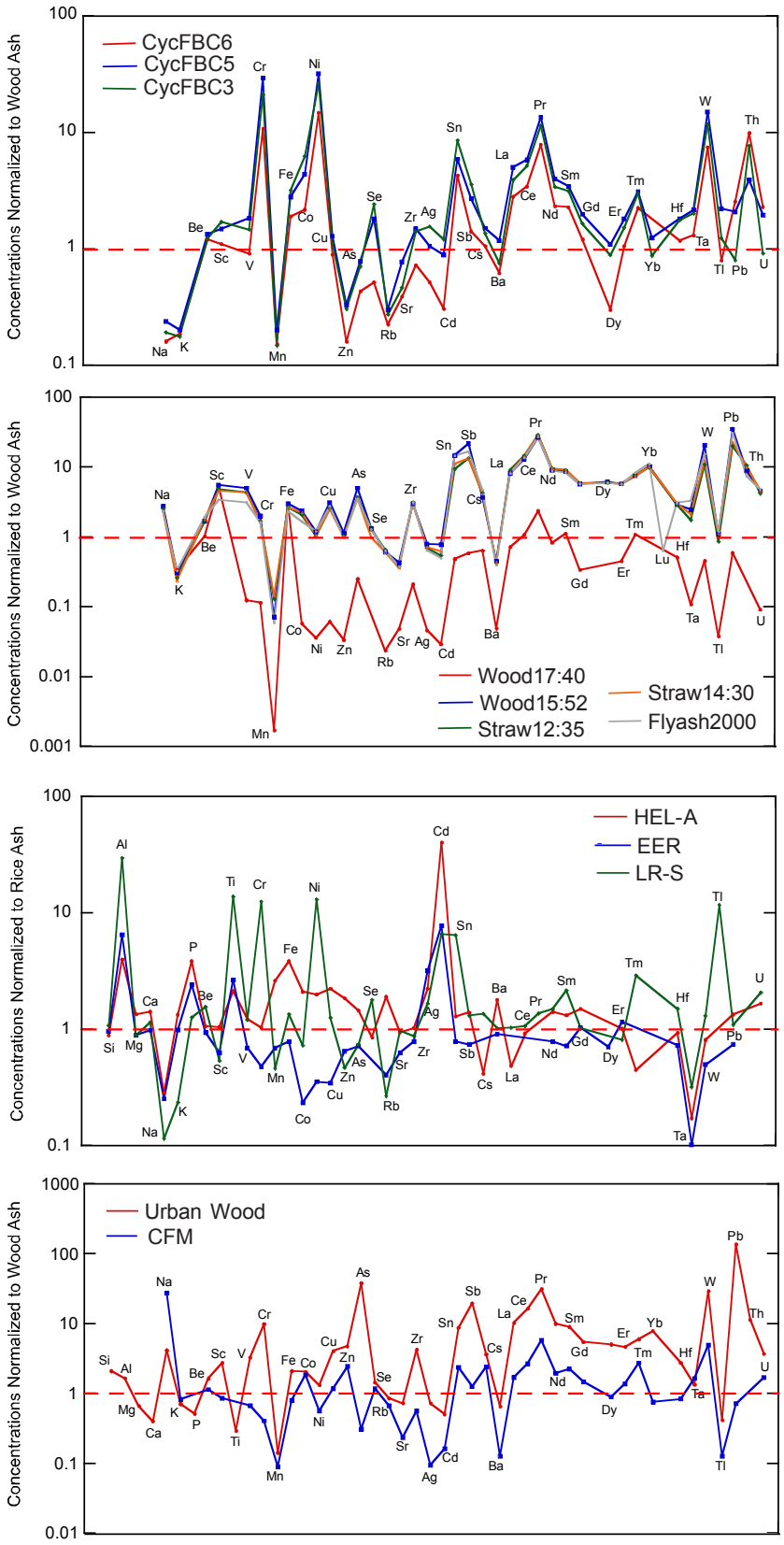

Figure 37. Normalized concentrations of major and trace elements (Table 17) arranged in order of increasing atomic number, with the exception that major elements are shown first in the sequence. Normalized to either wood or rice straw ash as indicated (Table 18).

A second set of experimental fly ashes (Table 17) was produced at an operating commercial, biomass-fueled, power plant (see Chapter 3) (Wood17.40, Wood15.52, Straw12.35, and Straw14.30). These ashes are shown in Figure 37 again normalized to the wood ash investigated in this study. The wood fuel utilized in the experiment was a blend between orchard pruning and urban wood fuel. The experiments prefixed 'straw' were based on blending leached rice straw with the base wood fuel (1:3 ratio, respectively). There is again a remarkable similarity between the fly ashes. The systematic low values for many elements by a factor of 10 obtained on Wood17.40 cannot be related to the fuel source and is most likely due to a dilution error made during preparation for ICPMS analysis. This is supported by the observation that the elements determined by INAA do not show the same dilution.

The analytical results for the fly ash from the commercial power plant indicate depletion in K and Mn and some enrichment in Sn, Sb, some rare earth elements, W, and Pb. The enrichments in Sb and Pb were not seen for the laboratory fluidized bed experiments and may be related to the use of urban wood in the fuel blends. It is further remarkable that the a fly ash collected a few years after the original power plant experiments (Flyash2000) shows very similar results suggesting strong consistency in the fuel plant intake blends and fuel source trace element compositions.

A group of ashes produced from firing rice straw at 575 ^{o}C are also illustrated in Figure 37 (HEL-A, EER, LR-S) normalized to the presently investigated rice straw ash (Table 18). The LR-S ash was produced from leached rice straw, while the remaining were produced from unleached, crude rice straw. The analytical results show remarkably large sample-to-sample variation that may be related to seasonal and geographical origin of the straws. The strong enrichment for the leached rice straw (LR-S) in Al and Ti may partly be explained by the strong loss of K, Na, and Cl by leaching and differences in soil contamination between the samples. That Si does not show the same enrichment is the result of the high silica concentration in straw, so that the enrichment ratio remains near unity. High enrichments in Cr and Ni are most likely the result of contamination from milling equipment used in particle size reduction. Two additional ashes were analyzed as part of this study and are shown in Figure 37 (Urban Wood, CFM). The first of these is an urban wood fuel obtained from an operating biomass power plant. Compared to the clean wood ash investigated in this study, the urban wood ash shows increases in Cr, As, Sn, As, Zr, rare earth elements, W, and Pb reflecting the mixed source wood as well as

some contamination from boiler materials. The ash identified by CFM (California cattle feedlot manure ash) shows less dramatic variations when normalized to wood ash. The most notable feature is the high concentrations in Na and Cl stemming in part from salt additions to cattle feed rations (see Table 17).

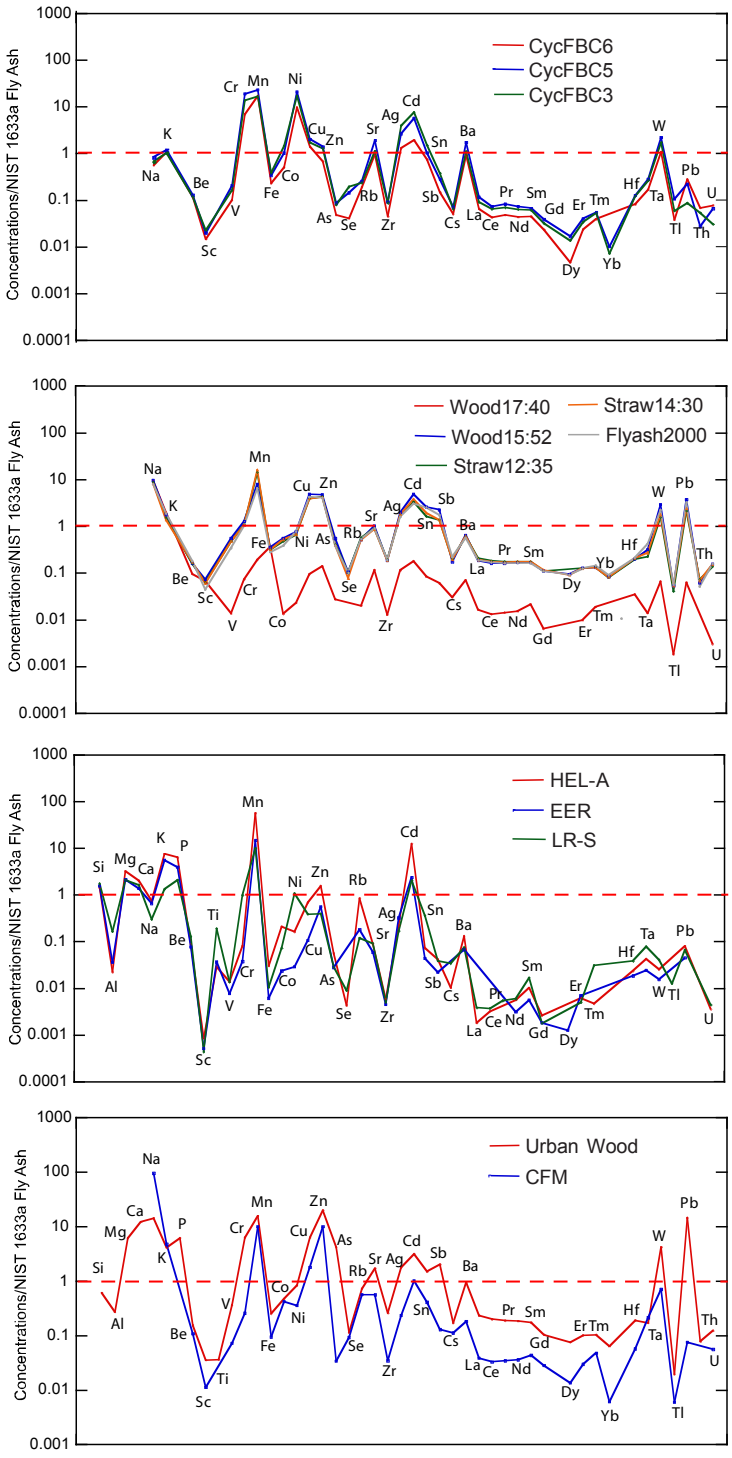

Figure 38. Normalized concentrations of major and trace element concentrations (Table 17) arranged in order of increasing atomic number, with the exception that major elements are shown first in the sequence. Normalized to NIST Flyash 1633a (Table 18).

The same groups of ashes are shown in Figure 38 normalized to the NIST Flyash 1633a (Table 18) that is representative for fly ash from a typical coal fueled power plant. There are some interesting systematic features for the wood based ashes, when compared to the coal fly ash. The rare earth elements are systematically low compared to coal fly ash. Many heavy elements also have low concentrations (Hf, Ta, W, Pb, Th, U) except where an urban waste was blended into the fuel. Similarly, some transition metals variably show high concentrations in the wood based fuels (Cr, Mn, Cu, Zn) that may either be related to the use of urban wood components in the source fuel or to contamination from boiler materials.

The trace element concentrations shown in Figure 39 are the same analyzes as previously shown (Table 17) normalized to the wood ash (Table 18). Instead of sequencing the trace elements in order of increasing atomic number, they have now been arranged in order of decreasing continental crust abundances when normalized to primitive mantle (Gillardet et al., 1999). This order is equivalent to decreasing magmatic compatibility and has been widely used to study river water and their suspended sediment loads (Gillardet et al., 1999, 2004). This approach to ordering the elements, as determined by important processes being studied, has been widely successful in geochemical studies. It provides a coherent order and groups elements that behave in similar fashions. There are some reasons for using the upper continental crust sequencing for studing trace elements in organic material such as the availability of material for weathering and soil formation. The most mobile elements are dissolved in interstial waters in soil. The remaining elements are incoporated into secondary clay and oxy-hydroxide products. Both groups of elements are transported in run-off water either dissolved or as suspended sediment particles that eventually provides nutritional components for plant growth. The success of this element sequencing in clearly displaced in Figure 39 by strongly reducing the irregularity in the plot and by grouping elements.

This brief survey of some fuel or potential fuel ashes was not intented as a comprehnsive study. Detailed studies of the fractionation during combustion are essential for better understanding trace element behavior. Also required is a better overall understanding of the trace element compositions of biomass material, including well characterized biofuel standards. It is finally clear from this brief survey that biological processes in part control partitioning of trace elements into annual growth material and that the trace pattens cannot only be explained by passive uptake from the soil and water substrata.

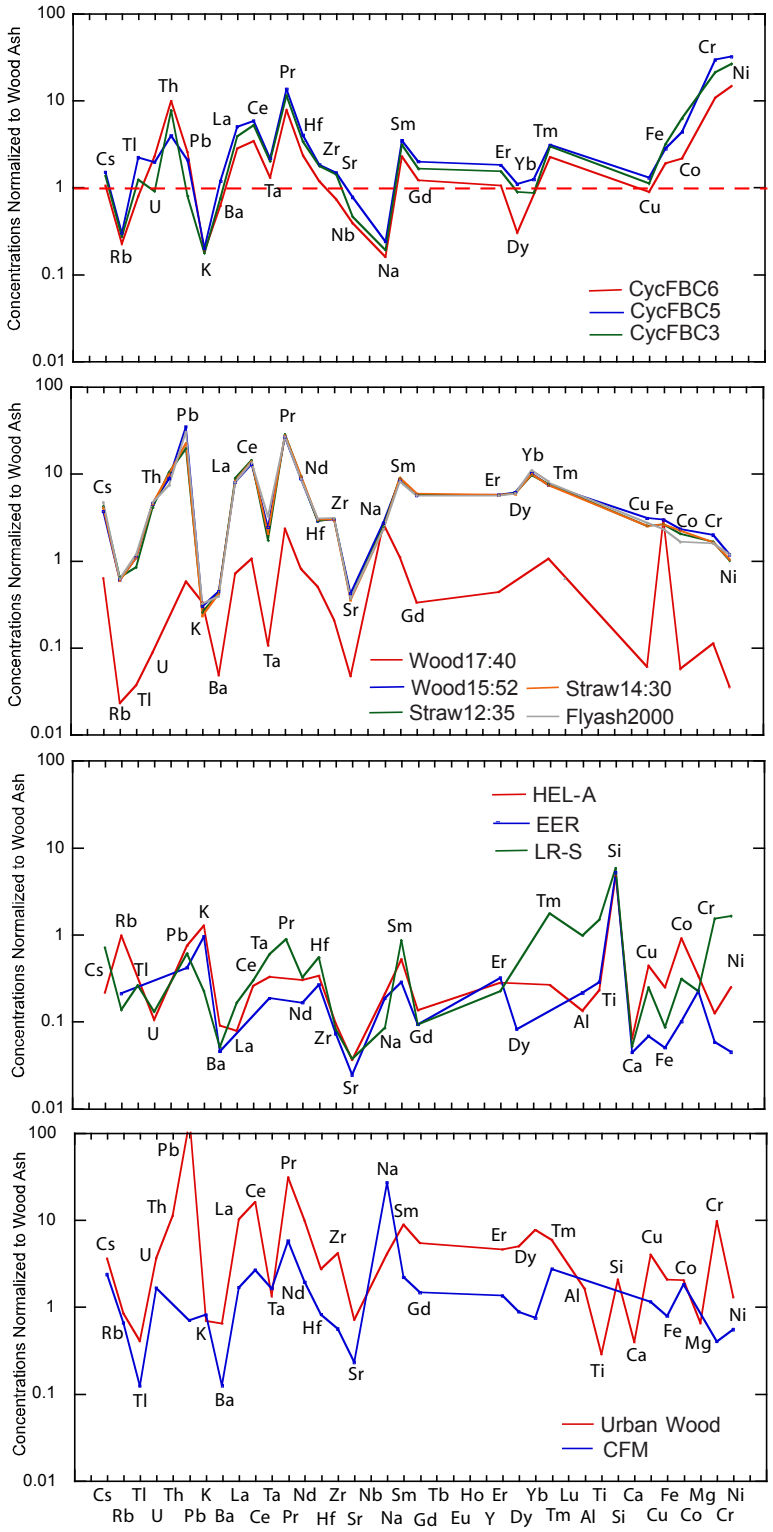

Figure 39. Major and trace element conentrations of fly ash (Table 17) normalized to wood ash (Table 18). Arranged in order of decreasing continental crust abundances (toward the right) when normalized to primitive mantle (Gillardet et al., 1999). This order is equivalent to decreasing magmatic compatibility.

9. Toxicity

United States Environmental Protection Agency's 'Toxicity Characteristic Leaching Procedure' determines the mobility of both organic and inorganic compounds present in solid wastes. The toxicity analysis simulates landfill conditions and determines the concentrations of contaminants present in extracted leachate and determines if a waste meets the definition of toxicity and will require handling as a hazardous waste. For solid wastes (like ashes and slag), the regulations allow the use of a total constituent analysis instead of the more involved extraction analysis. The result of a total constituent analysis is divided by twenty to convert into an equivalent leachable concentration that thus carries the toxicity characteristics.

The Environmental Protection Agency's heavy trace element toxicity limits are given in Table 19 and compared to the average ash and fly ash compositions determined in this study. In bold are identified the elements for which the equivalent leachable concentrations exceeds the permitted concentrations. For wood ash, these are Ba and Cr that barely exceed the limits. The straw ashes are all well below the permitted limits. For ashes and fly ashes for which a significant component of urban wood material are involved, As, Cr, and Pb may variably exceed the limits. For many of these types of ashes, a regular extracted leachate may be better suited to identify possible toxic concentrations. Many biomass power plants already analyze ash to test for compliance.

Table 19. Toxicity of Fuel Ashes

EPA Hazardous Waste Code	Element	EPA limits* (ppm)	Wood Ash (ppm)	C/20	Rice Straw Ash (ppm)	C/20	Wheat Straw Ash (ppm)	C/20	Urban Wood Ash (ppm)	C/20	Fly Ash (ppm)	C/20
D004	Arsenic (As)	5	16.1	0.81	6	0.28	5.2	0.26	603	**30**	56	2.8
D005	Barium (Ba)	100	2222	**111**	112	5.6	743	37	1429	71	861	43
D005	Cadmium (Cd)	1	6.7	0.34	0.3	0.02	1.6	0.08	3.3	0.17	3.3	0.17
D007	Chromium (Cr)	5	118	**6**	14.5	0.73	36	1.8	1140	**57**	188	**9**
D008	Lead (Pb)	5	7.1	0.36	4	0.2	5.7	0.29	959	**48**	215	**11**
D009	Mercury (Hg)	0.2	(35 ppb)									
D010	Selenium (Se)	1	1	0.05	0.1	0.01	2	0.1	1.4	0.07	1.2	0.06
D011	Silver (Ag)	5	1.5	0.08	0.1	0.01	0.1	0.01	1.1	0.06	0.96	0.05

*Elemental limits following the EPA Toxic Characteristic Leaching Procedure.
C/20, concentration divided by 20. Bold indicate adjusted concentrations exceeding EPA limits.

10. Conclusions

10.1. Summary

Use of biomass fuel, such as wood and straw materials, for power and fuel generation result for most combustion systems in atmospheric emissions (gas, aerosol) and a significant volume of solid byproducts, including fly ash. Increased utilizing of such byproducts as a partial substitute for soil fertilizers has lead to concerns, particularly as increase use is made of municipal and industrial solid wastes. Understanding of the partitioning of major and trace elements between solid and gas has thus become critical for environmental and regulatory purposes and for plant operation.

This report present analytical results on the major and trace element concentrations and their mobility in three series of temperature-controlled, experimental ashes produced from wood, rice straw, and wheat straw fuels. The fuels utilized are relatively void of domestic and industrial components and provide the base for evaluating trace elements and their behavior in potential biomass fuels. The experimental results were tested by analyzing a series of fly ashes (and other ashes) produced from fuel-intake-controlled, laboratory-scale, fluidized bed-combustor and an commercial operating, biomass-fueled, power plant.

Ashing experiments as a function of fuel type and firing temperature (wood, rice straw, and wheat straw) reveal systematic mineralogical and compositional variations. At low ashing temperatures, wood fuel decomposes leaving significant carbonates and amorphous silicate in the solid fraction together with mainly carbon residuals such as graphite. Straw fuels decompose leaving amorphous silicate and halite salts in the solid residue. Increasing combustion temperature drives off the remaining carbon and salt at temperatures determined by mineralogical and bulk chemical compositions. Carbonates decompose at about 700 ^{o}C and give way to silicate and oxide minerals in the residue prior to partial melting at very high temperatures from about 1350 ^{o}C. The straw ashes become increasingly void of graphite with increasing crystallinity (silica minerals) and show breakdown of halite salts (principally sylvite) from about 1000 ^{o}C. The straw ashes melt at a relatively low temperature dependent on potassium and silica contents (wheat straw from 800 ^{o}C).

Potassium and sodium are for all fuels also lost as a function of firing temperature. These changes and transformations as a function of firing temperature result in marked elemental losses amounting to a maximum of about 40 % by weight for wood fuel. The weight losses from the straw fuels amounts in contrast to a maximum of 20 %. These fundamental processes will be manifested in two competing factors when considering trace element abundances. The first is that structural and mineralogical transformations in the solid residue can control the fate of trace elements. The second is that the abundances of trace elements are influenced by enrichment controlled by volatile releases (amounting to a maximum of 40 %) and depletions resulting from removal with the volatile components. The latter depletion can be so severe that some elements can be completely removed from the solid fraction (potassium and sodium).

The concentrations of major and trace elements in the experimental ash and slag were analyzed using various multielement instrumental techniques. The majority of major and minor elements were analyzed using X-ray fluorescence spectroscopy (XRF) (Si, Ti, Al, Fe, Mn, Mg, Ca, Na, K, P). Some major and minor elements were in addition analyzed by instrumental neutron activation techniques (INAA) (Fe, Mn, Na, K). The majority of the trace elements were analyzed by inductively coupled plasma mass spectroscopy (ICPMS) with about 40 elements detected in most ashes. INAA using short irradiation duration techniques proved very successful in analyzing Na, Cl, K, Mn, and Sr. These results nicely supplemented the XRF results and added chlorine to the list of analyzed elements. The remaining elements were analyzed by INAA using long irradiation duration with variable results because of very low concentrations. It was possible to detect many of the transition and alkali metals, however, most of the rare earth and heavier elements could not be detected using INAA. Some elements, including mercury, could not be detected with either of the used methods. The recommended analytical methods and element combinations consist of XRF (or similar methods) for major and minor elements, the majority of trace elements using ICPMS, and short irradiation duration INAA for the alkali metals and chlorine. Additional analyzes for mercury (and other potential volatile elements such as As, Se, Sn, Sb) should be done using cold-vapor atomic absorption spectroscopy not evaluated here.

The resultant list includes all elements recommended by the European Union's Bionorm Project (Baernthaler et al., 2006) with the exception of molybdenum (Mo) that was not analyzed and mercury that could not be detected as discussed above.

There are distinct differences between the individual fuel types examined in this study. The average concentrations of major and trace elements in the ashes and slag were summarized in Tables 11 and 15. The wood ash is composed of the major oxides SiO_2, Al_2O_3, Fe_2O_3, MnO, CaO, K_2O, and P_2O_5 (all in concentrations above 1 wt. %) with SiO_2 and CaO by far dominating (~60 % of total) and with the minor oxides TiO_2 and Na_2O. The concentrations of titanium are low and could with advantage have been analyzed as a trace element. Trace elements in high concentrations in wood ash are Mn (20,000 ppm), Sr (2,200 ppm), and Ba (2,200 ppm). The concentrations of manganese are so high that this element should be classified as a major element. Elements in intermediate concentrations (100-10 ppm range) are many of the transition metals (V, Cr, Co, Ni, Cu, Zn), Zr, and Rb. Elements in the range 10-1 ppm include Be, As, Se, Cd, Sn, La, Ce, Nd, and Pb. The average lead concentration is 7 ppm. The remaining analyzed elements occur in concentrations below 1 ppm. Chlorine is not detected in the wood ash.

The rice straw ash is composed of the major oxides SiO_2, MgO, CaO, and K_2O (above 1 %) with SiO_2 and K_2O by far dominating (~90 % of total) and the minor oxides Al_2O_3, Fe_2O_3, MnO, Na_2O, and P_2O_5. The element titanium is near the detection limit and could together with aluminum and iron with advantage had been analyzed as trace elements. The only trace element in high concentrations in rice straw ash is manganese (4,000 ppm). Other elements in intermediate concentrations (200-10 ppm range) are many transition and alkali metals (Cr, Cu, Zn, Rb, Sr, Ba). Elements in the range 10-1 ppm include V, Co, Ni, Zr, and Pb. The average lead concentration is 4 ppm. The remaining analyzed elements occur in concentrations below 1 ppm. Chlorine occurs as a major element in concentrations up to 3.5 wt. %.

The wheat straw ash shows many features in common with rice straw and is composed of the major oxides SiO_2, MgO, CaO, Na_2O, K_2O, and P_2O_5 (above 1 %) with SiO_2 and K_2O by far dominating

(~80 % of total) and the minor oxides TiO_2, Al_2O_3, Fe_2O_3, MnO, Na_2O, and P_2O_5. The concentrations of Ti, Al, and Fe are low or near the detection limit and could with advantage have been analyzed as trace elements. The only trace elements in high concentrations in wheat straw ash are Mn (800 ppm), Ba (750 ppm), and Sr (250 ppm). Elements in intermediate concentrations (100-10 ppm range) are many of the transition and alkali metals (V, Cr, Ni, Cu, Zn, Rb). Elements in the range 10-1 ppm include Co, As, Se, Zr, Cd, Ce, Nd, and Pb. The average lead concentration is 6 ppm. The remaining analyzed elements occur in concentrations below 1 ppm. Chlorine occurs as a major element in concentrations up to 4.5 wt. %.

The concentrations of many major and trace elements depend on firing temperature. The alkali metals Na, K, Rb, and Cs show strong depletion with increasing firing temperature from 800 to 1000 ^oC, attributable to the removal of these elements from the ash or slag as a result of the decomposition of carbonate minerals. The same elements in the straw ashes show, particularly for potassium, similar depletions; however, the trace elements rubidium and cesium do not show detectable depletions because of the much lower concentrations and the concurrent enrichment due to the removal of more volatile constituents. Other elements that indicate increasing depletions with temperature are Ag, Cd, As, Se, and Pb. There is a general increase in residual concentrations of many elements with the removal of volatile constituents and increasing temperature that may amount to 60 % for wood ash.

Depletion was with increasing firing temperature observed for Cl, Na, K, Rb, Cs, Ag, Cd, As, Se, and Pb. The losses for the alkali metals in high concentrations, together with chlorine, were expected and are well established in the literature (Dayton et al., 1995; Björkman and Strömberg, 1997; Keown et al., 2005; Thy et., 2006a,b). It is thus not surprising that the trace alkali metals behave in a similar fashion. In a recent study of the effects of high (1000 ^oC) and low (<150 ^oC) ashing Richaud et al. (2004) detected variably high and/or temperature release of As, Se, Cd, Hg, Zn, Pb, and Mn from coal. Various forest residue and wood materials indicated release of Zn, Pb, Hg, and Mn. These results are in good correspondence with the present results, except that we did not observe loss of zinc and manganese. The loss observed for silver must be viewed with some caution, since the recovery of this element during analysis was at best poor (see Table 10).

Two fly ash sets produced during fuel-intake controlled experiments using either a laboratory-scale fluidized bed combustor or a full-scale operating biomass-fueled power plant were also included in the analytical program. These fly ashes are particularly of interest since they used fuel or fuel components investigated as part of this study. There are several important observations relating to the trace element compositions of these fly ashes. The first is that very strong fractionation occurs during combustion to the extent that trace element concentrations show little similarities to those observed in the corresponding fuel ashes. The second is that fly ashes collected over the duration of the experiments are remarkably similar. The third is that the minor straw components (leached or unleached) have little effect on fly ash trace element concentrations for a base wood fuel. The fourth is that the trace element concentrations can be strongly affected by contamination from plant construction materials such as steel. The final is that incorporation of urban fuel types may strongly affect many heavy metals including lead. The survey of some relevant fly ashes was not intended as a comprehensive study. Further experimental and practical studies of the partitioning of key trace elements between the various solid and vapor components are required to better understand the behavior of trace elements during biomass combustion.

This report advocates the use of normalized multielement diagrams to allow easy survey and interpretation of large numbers of trace element analyses. The usefulness of such ‘spider diagrams’ is determined by two factors. The first is that the normalizing values should represent unaffected and uncontaminated material for processes under investigation. The second is that the order in which the elements is presented likewise should reflect the processes being investigated. Different normalizing values and order of presentation would therefore ideally be required for studies of elemental losses during ashing or studies of plant intake of trace elements during growth. Further work along these lines is required to develop this approach into a powerful tool for studying trace element partitioning into plants and their fate during combustion or during other chemical and thermal processing. An obvious hindrance is the lack of chemically well-characterized, biofuel standard materials, including a comprehensive set of major, minor, and trace elements. Such standard materials would also be highly valuable for quality control purposes during analyses.

The study of trace element abundances in common biomass material during combustion provides the foundation for understanding the behavior of these elements as well as outlines the baseline abundance that can be expected in biomass and waste materials.

10.2. Recommendations

It is recommended that a broad survey of trace element contents of potential biomass fuels are conducted in order to determine for example the dependencies of soil type, irrigation water quality, and atmospheric pollution. Such a study will supplement the results of this study mainly concerned with the effects of firing temperature on the mobility of trace elements in biomass fueled power plant.

It is recommended that a detailed study be initiated of the fractionation of trace elements during combustion in model boilers as well as full-scale power plants.

It is further recommended that a set of biofuel multielement analytical standards be developed. This should include common and potential biomass ashes as well of fly ashes from biomass fueled power plants. The current situation is that the only relevant multielement standard available is a fly ash from a coal-fueled power plant (NIST 1633). The potential for high heavy element abundance in some fuel types warrant precise analyses of biomass and byproducts from thermal conversions. Such analyses would be greatly aided by high quality analytical standards resembling the fuel material in question.

10.3. Public Benefits to California

The results allow predictions of the concentrations of the trace elements in common biomass materials and provide a necessary foundation for monitoring heavy element emission and the utilization and disposal of residues and waste from biomass fueled power plants and other conversion facilities.

References

Baernthaler, G., Zischka, M., Haraldsson, C., and Obernberger, I., 2006. Determination of major and minor ash-forming elements in solid biofuel. Biomass & Bioenergy 30, 973-997.

Bale, C.W., Chartrand, P., Degterov, S.A., Eriksson, G., Hack, K., Ben Mahfoud, R., Melançon, J., Pelton, A.D., and Petersen, S., 2002. FactSage thermochemical software and databases. Calphad 26, 189-228.

Baxter, L.L., Miles, T.R, Miles, T.R. Jr, Jenkins, B.M., Milne, T., Dayton, D., Bryers, R.W., and Oden, L.L., 1998. The behavior of inorganic material in biomass-fired power boilers: field and laboratory experiences. Fuel Processing Technology 54, 47-78.

Cali, J.P., 1975. Certificate of Analysis. Standard Reference Material 1633. Trace Elements in Coal Fly Ash. Office of Standards Reference Materials, Washing DC.

Chadwick, M.J., Highton, N.H., and N. Lindman, 1987. Environmental Impacts of Coal Mining and Utilization. Pergamon Press, Oxford.

Dayton, D.C., French, R.J., and Milne, T.A, 1995. Direct observation of alkali vapor release during biomass combustion and gasification. 1. Application of molecular beam mass spectrometry to switchgrass combustion. Energy and Fuels 9, 855-865.

Gaillardet, J., Viers, J., and Dupre, B., 2004. Trace elements in river water. In (Drever, J.I., ed.), Treatise on Geochemistry, Volume 5, Surface and Ground Water, Weathering, and Soils, 225-272. Elsevier and Pergamon, Amsterdam.

GeoReM, 2006. Geological and Environmental Reference Materials. http://georem.mpch-mainz.gwdg.de/start.asp.

Gills, T.E., 1993. Certificate of Analysis. Standard Reference Material 1633b. Constituent Elements in Coal Fly Ash. National Institute of Standards and Technology, Gaithersburg, GA.

Govindaraju, K., 1994. 1994 compilation of working values and sample description for 383 geostandards. Geostandards Newsletter 18, 1-158.

Hasler, P. T. Nussbaumer, R. Buhler. 1994. Vergasung von biomassse fue die methanol-synthese. Schlussbericht im Sektor Technik Projeckt BIOMETH, as reported by von Scala, C. R. Struis and S. Stucki, 2000. The influence of heavy metals on the gasification of wood. http://lem.web.psi.ch/frame.htm.

Holland, H.D., 1978. The Geochemistry of the Atmosphere and Oceans. Wiley-Interscience, New York.

Jenkins, B.M., Mehlschau, J.J., Williams, R.B., Solomon, C., Balmes, J., Kleinman, M., and Smith, N., 2003. Rice straw smoke generation system for controlled human inhalation exposures. Aerosol Science and Technology 37, 437-454.

Jenkins, B.M., Williams, R.B., Bakker, R.R., Yomogida, D.E., Blunk, S.L., Pfaff, D., Goronea, M., Baxter, L.L., Carlson, W., Duffy, J., Rovenstine, J., Bates, R., Smith, T., Sugaoka, A., Stucki, K., and Reynolds, S., 1999. Fuel Selection and Furnace-Control in Reduction of Operating Costs for Biomass Boilers. Volume 3. California Energy Commission, Interagency Agreement 500-94-025, Final Report, Sacramento, California.

Jochum, K.P., Nohl, U., Herwig, K., Lammel, E., Stoll, B., and Hofmann, A.W., 2005. GeoReM: a new geochemical database for reference materials and isotopic standards. Geostandards and Geoanalytical Research 29, 333-338.

Kouvo, P. and Backman, R., 2003. Estimation of trace element release and accumulation in the sand bed during bubbling fluidised bed co-combustion of biomass, peat, and refuse-derived fuels. Fuel 82 741-753.

Livingstone, D.A., 1963. Chemical composition of rivers and lakes. Data of Geochemistry. US Geological Survey Professional Paper 440G, G1-G64.

Llorens, J.F., Fernandez-Turiel, J.L., and Querol, X., 2001. The fate of trace elements in a large coal-fired power plant. Environmental Geology 40, 409-416.

Meister, B.C., Williams, R.B., and Jenkins, B.M., 2005.Utilization of Wastre Renewable Fuels in Boilers with Minimization of Pollutant Emissions. Laboratory Scale Gasification Screening Experiments. PIER Final Report CEC-500-2005-134. California Energy Commission, Sacramento, California.

Meybeck, M., 2004. Global occurrence of major elements in rivers. In (Drever, J.I., ed.) Treatise on Geochemistry, Vol. 5, Surface and Ground Water, Weathering, and soils, 207-223. Elsevier and Pergamon, Amsterdam.

Miles, T.R, Miles, T.R. Jr, Baxter, L.L., Bryers, R.W., Jenkins, B.M., and Oden, L.L., 1995. Alkali Deposits Found in Biomass Power Plants. A preliminary Investigation of Their Extent and Nature. Summary Report. National Renewable Energy Laboratory, Golden, Colorado.

Obernberger, I. and Biedermann, F., 1997. Fractionated heavy metal separation in biomass combustion plants – possibilities, technological approach, experiences. Proceedings of the International Conference "The Impact of Mineral Impurities in Solid Fuel Combustion", Engineering Foundation, Kona, Hawaii.

PHYLLIS database for biomass and waste, Netherlands Energy Research Foundation, ECN, http://www.phyllis.nl/.

Querol, X., Fernandez-Turiel, J.L., and Lopez-Soler, A., 1995. Trace elements in coal and their behavior during combustion in a large power station. Fuel 74, 331-343.

Raask, E. 1985. Mineral impurities in coal combustion. Hemisphere Publishing, Washington, D.C.

Rasberry, S.D., 1985. Certificate of Analysis. Standard Reference Material 1633a. Trace Elements in Coal Fly Ash. National Institute of Standards and Technology, Gaithersburg, GA.

Richaud, R., Herod, A.A., and Kandiyoti, R., 2004. Comparison of trace element contents in low-temperature and high-temperature ash from coals and biomass. Fuel 83, 2001-2012.

Roelandts I. and Gladney E. S. (1998) Consensus values for NIST biological and environmental standard reference materials. *Fresenius J. Anal. Chem.* **360,** 327-338.

Roy, W.R., Thiery, R.G., Schuller, R.M., and Suloway, J.J., 1891. Coal fly ash: a review of the literature and proposed classification system with emphasis on environmental impacts. Environmental Geology Notes 96, Illinois Institute of Natural Resources, State Geological Survey Division.

Rudnick, R.L. and Gao, S., 2004. Composition of the continental crust. In (Rudnick, R.L., ed.) Treatise on Geochemistry, Volume 3, The Crust, Elsevier and Pergamon, Amsterdam.

Spears, D.A., 2004. The use of laser ablation inductively coupled plasma-mass spectrometry (LA ICP-MS) for the analysis of fly ash. Fuel 83, 1765-1770.

Struis R.P.W.J., von Scala C, Stucki S, Prins R. 2002. Gasification reactivity of charcoal with CO2. Part II: Metal catalysis as a function of conversion. Chemical Engineering Science 57 (17): 3593-3602.

Thy, P., Jenkins, B.M., and Lesher, C.E., 1999. High temperature melting behavior of urban wood fuel ash. Energy and Fuel 13, 839-850.

Thy, P., Lesher, C.E., Jenkins, B.M., 2000. Experimental determination of high temperature elemental losses from biomass fuel ashes. Fuel 79, 693-700.

Thy, P., Lesher, C.E., Jenkins, B.M., and Williams, R.B., 2004. Controlling Fouling with Rice Straw Blends in Biomass Boilers. California Energy Commission, Energy Innovations Small Grant Program, Final Report, Sacramento, California.

Thy, P., Grundvig, S., Jenkins, B.M., Shiraki, R., and Lesher, C.E., 2005. Analytical controlled losses of potassium from straw ashes. Energy and Fuels 19, 2571-2575.

Thy, P., Jenkins, B.M., Lesher, C.E., and Grundvig, S., 2006a. Compositional constraints on slag formation and potassium volatilization from rice straw blended wood fuel. Fuel Processing Technology 87, 383-408.

Thy, P., Jenkins, B.M., Grundvig, S., Shiraki, R., Lesher, C.E., 2006b. High temperature elemental losses and mineralogical changes in common biomass ashes. Fuel 85, 783-795.

Tillmann, D.A., 1994. Trace Metals in Combustion Systems. Academic Press, San Diego.

www.eia.doe.gov, 2003. www.eia.doe.gov/cnef/solar.renewables/page/rea_data/table5.

Appendices

Appendix 1. Elements Analyzed

Atomic Number Order			Alphabetic Order		
Be	4	beryllium	Ag	47	silver
Na	11	sodium	Al	13	aluminum
Mg	12	magnesium	As	33	arsenic
Al	13	aluminum	Ba	56	barium
Si	14	silicon	Be	4	beryllium
P	15	phosphorus	Ca	20	calcium
Cl	17	chloride	Cd	48	cadmium
K	19	potassium	Ce	58	cerium
Ca	20	calcium	Cl	17	chloride
Sc	21	scandium	Co	27	cobolt
Ti	22	titanium	Cr	24	chromium
V	23	vanadium	Cs	55	cesium
Cr	24	chromium	Cu	29	copper
Mn	25	manganese	Dy	66	dysprosium
Fe	26	iron	Er	68	erbium
Co	27	cobolt	Eu	63	europium
Ni	28	nickel	Fe	26	iron
Cu	29	copper	Gd	64	gadolinium
Zn	30	zinc	Hf	72	hafnium
As	33	arsenic	Ho	67	holmium
Se	34	selenium	K	19	potassium
Rb	37	rubidium	La	57	lanthanum
Sr	38	strondium	Lu	71	lutetium
Zr	40	zirconium	Mg	12	magnesium
Ag	47	silver	Mn	25	manganese
Cd	48	cadium	Na	11	sodium
Sn	50	tin	Nd	60	neodymium
Sb	51	antimony	Ni	28	nickel
Cs	55	cesium	P	15	phosphorus
Ba	56	barium	Pb	82	lead
La	57	lanthanum	Pr	59	praseodymium
Ce	58	cerium	Rb	37	rubidium
Pr	59	praseodymium	Sb	51	antimony
Nd	60	neodymium	Sc	21	scandium
Sm	62	samarium	Se	34	selenium
Eu	63	europium	Si	14	silicon
Gd	64	gadolinium	Sm	62	samarium
Tb	65	terbium	Sn	50	tin
Dy	66	dysprosium	Sr	38	strondium
Ho	67	holmium	Ta	73	tantalum
Er	68	erbium	Tb	65	terbium
Tm	69	thulium	Th	90	thorium
Yb	70	ytterbium	Ti	22	titanium
Lu	71	lutetium	Tl	81	thallium
Hf	72	hafnium	Tm	69	thulium
Ta	73	tantalum	U	92	uranium
W	74	tungsten	V	23	vanadium
Tl	81	thallium	W	74	tungsten
Pb	82	lead	Yb	70	ytterbium
Th	90	thorium	Zn	30	zinc
U	92	uranium	Zr	40	zirconium

Appendix 2. Abbreviations, Acronyms, and Dictionary

Abbreviations and Acronyms

Å, Ångstrom
d-values, used in crystallography for the average spacing between identical planes (measured in Ångstrom)
EPA, Environmental Protection Agency
FBC, fluidized-bed combustion
ICPMS, inductively coupled plasma mass spectroscopy
INAA, instrumental neutron activation
LOI, loss-on-ignition
MPa, unit of pressure
NIST, National Institute of Standards and Testing
ppb, parts per billion on a weight basis
ppm, parts per million on a weight basis
PURPA, Public Utilities Regulatory Policy Act
RSD, relative standard deviation
S-type thermocouple, temperature sensor made from a Platinum-10% Rhodium alloy against pure Platinum
XRF, X-ray fluorescence spectroscopy

Non-Technical Meaning of Selected Terms

amorphous, without the regular, ordered structure of crystalline solids
Ångstrom, one ten-billionth of a meter after Swedish chemist Anders Ångström
ash, inorganic, non-combustible residue left after complete combustion of a material
baghouse, facility that removes fly ash from the flue gas by the use of fabric filter bags
bed media, sand or similar refractory particulate materials used in fluidized bed reactors for rapid heat exchange and prompt mixing of feedstock injected into the reactor
biomass, organic materials that are plant or animal based, including but not limited to dedicated energy crops, agricultural crops and trees, food, feed and fiber crop residues, aquatic plants, forestry and wood residues, agricultural wastes, biobased segments of industrial and municipal wastes, processing byproducts and other non-fossil organic materials
bottom ash, agglomerated ash particles formed in pulverized coal boilers that are too large to be carried in the flue gases and impinge on the boiler walls or fall through open grates to an ash hopper at the bottom of the boiler
calcite, a mineral consisting of calcium carbonate crystallized in hexagonal form
carbonate, mineral belonging to a group with the essential structural ion unit $(CO_3)^{-2}$), including calcite, dolomite, siderite, and magnesite.
co-firing, simultaneous use of two or more different fuels in the same combustion chamber of a power plant
combustion, thermal conversion of a carbon rich feedstock with an oxidant (excess air) to produce primarily heat energy, carbon dioxide, water and ash

convection pass, a heat exchange section of a boiler or other heat recovery device, typically coming after the furnace section and commonly employing cross-flow or parallel-flow tubular heat exchangers to preheat combustion air, evaporate water to steam, and superheat steam. In the laboratory reactor used for the experiments reported here, the convection pass included the vertical disengagement zone and the subsequent horizontal pass

cristobalite, high-temperature polymorph mineral of quartz or tridymite

crystallinity, the quantity or state of being crystalline (the amount of crystals)

cyclone, cone-shaped air-cleaning apparatus which operates by centrifugal separation that is used in particle collecting and fine grinding operations

decomposition, the separation of a substance into constituent parts or simpler compounds

disengagement zone, a zone following the primary bed section of a fluidized bed reactor designed to disengage larger particles from the flow and return them to the bed. Disengagement can be accomplished in a number of ways, including expanding the bed cross section to reduce the gas velocity and hence the drag force acting to carry particles on the flow, or by other means such as inertial separation using cyclones or multiclones, either internal or external to the reactor

***elemental analysis*,** quantification of the chemical physical components in a biomass or ash

fluidized-bed combustion (FBC), combustion by mixing with a bed material. The fuel and bed material mixture is fluidized during the combustion process to allow complete combustion

fly ash, biomass ash that exits a combustion chamber in the flue gas and is captured by air pollution control equipment such as electrostatic precipitators, baghouses, and wet scrubbers

fusing, transforming into a melt at relatively high temperature

generating bank, a specific section of the convection pass heat exchangers in a boiler used to evaporate water to steam. May be used in combination with a waterwall heat exchanger to increase steaming capacity

glass, amorphous inorganic, transparent or translucent, substance without strong crystalline structure as in minerals (supercooled liquid)

graphite, a mineral consisting of soft black lustrous carbon

***halite*,** mineral consisting of sodium chloride

heavy element, atomic metal or element of high density or atomic number

instrumental analysis, chemical analysis performed using an instrument. Often multielement analyses as opposed to traditionally titration based analyses

irradiation, exposure to rays such as X-rays

Kanthal furnace, furnace with heating elements made from an iron alloy marketed by AB Kanthal

larnite, loosely defined as calcium silicate mineral of the general form Ca_2SiO_4

leaching, process of separating the soluble components from some material by percolation water

liquidus, phase boundary or temperature above which a substance is completely liquid

loss-on-ignition (LOI), weight loss during firing or ignition

major element, chemical element or oxide in concentrations above 2 %

melting, transforming into a melt at relatively high temperature

minor element, chemical element or oxide in concentrations below 2 % and above 0.1 %

moisture content, amount of water contained in a material expressed as either on a wet weight basis or dry weight basis

muffle furnace, a front-loading box-type oven for high-temperature applications

mullite, orthorhombic mineral composed of silicate and aluminum of the general form $Al_6Si_2O_{13}$. Often used as a refractory.

multiclone, a device in which multiple cyclonic type separators (cyclones) are used to separate ash and other particles from the flue gas of a furnace or boiler

non-destructive analytical method, analytical method that do not destroy the nature or structure of the material being analyzed

oxide mineral, binary mineral of oxygen with an element

periclase, magnesia oxide mineral of the general formula MgO

proximate analysis, determination of moisture, volatile matter, ash and the calculation of fixed carbon in a material

pyroxene, a member of a group of silicate minerals closely related in crystal form and having the general formula $ABSi_2O_6$ where A represents Ca or Na and B is Mg, Fe, or Al

quenched melt, high temperature melt cooled to a glass and/or crystals

residue, material that remains after a portion is removed by a process, such as burning

silicate, member of a group of minerals with crystal structure characterized by fundamental units of SiO_4 tetrahedrons

sintering, process by which small particles coalesce to form larger masses, usually at high temperature

slag, ash that is or has been in a molten (or liquid) state or otherwise agglomerated

solid, substance that does not flow under moderate stress

solidus, temperature below which a substance is completely solid

solvent, substance like water able to dissolve another substances

spider diagram, multielement compositional diagram often normalized to a well known composition and with the element are arranged along the abscissa in a systematic fashion (like atomic number)

superheaters, heat exchangers used to superheat steam above its saturation temperature, commonly deployed in the high temperature zone in the entrance to the convection pass near the exit of the furnace

superliquidus, above temperature of the liquidus (see liquidus)

sylvite, potassium chloride mineral of the general chemical formula KCl

thermal conversion, transformation of biomass into bioenergy or biobased products

toxic element, element that in sufficient high concentrations may be toxic

trace element, element in concentrations below 0.1 % often given as parts per million (ppm)

tridymite, high-temperature polymorph of quartz

ultimate analysis**,** see Elemental Analysis

urban wood fuel, a class of biomass fuel representing wood separated from a waste typically including used pallets, crates, used construction forms, stumps, branches, and out-of-specification lumber. May also include contaminant materials such as plastics, textiles, and other wastes not completely removed in separation of the wood. Demolition waste may or may not be included depending on use, source, and composition. Demolition wastes are commonly avoided, particularly if lead-based paints are present on the wood

vesicle channels, interconnected channels in a solid formed by systematic alignment of elongated vesicles

volatiles**,** materials (such as vapors and gases) that vaporize from heated and non-heated biomass

volatilization, a process (usually pyrolysis) whereby volatile materials are removed from carbon rich feedstock

Analytical Tools

Agilent quadrupole ICP-MS, inductively coupled plasma mass spectrometry (ICP-MS) is a fast, precise, and accurate multielement analytical technique for the determination of trace element abundances. Because of its high sensitivity and capability of analyzing both solution and solid samples, ICP-MS has broad applications in many fields including the earth, environmental, materials, biological, and medical sciences. Manufactured and distributed by Agilent Technologies, Santa Clara, CA (US office).

BYK-Gardner Colour Guide, color-view spectrophotometer is used to qualify colors. Manufactured and distributed by BYK-Gardner GmbH, Geretsried, Germany

PANalytical X-ray spectrometer, a non-destructive X-ray analytical technique used to identify and determine the concentrations of elements present in solid, powdered and liquid samples. Capable of measuring elements from Beryllium (Be) to Uranium (U) and beyond from trace levels and up to 100%. Manufactured and distributed by PANalytical, Almelo, The Netherlands

SPEX wolfram carbide mill, sample preparation mill made from wolfram carbide. Manufactured and distributed by SPEX CertiPrep, Metuchen, NJ, USA

SuperQ Software, software package used for XRF elemental analysis. Written and distributed PANalytical, Almelo, The Netherlands

TRIGA nuclear reactor, research nuclear reactor used to radiate samples for INAA. Manufactured and distributed by General Atomics, San Diego, CA, USA